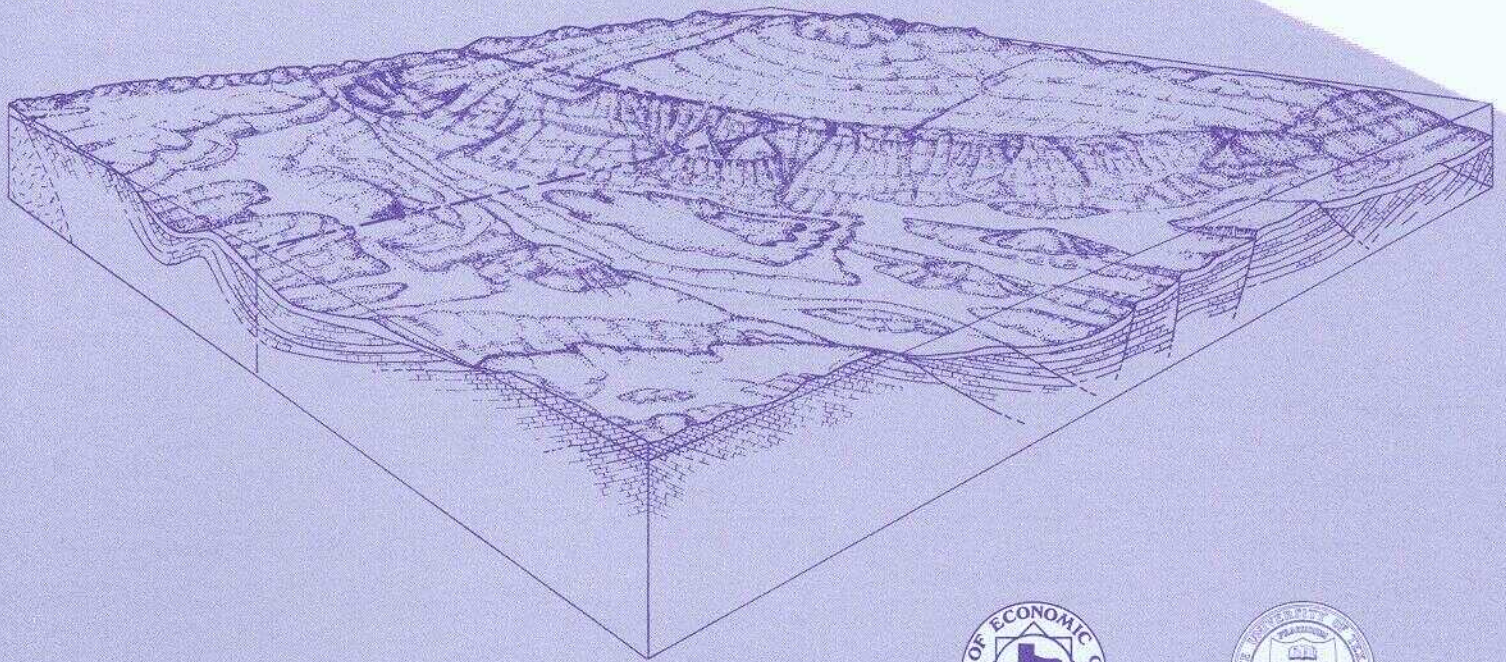


Stratigraphic Analysis of the Upper Devonian Woodford Formation, Permian Basin, West Texas and Southeastern New Mexico

John B. Comer



1991



Bureau of Economic Geology • W. L. Fisher, Director
The University of Texas at Austin • Austin, Texas 78713-7508

Report of Investigations No. 201

Stratigraphic Analysis of the
Upper Devonian Woodford Formation,
Permian Basin, West Texas and
Southeastern New Mexico

*John B. Comer**

*Current address
Indiana Geological Survey
Bloomington, Indiana 47405



1991



Bureau of Economic Geology • W. L. Fisher, Director
The University of Texas at Austin • Austin, Texas 78713-7508

Contents

Abstract	1
Introduction	1
Methods	3
Stratigraphy	5
Nomenclature	5
Age and Correlation	6
Previous Work	6
<i>Western Outcrop Belt</i>	6
<i>Central Texas</i>	7
<i>Northeastern Oklahoma and Northern Arkansas</i>	8
<i>Ouachita Fold Belt</i>	8
<i>Central and Southern Oklahoma</i>	8
<i>Permian Basin</i>	9
Formation Boundaries	9
Distribution	10
Northwestern Shelf and Matador Uplift	10
Eastern Shelf	10
Central Basin Platform and Pecos Arch	11
Delaware Basin	11
Midland Basin	11
Val Verde Basin	11
Diablo Platform and Western Outcrop Belt	12
Lithofacies	12
Black Shale	12
<i>Characteristic Features</i>	12
<i>Bedding and Sedimentary Structures</i>	12
<i>Texture</i>	13
<i>Composition</i>	13
Siltstone	16
<i>Characteristic Features</i>	16
<i>Bedding and Sedimentary Structures</i>	17
<i>Texture</i>	17
<i>Composition</i>	17
Formation-Boundary Lithologies	20
<i>Lower Contact</i>	20
<i>Upper Contact</i>	20
Lithofacies Correlation	22
Lithofacies Distribution	23
Depositional Processes	25
<i>Siltstone</i>	25
<i>Black Shale</i>	26
Lithologic Patterns and Origin of Sediments	26
Depositional Setting	30
Paleogeography	30
Paleotectonics	31
Paleoclimate	32
Paleoceanography	33

Depositional Mechanisms	34
Synopsis of Depositional History	35
Petroleum Potential	36
Summary	36
Acknowledgments	38
References	39
Appendices	
A. Location of cores and measured sections	43
B. Description of cores and measured sections	44
C. Point-count data for the Woodford Formation	60
D. Organic content of the Woodford Formation	61

Figures

1. Index maps showing structural provinces in the Permian Basin	2
2. Map showing lines of cross sections and locations of cores and measured sections	4
3. Correlation chart for Devonian and Mississippian Systems in West Texas and southeastern New Mexico	7
4. Photos of Woodford black shale	14
5. Photos of Woodford siltstone	18
6. Photos of Woodford contacts	21
7. Log correlation of Woodford lithofacies	23
8. Fence diagram of Upper Devonian units	24
9. Regional lithologic variations in Upper Devonian rocks in West Texas and southeastern New Mexico	26
10. Late Devonian paleogeography of West Texas and southeastern New Mexico	30
11. Late Devonian paleogeography of North America	32
12. Model of Late Devonian circulation during eustatic highstand	34

Plates (in pocket)

1. Structure map of Woodford Formation, Permian Basin.
2. Isopach map of Woodford Formation, Permian Basin.
3. West-east cross section A–A'. Line of section in figure 2.
4. West-east cross section B–B'. Line of section in figure 2.
5. West-east cross section C–C'. Line of section in figure 2.
6. North-south cross section D–D'. Line of section in figure 2.
7. North-south cross section E–E'. Line of section in figure 2.

Abstract

The Upper Devonian Woodford Formation is an organic-rich petroleum source rock that extends throughout West Texas and southeastern New Mexico and currently is generating oil or gas in the subsurface. The Woodford is a potential hydrocarbon reservoir in areas where it is highly fractured; the most favorable drilling targets are fractured siltstone or chert beds in densely faulted regions such as the Central Basin Platform, southernmost Midland Basin, and parts of the Northwestern Shelf. Stratigraphic analysis was undertaken to determine how the Woodford was deposited and why its petroleum source potential is so great.

The Woodford consists of two lithofacies, black shale and siltstone. Black shale, the most widely distributed rock type, is very radioactive and contains varvelike parallel laminae, abundant pyrite, and high concentrations of marine organic matter. Siltstone, typically a basal facies, in deep basin and proximal shelf settings, exhibits disrupted stratification, graded layers, fine-grained Bouma sequences, and a subequal mixture of silt-sized quartz and dolomite. Black shale is mostly pelagic and represents an anaerobic biofacies, whereas siltstone is the result of bottom-flow deposition and represents a dysaerobic biofacies.

The depositional model developed herein for the Woodford was based on stratigraphic sequence, patterns of onlap, and lithologic variations, together with published information about global paleogeography, paleoclimate, and eustasy. During the Late Devonian, the Permian Basin was a low-relief region located on the western margin of North America in the arid tropics near 15 degrees south latitude. Worldwide marine transgression caused flooding of the craton and carried water from a zone of coastal upwelling into the expanding epeiric sea. Strong density stratification developed, due partly to accumulation of hypersaline bottom water that formed locally in the arid climate. Anaerobic conditions resulted from poor vertical circulation and from high oxygen demand, which was caused by the decay of abundant organic matter produced in the nutrient-rich surface waters. Continuous, slow deposition of pelagic material was interrupted by episodic, rapid deposition of silt and mud from bottom flows generated during frequent tropical storms.

This report documents the composition, distribution, and structure of the Woodford Formation in a major hydrocarbon-producing basin. Petrologic and organic geochemical data helped explain the origin of the unit and provided information necessary for predicting potential locations and lithologies of commercial petroleum reservoirs within the Woodford. Combining comprehensive stratigraphic, petrologic, and geochemical data was useful for developing a depositional and exploration model of Devonian black shale in West Texas and New Mexico. Similar studies should be conducted elsewhere to enable discovery of unconventional hydrocarbon reserves in black shales.

Keywords: Upper Devonian, Woodford, black shale, siltstone, source rocks, unconventional reservoirs, depositional model, paleogeography

Introduction

This report presents a stratigraphic analysis of the Woodford Formation (Upper Devonian) in the Permian Basin of West Texas and southeastern New Mexico (fig. 1a, b). The study is

part of a larger project undertaken to determine how and why these enigmatic, organic-rich marine rocks were deposited and to document their petroleum-generation history. The part of

the project involved in this study entailed mapping, conducting lithologic studies of cores and outcrops, and reconstructing paleogeography and depositional environments.

The Woodford Formation has long been recognized by geologists working in the region as an important stratigraphic marker because of its black shale lithology, anomalously high radioactivity, and widespread distribution (Ellison, 1950; Wright, 1979). The organic-rich formation typically yields shows of oil from cuttings and cores and produces a gas response on mudlogs. The Woodford, acknowledged as a principal petroleum source rock in the Permian Basin (Galley, 1958; Jones and Smith, 1965; Horak, 1985), contains some intervals of "oil shale" as well (>10 gal of retortable oil per ton of shale). It is also a low-grade, subeconomic uranium and heavy metal deposit (Swanson, 1960; Landis, 1962; Duncan and Swanson, 1965).

The economic potential of black shales has prompted several studies of shale deposition. Previous publications describe and interpret the origin of Devonian black shales in the eastern United States (for example, Cluff, 1980; Ettensohn and Barron, 1981; Broadhead and others, 1982; Schopf, 1983; Ettensohn and Elam, 1985; Pashin and Ettensohn, 1987), but no com-

parable work has been published on equivalent strata in the southern Midcontinent. Developing a comprehensive depositional model of the Woodford was complicated in that no modern analog is available for comparison. During the Late Devonian a euxinic sea, in which broad expanses of marine black shale had been deposited, occupied most of the Midcontinent of North America. However, virtually no large euxinic epeiric seas on stable cratons and passive continental margins adjacent to the open ocean exist in the modern world. Why cratonic euxinic seas developed must be understood before the origin of the Woodford can be fully explained. Although global controls, such as deglaciation and ocean ridge expansion (Heckel and Witzke, 1979; Johnson and others, 1985), can account for the worldwide transgression in the Late Devonian, regional controls must be used to account for the strongly stratified water columns and widespread bottom anoxia that developed in North America. The depositional model described later herein shows that it was the unique relationship among geography, geomorphology, tectonics, climate, and oceanography that produced the uncommon environment and unusual lithology of the Woodford Formation.

Methods

Data for the project were obtained from 558 well logs, 13 cores, and 3 measured sections. Well control is plotted on the structure and isopach maps (pls. 1, 2), and the location of cores, measured sections, and cross sections is shown in figure 2. An index of well names and locations is on open file at the Bureau of Economic Geology, and the core and measured section localities are listed in appendix A.

Plates 1 and 2 were contoured using the well data shown on each map. In areas of poor control, elevation of the Woodford (pl. 1) was inferred using the *Tectonic Map of Texas* (Ewing, 1991), which was contoured on top of the Ellenburger Formation (Lower Ordovician) in West Texas and on top of the Silurian-Devonian carbonate section in southeastern New Mexico.

Faults mapped in this report were redrawn from Ewing's map.

Outcrops in the Hueco, Franklin, and Sacramento Mountains were described to compare these well-studied measured sections in the west with the poorly known rocks in the subsurface. Outcrops were chosen that had been mapped previously and for which paleontological analysis had established relative ages.

The Woodford Formation was identified from well logs, primarily by high radioactivity on the gamma-ray log (pls. 3 through 7), and by its stratigraphic position between carbonates. Although other highly radioactive strata lie in the Permian Basin, the Woodford is the most laterally persistent and typically exhibits the strongest radioactivity anomaly.

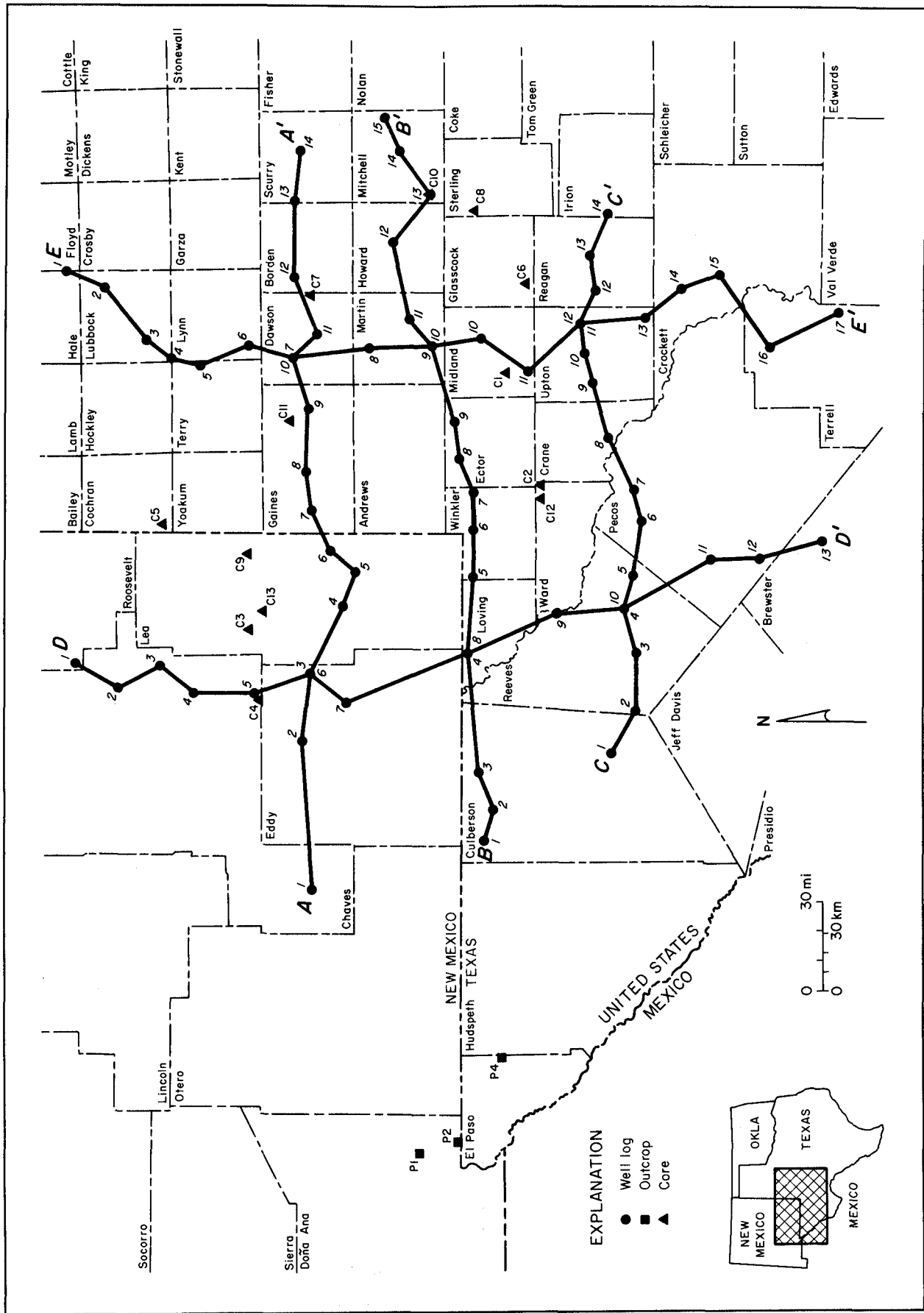


FIGURE 2. Map showing lines of cross sections (pls. 3 through 7) and locations of cores and measured sections (app. A).

The Woodford was more difficult to identify where it is overlain by radioactive, fine-grained carbonates or shales (for example, pl. 5, logs 9 through 14; pl. 6, logs 9 through 13; pl. 7, logs 10 through 12 and 16, 17) and where the lower part of the formation is much less radioactive than the upper part (for example, pl. 4, logs 9, 11; pl. 7, logs 7, 8). In such sections, the upper and lower contacts were picked from cores, if available, or on sonic, resistivity, and neutron logs. Typically the Woodford Formation exhibits low sonic velocity, low resistivity, and low neutron-induced radiation.

In cores and outcrops, the Woodford and correlative formations were identified by their high radioactivity and unique lithology. A radioactivity profile (counts per second [CPS]) was made for each core and outcrop using a hand-held scintillometer (Ettensohn and others, 1979). Discrepancies between log depth and core depth were corrected by comparing the radioactivity profile and the wireline gamma-ray log. Lithologically, Woodford black shale contrasts sharply with the light-colored Silurian-Devonian carbonates below and Mississippian carbonates above. Where differences in color and composition are less obvious, continuous, varvelike parallel laminae and abundant pyrite distinguish the Woodford.

Petrologic analysis was conducted using slabbed cores, outcrops, slabbed hand specimens, and thin sections (app. B). Uncovered thin sections were X-rayed to identify the clay minerals and to distinguish calcite and dolomite, and selected thin sections were point counted (app. C).

Stratigraphy

Nomenclature

The name Woodford was first used by Taff (1902) to describe exposures of chert and black shale along the southern flank of the Arbuckle Mountain anticline in Carter County, Oklahoma. Both Woodford Chert and Woodford Shale are established as formation names (Keroher and others, 1966), but the term Woodford Formation also appears in the literature. In this report, "Woodford Formation" is used because of the wide variety of lithologies that compose the

Woodford lithofacies were correlated in the subsurface using gamma-ray logs (pls. 3 through 7). The two dominant lithofacies, black shale and siltstone, are readily identified because siltstone is markedly less radioactive than black shale (app. B; C5, C9).

Total organic carbon (TOC), vitrinite reflectance (% R_o), and kerogen morphology data (app. D) were valuable in interpreting the sediment provenance, paleogeography, climate, and oceanography during Woodford deposition. Recognition of pelagic and terrigenous sediment was aided by distinguishing between amorphous kerogen, which derives from organic matter of aquatic origin, and structured kerogen, which is mostly the debris of land plants (Hunt, 1979; Tissot and Welte, 1984). Large concentrations of organic matter, recorded in the rocks as high TOC values, indicate high primary productivity, rapid sedimentation, or anoxic conditions; kerogen type records relative influences of terrigenous, paralic, or marine sources and indirectly reflects depositional processes, paleosalinity, paleoclimate, and proximity to land (Byers, 1977; Hunt, 1979; Demaison and Moore, 1980; Tissot and others, 1980; Tissot and Welte, 1984; Stein, 1986; Pedersen and Calvert, 1990). Vitrinite reflectance, which records maximum paleotemperature (Dow, 1977; Hunt, 1979; Tissot and Welte, 1984), allows inferences to be made about structural evolution, thermal events, and burial history of the basin during and after the Late Devonian and constrains models of mid-Paleozoic tectonics and paleogeography.

interval in the southern Midcontinent. The most readily apparent and dominant lithology is black shale; however, chert, dolostone, sandstone, siltstone, and light-colored shale are common (Harlton, 1956; Amsden and others, 1967; Amsden, 1975, 1980).

Correlation and nomenclature of Devonian and Mississippian formations are well known regionally (fig. 3), but within the Permian Basin, stratigraphy and correlation of Silurian, Devonian, and Mississippian strata are poorly

known. Throughout this report, therefore, carbonate rocks underlying the Woodford are referred to as Silurian-Devonian (undifferentiated), and those overlying the Woodford are referred to as Mississippian (undifferentiated), unless faunal or lithologic data indicate a specific system, series, or stage.

Age and Correlation

The Woodford Formation is mostly Late Devonian (Frasnian-Famennian) in age, although beds of latest Middle Devonian (Givetian) and earliest Mississippian (Kinderhookian) appear at some localities (Hass and Huddle, 1965; Amsden and others, 1967; Amsden and Klapper, 1972; Amsden, 1975, 1980). Ellison (1950) found Late Devonian conodont assemblages but no Mississippian fossils in the Woodford Formation in the Permian Basin, and he documented the correlation between the Woodford in the Permian Basin and the Percha Formation in southeastern New Mexico and West Texas (fig. 3). The Late Devonian age of the Percha and Sly Gap Formations (fig. 3) has been established by faunal analysis (Stevenson, 1945; Laudon and Bowsher, 1949).

The Woodford is stratigraphically equivalent to several Devonian black shales in North America, including the Antrim Shale in the Michigan Basin, the Chattanooga and Ohio Shales in the Appalachian Basin, the New Albany Shale in the Illinois Basin, the Bakken Formation in the Williston Basin, and the Exshaw Formation in the Western Canada Basin (Meissner, 1978; Cluff and others, 1981; Roen, 1984; Burrowes and Krause, 1987). Correlative rocks exposed in uplifts in the southern Mid-continent include the Houy Formation in the Llano Uplift of Central Texas; the Chattanooga Shale in the Ozark Uplift of northeastern Oklahoma, southern Missouri, and northern Arkansas; the middle division of the Arkansas Novaculite in the Ouachita Mountains of southeastern Oklahoma and west-central Arkansas; the upper part of the Caballos Novaculite in the Marathon region of West Texas; the Percha Formation in the Hueco and Franklin Mountains of West Texas; and the Sly Gap Formation in the Sacramento Mountains of southeastern New

Mexico (King and others, 1945; Stevenson, 1945; Laudon and Bowsher, 1949; Graves, 1952; Cloud and others, 1957; Huffman, 1958; Hass and Huddle, 1965; Amsden and others, 1967).

Previous Work

Western Outcrop Belt

Throughout the Franklin, Hueco, and Sacramento Mountains, Middle and Upper Devonian rocks unconformably overlies massive beds of the Lower Silurian Fusselman Dolomite (King and others, 1945; Stevenson, 1945; Laudon and Bowsher, 1949; LeMone, 1971; Lucia, 1971). In the Franklin and Hueco Mountains and at Bishop Cap, New Mexico, the Fusselman is overlain by the upper Middle to lower Upper Devonian Canutillo Formation, which is overlain conformably by the Upper Devonian Percha Formation (King and others, 1945; Rosado, 1970) (app. B; Pl, P4). The Canutillo consists of dark cherty and noncherty dolostone (Rosado, 1970), and the Percha is black, fissile, nonfossiliferous shale (Stevenson, 1945). The Canutillo-Percha contact is sharp, and the lithologic transition abrupt.

In the Sacramento Mountains, the Fusselman is overlain by the upper Middle to lower Upper Devonian Onate Formation, which is overlain by the lower to middle Upper Devonian Sly Gap Formation (Stevenson, 1945; Laudon and Bowsher, 1949; Kottowski, 1963; Rosado, 1970; Bolton and others, 1982). Locally, rocks assigned to the Percha overlies the Onate or the Sly Gap (Pray, 1961; Bolton and others, 1982). The Onate-Sly Gap contact was found to be conformable by Stevenson (1945) but locally eroded and disconformable by Pray (1961). Kottowski (1963) suggested that the Onate may be a basal facies of Sly Gap because the contact is gradational or only slightly erosional. The Onate consists of interbedded gray-brown shale, siltstone, fine sandstone, and carbonate (Stevenson, 1945), and the most common lithology is dolomitic siltstone (Kottowski, 1963). The Sly Gap is fossiliferous and consists of thinly interbedded, mostly tan to pale-yellow shale, siltstone, and limestone, along with a few dolomitic beds (Stevenson, 1945; Rosado, 1970). The Sly Gap is distinguished from the Onate in the field by color; and the Sly

SYSTEM	SERIES	Sacramento Mountains New Mexico	Franklin Mountains Texas	Hueco Mountains Texas	Permian Basin New Mexico and Texas		
					Delaware Basin	Central Basin Platform and Midland Basin	
MISSISSIPPIAN	Chesterian	Helms Formation	Helms Formation	Helms Formation	Helms Formation	Mississippian Limestone	
	Meramecian	Rancheria Formation	Rancheria Formation		Rancheria Formation		
		Las Cruces Formation	Las Cruces Formation				
	Osagean	Lake Valley Formation					
	Kinderhookian	Caballero Formation					
DEVONIAN	Upper	Famennian	Percha Fm.	Percha Formation	Percha Formation	Woodford Formation	Woodford Formation
		Frasnian	Sly Gap Fm.	Percha Formation	Percha Formation	Woodford Formation	Woodford Formation
	Middle	Givetian	Ouate Formation	Canutillo Formation	Canutillo Formation	Thirtyone Formation	Devonian Limestone
		Eifelian					
		Emsian					
	Lower	Pragian					
		Lochkovian					

QA 14569c

FIGURE 3. Correlation chart for Devonian and Mississippian Systems in West Texas and southeastern New Mexico. Adapted from Rosado (1970), LeMone (1971), Hoenig (1976), Bolton and others (1982), Lindberg (1983), and Hills (1984).

Gap has more shale and fewer massive, resistant beds than does the Onate (Stevenson, 1945). In the Sacramento Mountains, the Sly Gap gradually thins to the east and south and contains more black shale than do exposures farther west (Stevenson, 1945), reflecting a facies relationship with the Percha (Rosado, 1970).

At most localities in the Franklin, Hueco, and Sacramento Mountains, the Percha and Sly Gap Formations are overlain disconformably by Mississippian limestones (King and others, 1945; Rosado, 1970) (app. B; P2, P4). At Bishop Cap, New Mexico (app. B; P1), and locally in the Sacramento Mountains, Upper Devonian rocks are overlain conformably by the Kinderhookian Caballero Formation (Rosado, 1970; Bolton and others, 1982) (fig. 3).

Central Texas

In the Llano region of Central Texas, the Houy Formation disconformably overlies rocks of Early to Middle Devonian and Early Ordovician age (Cloud and others, 1957). Rocks below the unconformity are carbonates, and most are cherty. In upward succession, the Houy consists of a lower or basal chert breccia (Ives Breccia Member), black shale (Doublehorn Shale Member), and an upper, unnamed phosphatic unit. The Ives Breccia consists mostly of angular fragments and unbroken nodules of chert and locally contains angular blocks of dolostone, all of which appear to be little-moved lag deposits (Cloud and others, 1957). The Doublehorn Shale is fissile, radioactive, spore-bearing black shale, and the upper phosphatic unit contains phosphatic

debris such as fish bones, pellets, and conodonts. The Houy is predominantly Late Devonian, but locally the lowermost Houy may be Middle Devonian and the upper phosphatic unit partly Early Mississippian (Kinderhookian) (Cloud and others, 1957).

The Houy is conformably overlain by the Kinderhookian Chappel Limestone (Cloud and others, 1957). However, the upper Houy has thin beds, interrupted faunal zones, and intervals containing mixed Mississippian and Devonian fossils, all of which make correlation, age, and vertical continuity difficult to determine (Cloud and others, 1957).

Northeastern Oklahoma and Northern Arkansas

In the Ozark Uplift, the Chattanooga Shale rests disconformably on rocks ranging in age from Devonian to Ordovician (Huffman, 1958). The Sylamore Sandstone Member constitutes the lower part of the formation at many localities, and its age is late Middle Devonian to late Kinderhookian (Freeman and Schumacher, 1969; Pittenger, 1981). The black shale interval, sometimes called the Noel Shale Member (Huffman and Starke, 1960), is predominantly Late Devonian but ranges in age from early Late Devonian to Kinderhookian (Amsden and others, 1967). The Sylamore is submature to supermature quartzarenite that contains minor phosphate, glauconite, and locally abundant dolomite (Pittenger, 1981). Quartz was reworked from contemporaneous exposures of the Middle Ordovician Bergen Sandstone (Pittenger, 1981). Locally the basal layer of the Sylamore is chert breccia (Amsden and others, 1967). The Noel is black, fissile, radioactive shale and is the most abundant Chattanooga lithology. The Chattanooga is overlain disconformably by limestones and cherts of the Mississippian Boone Group. The Boone is predominantly Osagean but ranges in age from middle Kinderhookian to early Meramecian (Sutherland and Manger, 1979).

Ouachita Fold Belt

The middle division of the Arkansas Novaculite in Oklahoma and Arkansas is from Late Devonian to Kinderhookian age and represents, at least partly, a lateral facies of the

Woodford (Hass, 1951; Amsden and others, 1967). Likewise, the upper Caballos Novaculite in West Texas is a Late Devonian (Graves, 1952) lateral facies of the Woodford. Faunal data are scarce and contact relationships problematic, but vertical lithologic continuity suggests that the Woodford-equivalent interval in the novaculite formations is bounded conformably by the underlying and overlying beds. The upper Caballos contains mostly white novaculite, and the middle division of the Arkansas Novaculite contains interbedded dark-gray and greenish-gray shales and dark-gray novaculite (Hass, 1951; Amsden and others, 1967).

Central and Southern Oklahoma

In central and southern Oklahoma, the Woodford Formation rests disconformably on rocks of late Early Devonian to Ordovician age (Amsden, 1975, 1980). The Woodford is mostly Late Devonian but ranges in age from Givetian to Kinderhookian (Hass and Huddle, 1965; Amsden and others, 1967; Amsden and Klapper, 1972; Amsden, 1975, 1980). A basal clastic unit, the Givetian to early Famennian Misener Sandstone, is present in some areas (Amsden and Klapper, 1972). Woodford black shale is Frasnian to Kinderhookian (Hass and Huddle, 1965; Amsden and others, 1967).

Rocks underlying the Woodford are predominantly carbonates, and some are cherty. In southern Oklahoma, the Misener is sandstone, siltstone, green shale, dolostone, or chert breccia, whereas in north-central Oklahoma it is mostly mature quartzarenite containing minor glauconite and phosphate and locally abundant dolomite (Harlton, 1956; Amsden and others, 1967; Amsden and Klapper, 1972; Amsden, 1980; Francis, 1988). Quartz was derived with little transport from Middle Ordovician Simpson sandstone in north-central Oklahoma and from the Ouachita province in southern Oklahoma (Amsden and Klapper, 1972). Black shale is the most widespread Woodford lithology. It is fissile, spore-bearing, and highly radioactive, and in the Arbuckle Mountains it is interbedded with chert (Amsden and others, 1967; Amsden, 1975, 1980). Woodford chert is dark and rich in radiolarians and marine organic matter (Comer and Hinch, 1987). The Misener-Woodford sequence is stratigraphically equivalent to the

Sylamore-Chattanooga sequence in the Ozark Uplift, and the lower boundary of both sequences is diachronous, onlapping parts of the northern Oklahoma shelf and the Ozark Uplift (Freeman and Schumacher, 1969; Amsden and Klapper, 1972; Amsden, 1980).

In the Arbuckle Mountains, the Woodford is conformably overlain by the Sycamore Formation. The Sycamore consists of poorly fossiliferous, fine-grained, silty limestone interbedded with dark shale, and its age spans the Early to Middle Mississippian (Kinderhookian to Meramecian) (Ham, 1969). In the subsurface, the Woodford is overlain by Mississippian rocks (mostly limestones), but the stratigraphic relationship is problematic. In basinal regions, evidence of unconformity is obscure, although the contact is probably disconformable (Ham and Wilson, 1967; Frezon and Jordan, 1979). Locally the contact appears to be gradational, and the unconformity, if present, represents only a minor stratigraphic break (Frezon and Jordan, 1979).

Permian Basin

In the Permian Basin, lithologic, electric-log, and sparse faunal data indicate that the Woodford unconformably overlies rocks ranging in age from Devonian to Ordovician (Lloyd, 1949; Ellison, 1950; Peirce, 1962; McGlasson, 1967; Munn, 1971; Hoenig, 1976). The Woodford is overlain disconformably by Mississippian limestone (fig. 3) and locally by rocks as young as Early Permian (Lloyd, 1949; Wright, 1979). Lloyd (1949) assigned the Mississippian limestone section in the subsurface to the Meramecian Rancheria Formation on the basis of a few fossils and lithologic similarity to rocks exposed in the Sacramento Mountains. Older, Osagean and Kinderhookian rocks have not generally been recognized in the basin, although Kinderhookian strata were postulated to exist in a small area of eastern Chaves, southwestern Roosevelt, and northwestern Lea Counties, New Mexico, on the basis of lithologic similarity to the Caballero Formation in the Sacramento Mountains (Lloyd, 1949).

Ellison (1950) divided the Woodford Formation into three units using radioactivity, log response, and lithology. The lower unit was calcareous and cherty, and it had the lowest radioactivity; the middle unit had the most

resinous spores and the highest radioactivity; and the upper unit had few spores and intermediate radioactivity (Ellison, 1950). The middle unit was the most widespread, comprising the black shale lithology characteristic of the Woodford throughout the basin, and the lower unit was the most areally restricted. A correlation may exist between Ellison's lower Woodford unit and the Ives Breccia Member and between the middle Woodford unit and the Doublehorn Shale Member of the Houy Formation in Central Texas (Wright, 1979).

Formation Boundaries

The lower boundary of the Woodford and its stratigraphic equivalents represents a major regional unconformity that extends across the southern Midcontinent and records a major period of uplift and erosion that is at least partly Devonian (Galley, 1958; Amsden and others, 1967; Ham and Wilson, 1967; Ham, 1969). During this regressive episode, older Devonian and Silurian strata were removed over broad areas of the Midcontinent, and rocks below the unconformity became locally deeply eroded (Ham and Wilson, 1967; Ham, 1969; Amsden, 1975). In basinal regions, such as the Anadarko Basin, the unconformity marks the end of early Paleozoic shallow-water carbonate sedimentation and the beginning of deep-water carbonate and clastic deposition (Ham, 1969). The Woodford and correlative formations are diachronous and represent onlapping sediments (Freeman and Schumacher, 1969; Amsden and Klapper, 1972) deposited during worldwide Late Devonian marine transgression (Johnson and others, 1985). The coarse sandstone and breccia occurring locally above the unconformity are lag deposits derived from older formations (Cloud and others, 1957; Amsden and others, 1967; Amsden and Klapper, 1972; Amsden, 1975, 1980; Pittenger, 1981), and the black shale represents strongly reduced mud laid down on the anoxic floor of an epeiric sea (Ellison, 1950; Wright, 1979).

The upper boundary of the Woodford represents only a minor stratigraphic break (Ham and Wilson, 1967; Frezon and Jordan, 1979; Click, 1979; Mapel and others, 1979). It is disconformable at some localities (for example, the

Ozark Uplift and parts of the western outcrop belt and Oklahoma subsurface) and conformable at others (for example, Central Texas, the Arbuckle Mountains, and the Ouachita Fold Belt). The local occurrence and minor stratigraphic expression of unconformities indicate

Distribution

Distribution of the Woodford Formation in the Permian Basin is illustrated in plates 1 through 7. The area contoured in plates 1 and 2 was not extended to the western outcrop belt because of limited well control in Chaves, Eddy, Otero, and Lincoln Counties, New Mexico, and Culberson, Hudspeth, and El Paso Counties, Texas.

Relief on the present-day Woodford surface is more than 20,000 ft in the subsurface (pl. 1) and more than 25,000 ft if elevations in the western outcrop belt are included. Most of the relief in the basin developed as a result of deformation during the late Paleozoic Ouachita orogeny (Galley, 1958; Muehlberger, 1980), whereas relief in the outcrop belt and Diablo Platform was strongly influenced by later Laramide deformation (Muehlberger, 1980).

The Woodford Formation ranges in thickness from 0 to 661 ft (pl. 2) and is thickest in structural lows and thinnest or absent on structural highs. Thicknesses shown on plate 2 were not corrected for dip and do not everywhere represent true stratigraphic thicknesses. The Woodford is more nearly flat-lying in basin and shelf settings farthest from major faults (for example, on the Eastern Shelf and in most parts of the Midland Basin and Northwestern Shelf).

Northwestern Shelf and Matador Uplift

The Woodford Formation is present at most localities on the Northwestern Shelf but is absent on and north of the Matador Uplift (fig. 1a; pls. 1, 2, 7) (Ellison, 1950; Wright, 1979; Dutton and others, 1982; Ruppel, 1985). In northern Lea County, New Mexico, elevation of the Woodford increases northward, but the pattern is broken by several faults (pl. 1). These faults trend north-south or northwest-southeast, generally parallel

low-lying land masses in the latest Devonian or earliest Mississippian and an episode of minor epeirogenic uplift, slight sea-level fluctuations, and brief interruption of marine sedimentation (Stevenson, 1945; Ham and Wilson, 1967; Frezon and Jordan, 1979; Mapel and others, 1979).

to the Central Basin Platform and the axis of the Delaware Basin.

The Woodford thins northwestward across Eddy County, New Mexico, away from the Delaware Basin (pls. 2, 6), the gradual thinning coinciding with the increase in elevation (pl. 1). In eastern Chaves and northern Eddy Counties, New Mexico, thin and thick areas are irregularly distributed and are not clearly related to structure (pl. 2). In the northernmost part of the map, Woodford thickness appears to be structurally controlled because isopach contours are oriented east-west, parallel to the structural trend of the Matador Uplift (pl. 2).

Eastern Shelf

The Woodford Formation was previously thought not to extend onto the Eastern Shelf (Ellison, 1950; Wright, 1979), but in the present study no clearly defined eastern limit for the Woodford was found (pls. 1, 2). The formation is absent in northeastern Crockett County, in most of western Irion County, and in a large area that includes parts of Scurry, Borden, and Garza Counties. However, the formation is present across Sterling, Mitchell, and most of Scurry Counties.

The wide spacing of structural contours in the eastern part of the map (pl. 1) documents a gradual increase in elevation of the Woodford from the Midland Basin onto the Eastern Shelf. The Woodford also thins gradually in the same direction (pls. 2 through 5). On the Eastern Shelf, the Woodford is thin, and the distribution is somewhat irregular and patchy (note thicknesses in Scurry, Mitchell, and Sterling Counties, pl. 2). These structural and isopach trends are uninterrupted except in southern Irion and northern Crockett Counties, where large-scale faults cut the section.

Central Basin Platform and Pecos Arch

The Central Basin Platform and Pecos Arch are the diverging structural highs in the center of the map that meet in Crane and northeastern Pecos Counties (fig. 1a; pls. 1, 2). Faults bounding the Pecos Arch trend east-west, whereas those along the Central Basin Platform trend northwest-southeast. Some of the largest faults, those having throws of a few thousand feet, are normal or high-angle reverse faults, although some show evidence of strike-slip motion (Galley, 1958; Walper, 1977; Muehlberger, 1980; Hills, 1984).

The Woodford is absent from the Pecos Arch and from many of the faulted structures on the Central Basin Platform (Ellison, 1950; Galley, 1958) (pls. 1, 2, 7). Elevations of the Woodford or the unconformity representing the Woodford range from 980 ft below sea level in northern Pecos County to more than 7,000 ft below sea level in eastern Winkler County. The Woodford thins over the Central Basin Platform in most places, but in some areas, such as southern Ector and Winkler Counties, the thickness steadily increases westward (pl. 2).

Delaware Basin

The Woodford Formation reaches its maximum thickness of 661 ft in the Delaware Basin structural low in western Winkler County (pls. 1, 2). The Woodford is more than 600 ft thick in central and southwestern Winkler, southeastern Loving, and northern Ward Counties. The top of the deepest Woodford is more than 16,000 ft below sea level in eastern Loving County and more than 15,000 ft below sea level in east-central Reeves County (pl. 1). Several isolated thick areas whose distribution is fault controlled appear in Reeves County (pl. 2); in the north-central part of the county, thickness locally exceeds 500 ft, and in central and southeastern areas, 400 ft.

Midland Basin

The axis of the Midland Basin is approximately outlined by the closed -9,000-ft structural contours east of the Central Basin Platform in

Texas (pl. 1). The deepest Woodford is nearly 9,800 ft below sea level in northeastern Gaines County (pl. 1). Within the basin thickness trends are subtle (pl. 2); the Woodford at its thickest is 135 ft in north-central Martin County. Two thick areas are indicated by the closed 100-ft isopach contours in Dawson, Gaines, Andrews, and Martin Counties. Between the thick areas lies an east-west trend of relatively thin Woodford (50 to 100 ft). Another narrow thin trend (<50 ft) lies in southern Martin and southeastern Andrews Counties. These trends parallel structural and isopach trends along the Matador Uplift and Pecos Arch and are at a high angle to those along the Central Basin Platform immediately to the west.

Val Verde Basin

The Woodford is present in the Val Verde Basin of southern and southeastern Pecos, southern Crockett, northern Terrell, and northern Val Verde Counties (fig. 1a; pls. 1, 2, 7). In northern Brewster and southern Pecos Counties, the Woodford Formation, along with a carbonate sequence typical of the Paleozoic section of the craton, lies beneath allochthonous rocks of the Ouachita Fold Belt (pls. 1, 2, 6 [D-D', well 13]).

Two structural trends are present in the Val Verde Basin (pl. 1). In south-central Pecos County, faults and structural contours trend northwest-southeast, and elevation of the Woodford Formation increases from central Pecos County south westward and westward. In Terrell, southern Crockett, Val Verde, and eastern Pecos Counties, faults trend east-west, and elevation of the Woodford increases northward from the Ouachita Fold Belt to the Pecos Arch.

In central Pecos County, the Woodford was inferred to be more than 21,000 ft below sea level (pl. 1) on the basis of the elevation of the Ellenburger Formation (Ewing, 1991), and it was inferred to be more than 300 ft thick (pl. 2) on the basis of nearby thickness trends. In central Terrell County, the Woodford was inferred to be more than 20,000 ft below sea level, and even deeper burial is likely beneath the Ouachita overthrust (pl. 1). Thicknesses in this part of the basin locally exceed 400 ft and may be 300 ft or more in central Terrell County beneath the Ouachita allochthon (pl. 2).

Diablo Platform and Western Outcrop Belt

The Diablo Platform (fig. 1a, b) is a major structural boundary between the Permian Basin to the northeast and the Chihuahua Tectonic Belt to the southwest that has been strongly affected by Laramide deformation (Muehlberger, 1980). Most of the faults along the platform trend northwest-southeast and follow Proterozoic basement faults (Walper, 1977; Muehlberger, 1980).

Lithofacies

Two lithofacies were identified in the Woodford Formation—black shale and siltstone. Black shale is pyritic and has parallel laminae; siltstone, a hybrid rock composed of silt-sized quartz and dolomite grains, is medium to dark gray and has discontinuous and disturbed bedding. Distinguishing between lithologies can be difficult because differences in color may be slight, and many layers contain subequal mixtures of silt- and clay-sized grains. Contacts between lithofacies may be sharp, particularly at the base of the siltstones, or gradational; and lithologies are commonly interbedded and interlaminated.

Lithofacies were defined and described from cores because weathering had severely oxidized the pyrite and organic matter in outcrop. Outcrops are medium to light shades of gray or brown, whereas cores are black (black shale) or light to dark gray (siltstone). Textures were found to be comparable in outcrop and core, and the mineralogy of the silicate and carbonate fraction was similar. Hence, lithofacies analysis was possible at all localities.

Black Shale

Characteristic Features

Parallel laminae are the most characteristic feature of black shale (fig. 4a, b). Other distinguishing features include abundant pyrite, fine grain size, black color, and high radioactivity. The black color is caused by high concentrations of pyrite (as much as 13 vol %; app. C) and organic

The Woodford is absent in the southeastern part of the Diablo Platform, southwest of the map area (Wright, 1979), but it is present in the northeastern part (Rosado, 1970) (pls. 1,2). The highest observed subsurface elevation (128 ft below sea level) is in northwestern Culberson County (pl. 1). The highest overall elevation (>5,000 ft above sea level) is in the western outcrops. From the Delaware Basin, elevation of the Woodford gradually increases westward across Reeves and Culberson Counties toward the Diablo Platform (pl. 1), and the formation gradually thins in the same direction (pl. 2).

carbon (as much as 35 vol % [app. C] or 12 wt % TOC; app. D), and high radioactivity is caused by uranium bound in the organic matter (Swanson, 1960, 1961; Leventhal, 1981).

Bedding and Sedimentary Structures

Continuous parallel laminae predominate (fig. 4a), but other stratification types include discontinuous, wavy, and lenticular laminae and thin beds. Most laminae have no internal structure but can be distinguished by subtle differences in color that result from differences in composition (for example, unequal amounts of detrital quartz, clay, pyrite, dolomite, and organic matter and different numbers of spores and radiolarians). These laminae typically have a varvelike appearance in slabs and thin sections (fig. 4a). Thin graded siltstone-shale couplets were found in some intervals, mostly in shelf regions (app. B; C3, C4, C13). Most graded couplets have sharp bases, and some exhibit primary sedimentary structures such as fading ripple forms.

Burrows are scarce but commonly cause disrupted or distorted layers (fig. 4a through c). Most burrows are confined to, or start in, siltstone laminae (fig. 4a, b), but a few were found exclusively in shale (fig. 4c). Flattened horizontal burrows were the most common type observed, and vertical burrows (fig. 4b, c) were found only locally. Burrows are filled by silt, secondary silica, carbonate, and pyrite in varying proportions, and some contain scattered remnants of anhydrite (fig. 4d).

Syneresis cracks (fig. 4e) were found locally on the Central Basin Platform in organic-rich, pyritic black shale. They are short, wide vertical fractures, linear in plan view and wedge shaped in cross section. Syneresis cracks are found in the middle of the black shale section and not at lithologic or formation contacts (app. B; C2). They are highly compacted and thus are inferred to be syndepositional or very early diagenetic. The cracks are filled mostly by secondary silica (including quartz, chert, and chalcedony) and locally contain carbonate, along with patchy remnants of anhydrite. Filling must have occurred shortly after the cracks formed because cementing phases are deformed, and the surrounding black shale is differentially compacted (fig. 4e). Subaerial exposure is not indicated because pyrite and organic matter in the host shale are unoxidized.

Texture

Black shale consists of more than 50 percent clay-sized material and less than 50 percent silt-sized particles (fig. 4a through c). Silt-sized grains may be randomly scattered (fig. 4c) or concentrated in laminae (fig. 4a, b). Lighter colored laminae will typically contain greater proportions of silt-sized particles than will the darker laminae.

Median grain sizes of the silt fraction are between 0.01 and 0.05 mm. Sand-sized grains are rare. A few large (as much as 5 cm long) greenish shale clasts exhibiting parallel laminae (fig. 4f) were found locally on the Central Basin Platform.

Composition

Clay-sized material consists of organic matter and illite, and the silt-sized fraction consists of mostly dolomite, quartz, pyrite, mica, feldspar, glauconite, biogenic pellets, spores, and radiolarians. Other types of fossils, including conodonts, brachiopods, trilobites, sponge spicules, and vertebrate debris, were found locally, but only rarely.

Organic carbon content in core samples ranges from 1.4 to 11.6 weight percent TOC (mean = 4.5 ± 2.6 wt % TOC for 72 samples), or from roughly 4 to 35 volume percent organic matter. Outcrops contain much less organic carbon than do the cores (<0.1 to 2.3 wt % TOC; mean =

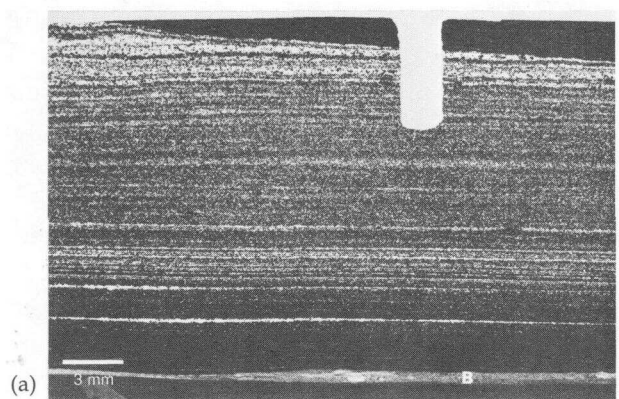
0.8 ± 0.6 wt % TOC for 25 samples) primarily because of oxidation during weathering. Average TOC concentration in each core ranges from 2.2 to 9.0 weight percent and in each outcrop from 0.1 to 1.1 weight percent (app. D).

Organic matter most commonly appears as fine-grained, disseminated, amorphous material (app. D), an oil-generating type. Woody particles were rare in thin sections and in separated kerogens. Large plant fragments appeared on a few bedding surfaces in cores from the Northwestern and Eastern Shelves. Recycled vitrinite occurs only in black shale from the Central Basin Platform, Eastern Shelf, and southern Midland Basin (app. D). The mean reflectance values of primary vitrinite in cores and outcrops range from 0.54 to 1.92 percent R (app. D) and represent hydrocarbon generation stages between early oil generation and late wet-gas generation (Hunt, 1979).

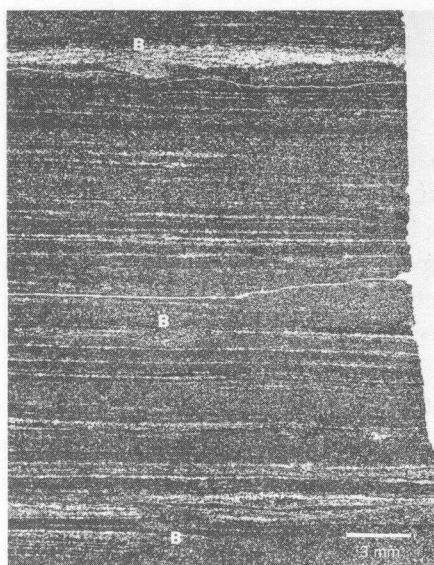
Illite is abundant in the black shale. Volume percentages range between 34 and 79 percent and average 59 ± 3 percent (app. C). The coarse clay mineral fraction (1 to $2 \mu\text{m}$) is detrital illite, whereas the fine clay mineral fraction ($<0.2 \mu\text{m}$) is diagenetic illite (Morton, 1985).

Dolomite and quartz are the most common silt-sized components. They occur randomly mixed in subequal proportions, and they have the same grain-size distribution. Dolomite grains in shale have no overgrowths—most are subhedral to anhedral and appear to be abraded (fig. 4g). Euhedral dolomite grains are abundant only locally in cores from the Central Basin Platform, Midland Basin, and Northwestern Shelf. Scattered silt- to sand-sized poikilotopic dolomite patches cement clay- or fine silt-sized particles in some samples.

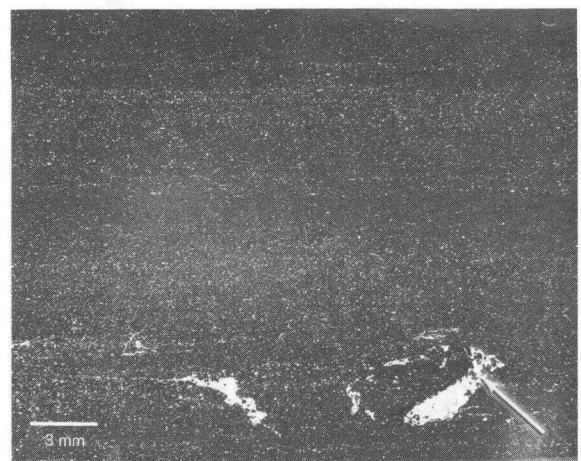
Pyrite is ubiquitous in cores and can be found in a variety of forms: (1) large (as much as 8 cm) nodules (some possessing cone-in-cone fabric), (2) irregular elongate patches, (3) thin streaks, (4) smooth elliptical masses having stromatolite-like or oncolitelike fabric, (5) scattered fine grains, (6) framboids, (7) aggregates (silt sized or finer), (8) fillings or replacements of minute organisms (for example, spores and radiolarians), (9) cement or replacement in burrows, and rarely, (10) fracture fillings. Weathering has altered pyrite in outcrop to various oxides and sulfates. Locally, gypsum lines joints and bed-



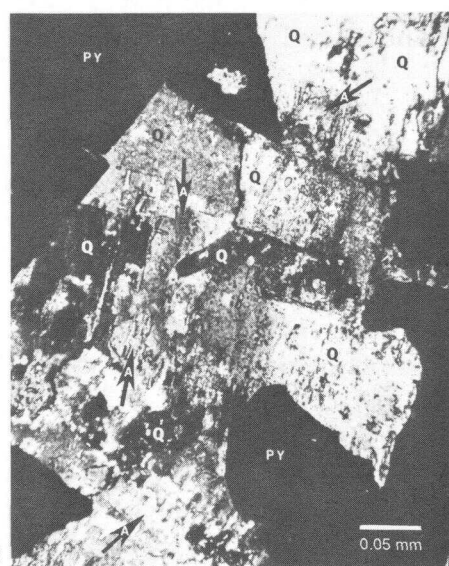
(a)



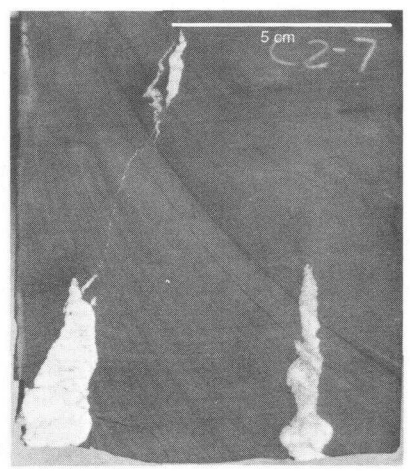
(b)



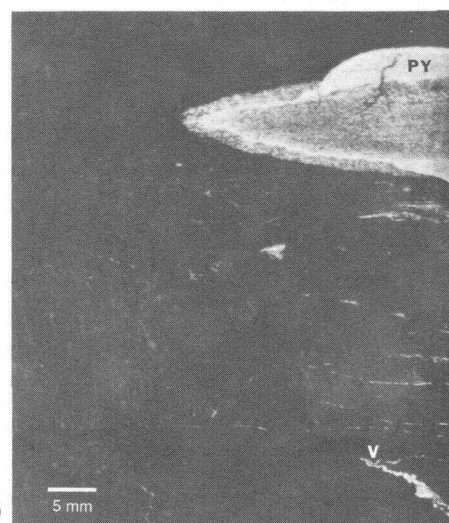
(c)



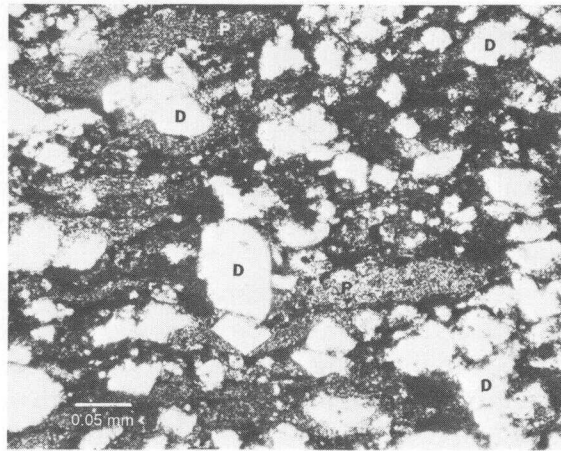
(d)



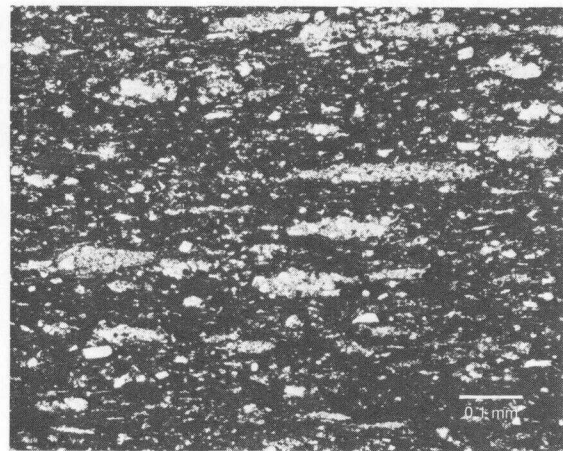
(e)



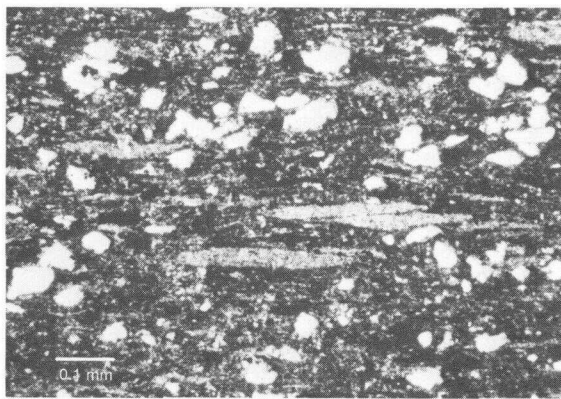
(f)



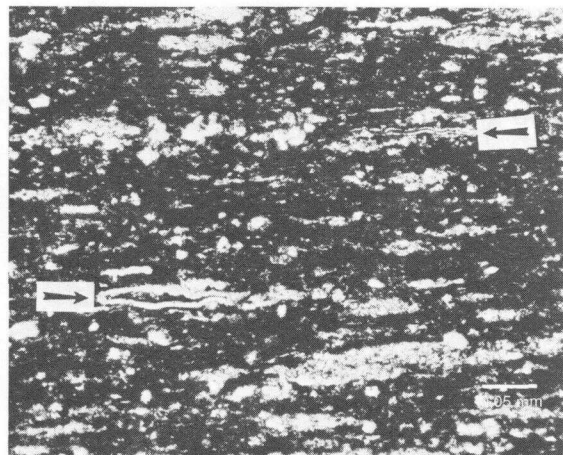
(g)



(h)



(i)



(j)

FIGURE 4. Photos of Woodford black shale. (a) Black shale exhibiting continuous parallel laminae at 11,555 ft in the No. 1918 Parks (app. B; C1, sample C1-10). Note cyclic change from black shale at base, siltstone laminae increasing upward, and abrupt return to black shale at top. Silty lamina at base, B, is burrowed. TOC = 4.2 wt %. (b) Disrupted parallel siltstone laminae in black shale at 10,914 ft in the No. 1 Champeau Federal (app. B; C4, sample C4-4). Disrupted areas, B, are burrows. TOC = 5.0 wt %; R_o = 1.03%. (c) Black shale exhibiting parallel laminae, scattered silt, and burrows at 12,228 ft in the No. 5 Pacific Royalty (app. B; C9, sample C9-2). TOC = 3.2 wt %. (d) Enlarged view of burrow in photo (c) (see arrow in photo [c]). Burrows are filled mostly by quartz, Q; pyrite, PY; and patchy remnants of anhydrite, arrows marked A. Rectangular habit indicates quartz is pseudomorph after anhydrite. Crossed nicols. (e) Syneresis cracks filled mostly by silica and carbonate and locally containing anhydrite at 7,179 ft in No. 43 Yarborough & Alien (app. B; C2, sample C2-7). Note differential compaction of black shale laminae and compactional deformation of syneresis structures. TOC = 8.5 wt % in host shale. (f) Shale clast in black shale at 7,177 ft in No. 43 Yarborough & Alien (app. B; C2, sample C2-6). Clast has parallel laminae, and the outer edge was pyritized, PY. Oblique calcite veins and pygmaic veinlets, V, reflect shearing. TOC = 11.2 wt % in host shale. (g) Silty shale at 7,172 ft (app. B; C2, sample C2-3). Silt is exclusively dolomite, D, and most grains are angular, broken, or abraded. Pellets, P, are elongate fine-grained aggregates and probably biogenic. Plane-polarized light. TOC = 8.5 wt %. (h) Pellets containing silt particles at 7,404 ft in the No. 1 Sealy Smith (app. B; C12, sample C12-4). Plane-polarized light. Dolomite/quartz ratio = 1.3/1.0; TOC = 10.2 wt %; R_o = 0.55%. (i) Pellets composed mostly of clay at 11,639 ft in the No. 1 Walker (app. B; C5, sample C5-2). Silt grains are dolomite and quartz. Plane-polarized light. Dolomite/quartz ratio = 1.3/1.0; TOC = 2.8 wt %. (j) Pellets and flattened spores at arrows from same thin section as those in photo (h). Spores are *Tasmanites*. Plane-polarized light.

ding planes, and iron oxide appears as pyrite pseudomorphs, indicating that these rocks were highly pyritic before weathering. Elsewhere, disseminated ferric oxides record the former abundance of pyrite in the Percha and Sly Gap Formations.

Muscovite flakes appear in all samples. Mica flakes and illite typically are well oriented parallel to bedding. In biogenic pellets, however, illite may comprise domains of differing orientations. Locally some mica flakes lie at high angles to bedding, a few flakes being oriented 90 degrees to bedding. Such flakes appear to be part of larger clumps of organic-bound sediment.

Feldspar (microcline) and glauconite are rare in black shale. Feldspar appears mostly in samples from the Northwestern Shelf, Central Basin Platform, and western Midland Basin (app. C; C1, C2, C4, C13). Glauconite occurs as an isolated grain or two in many thin sections.

Biogenic pellets are common (as much as 11%; app. C) in many black shale samples. They appear as flattened silt sized to fine sand sized aggregates and impart a microlenticular fabric to the rock when viewed in thin section (fig. 4h through j). Pellets are easily distinguished from burrows in plan view because pellets exhibit no trail-like patterns on bedding surfaces or in cross section because pellets show no cross-cutting contacts or internal stratification. Most pellets consist of illite, but some consist of silt-sized grains of quartz and dolomite (fig. 4h). Silty pellets commonly are cemented by carbonate and are flattened slightly less than clay pellets.

Spores are minor components in black shale, but they are widely distributed. Generally spores are flattened as a result of compaction (fig. 4j). However, in some intervals spores have been replaced by pyrite or infilled by pyrite, chert, or carbonate. Locally, early infilling is indicated by spores that are uncompacted or only slightly flattened.

Radiolarians also are a minor but widely distributed component. They are composed mostly of chert or chalcedony, but some have been partly or completely replaced by pyrite or carbonate. Spores and radiolarians may be randomly scattered throughout a laminated sequence or concentrated in laminae or thin beds. Radiolarian chert layers were observed locally

on the Central Basin Platform and in the southern Midland Basin (app. B; C2, C6).

Trilobite fragments are sparsely scattered in some intervals and locally occur alongside pellets. Most are carbonate, but a few have been partly replaced by chert. Trilobite fragments locally are common at the top of the formation along the unconformity with the Mississippian limestone (app. B; C10).

Brachiopods are scarce in the Woodford. Inarticulate brachiopods (*Lingula*) were recognized on bedding surfaces in cores from the Central Basin Platform and the Northwestern Shelf (app. B; C2, C4, C9). One silicified articulate brachiopod was found in black shale on the Central Basin Platform (app. B; C2). Elsewhere, articulate brachiopods are abundant only locally at the top of the formation (app. B; C10).

Phosphatic fossil debris is a minor component in black shale. Conodonts are scarce but widely distributed, and bone and teeth fragments and fish scales also are rare. Phosphatic debris sometimes is concentrated in the siltier shales and in interstratified siltstones.

Sponge spicules were found only locally in one core from the Central Basin Platform where monaxons were scattered parallel to stratification (app. B; C2). All of the spicules had altered to chert.

Secondary silica is the major constituent in some layers and sedimentary structures. Secondary silica in the form of chert, chalcedony, and megaquartz fills or replaces fossils and cements or replaces burrows and syneresis cracks (fig. 4c through e). Megaquartz that has pseudomorphic rectangular cleavage after anhydrite was found locally associated with anhydrite (fig. 4d). Also, some of the chalcedony in burrows and syneresis cracks is length-slow, suggesting that it replaced evaporites (Folk and Pittman, 1971).

Siltstone

Characteristic Features

Siltstone in the Woodford Formation is a hybrid siliciclastic-carbonate rock in which dolomite and quartz are the dominant silt-sized framework grains. Compared with black shale, siltstone has coarser grain size, lighter color,

more disrupted or discontinuous strata, and lower radioactivity. Siltstone, unlike the carbonate lithologies of bounding formations, has a more uniform silt-sized texture, abundant quartz grains, no chert, no large body fossils, and higher radioactivity.

Bedding and Sedimentary Structures

Stratification ranges from thin laminae to thin beds. Continuous, discontinuous, and wavy parallel laminae commonly are preserved, but stratification typically is disrupted by burrowing (fig. 5a, b) or, more rarely, contorted by soft-sediment deformation (fig. 5b, c).

Interbedded and interlaminated dark-gray to black shale, fine-grained dolomite grainstone, fine-grained lime grainstone, and lime mudstone locally are common (app. B; C9, C11). The interbedded shales and mudstones typically exhibit continuous, discontinuous, or wavy parallel laminae, and the grainstones, discontinuous and disturbed layers.

Most siltstones and grainstones have sharp lower contacts (fig. 5d through f), and many form graded couplets with shale (fig. 5e, f). Others have gradational upper and lower contacts (fig. 5g). Cores containing well-developed siltstone lithofacies commonly consist of vertically stacked couplets in which siltstone beds as thick as 10 to 15 cm grade upward into shale layers as thick as 5 cm (fig. 5a, b, e). Primary sedimentary structures include normal grading (fig. 5a, b, e, f), fading ripple forms (fig. 5e), climbing ripple cross-stratification (fig. 5d), horizontal stratification, soft-sediment deformation (fig. 5b), and flow-sheared laminae (fig. 5c). The vertical succession of structures typically comprises a partial or complete Bouma sequence (fig. 5e). Siltstone sequences such as these constitute a basal facies of the Woodford in the Northwestern Shelf and northern Midland Basin (app. B; C5, C9, C11).

Texture

Median grain sizes of siltstone are between 0.01 and 0.05 mm. Typically, little or no sand-sized material is present, although sand grains as large as the medium-sized grade were encountered locally. Clay-sized material ranges from 0 to almost 50 percent by volume. Silt-

stone is moderately to poorly sorted and rarely well sorted.

Composition

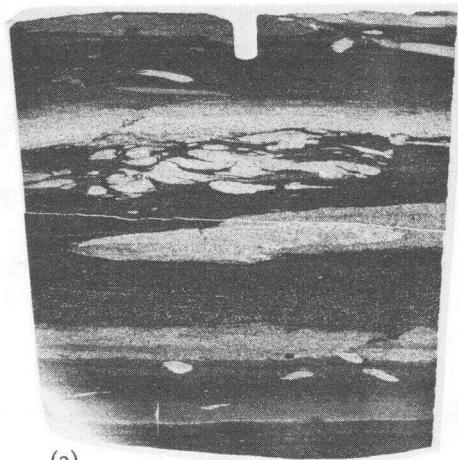
Quartz and dolomite are the most abundant framework grains in siltstone, and they typically have the same grain-size distribution (fig. 5h). They are commonly present in subequal proportions and are mixed with a variety of other components so that neither constitutes more than 50 percent of the rock. Dolomite is mostly subhedral or anhedral, and such grains commonly have an abraded appearance (fig. 5h). Euhedral grains were found locally, but many have anhedral or subhedral cores rimmed by euhedral overgrowths. In most siltstones, dolomite forms an interlocking mosaic with quartz, yet dolomite is rarely poikilotopic, even in dolomite grainstones. Locally, poikilotopic patches of dolomite cement a few angular silt-sized grains.

Other silt-sized constituents are pyrite, mica, feldspar, glauconite, phosphatic debris, and rare zircon and tourmaline. Pyrite is common and appears as nodules, euhedral crystals, irregular grains, aggregates, and framboids. In some beds, pyrite has subhedral and anhedral shapes similar to those of quartz and dolomite (fig. 5f, h) and may be reworked.

Mica (muscovite) was observed in all quartz-dominated siltstones and most dolomite-dominated siltstones; however, it is rare in carbonate mudstones and grainstones. Feldspar (microcline) is a minor component mostly in quartz-dominated siltstone. Both mica and feldspar are more abundant in the Northwestern Shelf and northern Midland Basin (app. B and C; C5, C11) where they occur along with minor amounts of the ultrastable silicates zircon and tourmaline.

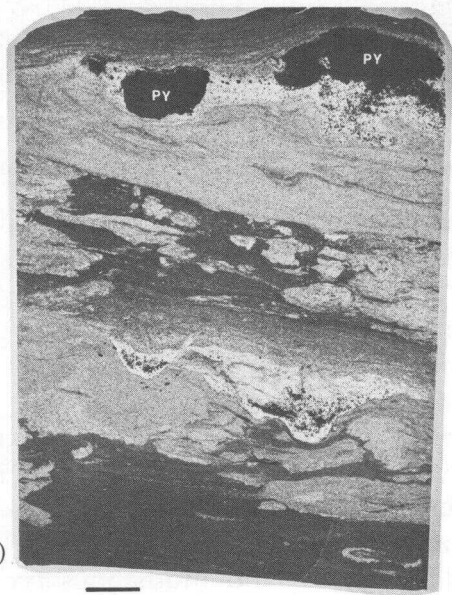
One or two grains of glauconite were seen in many samples, but glauconite is concentrated only locally at the top of the formation (app. B; C10, C13). Many core samples contained minor amounts of phosphatic debris, mostly conodonts and fish debris.

Illite and organic matter compose the fine fraction of siltstones, and in some samples the clay constitutes almost 50 percent of the rock. Illite is abundant in wispy laminae, in the upper part of graded layers, and in gradational shaly



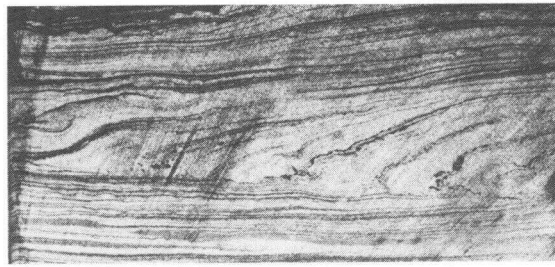
(a)

5 mm



(b)

5 mm



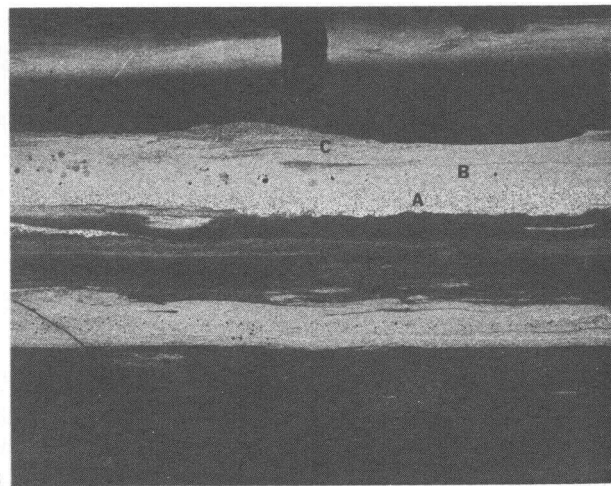
(c)

1 cm



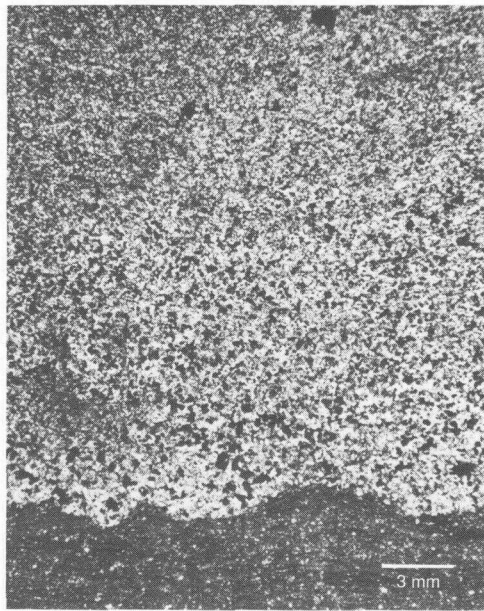
(d)

3 mm

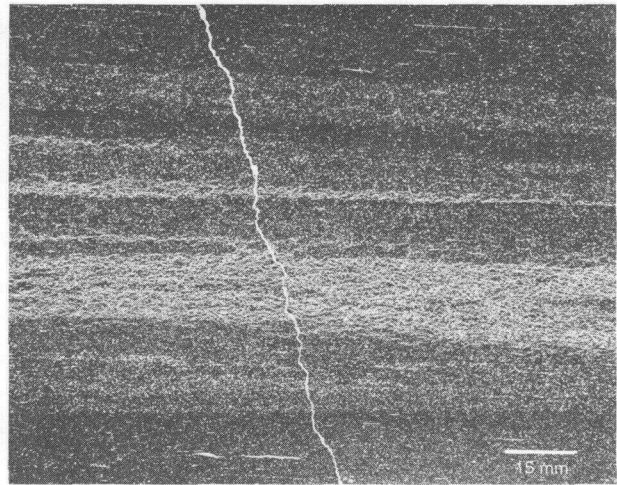


(e)

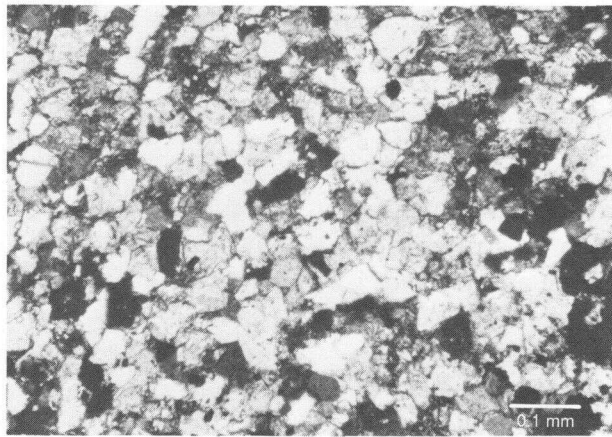
3 mm



(f)



(g)



(h)

FIGURE 5. Photos of Woodford siltstone. (a) Burrowed quartz-dominated siltstones and interlaminated shale in No. 1 Walker at 11,681 ft (app. B; C5, sample C5-12). Mean TOC of interlaminated interval = 0.2 wt %. (b) Quartz-dominated siltstone in No. 1 Williamson at 13,064 ft (app. B; C11, sample C11-10). Note soft-sediment deformation fabric just below pyrite, PY, nodules. Mean TOC of interlaminated interval = 0.7 wt %. (c) Core chip showing fine-grained dolomite grainstone in No. 1 Federal Elliott at 14,638 ft (app. B; C13, sample C13-6). Contorted laminae record flow shear during rapid deposition in a bottom flow. Dolomite/quartz ratio = 40/1. (d) Very thin dolomite-dominated siltstone bed in No. 1 A. E. State at 13,771 ft (app. B; C3, sample C3-6). Bed contains small-scale climbing ripple cross-laminae and grades into silty shale at top. Dark patches, PY, are pyrite. TOC in underlying shale bed = 2.3 wt %. (e) Dolomite-dominated siltstone laminae in No. 1 A. E. State at 13,768 ft (app. B; C3, sample C3-5). Middle lamina shows Bouma sequence that has graded, A; flat, B; and rippled, C, intervals. Ripple crests are spaced roughly 1.5 cm apart. Mean TOC in shale laminae = 1.6 wt %. (f) Enlarged view of graded interval, A, in photo (e). Silt is a subequal mixture of dolomite, quartz, and pyrite. (g) Dolomite-dominated siltstone laminae in No. 43 Yarborough and Alien at 7,172 ft (app. B; C2, sample C2-3) having indistinct contacts and lacking internal structure. (h) Magnified view of quartz-dominated siltstone shown in photo (b). White and dark-gray grains are quartz, pale-gray grains are dolomite, black grains are pyrite. Note angular and abraded appearance of some dolomite grains. Dolomite/quartz ratio = 0.95/1.0. Crossed nicols.

intervals between black shale and siltstone (fig. 5a, b, d through g).

Organic matter is not abundant, and siltstone cores and outcrops average less than 1 weight percent TOC (app. D). In individual samples TOC concentrations range between 0.1 and 1.1 weight percent (mean = 0.5 ± 0.3 wt % TOC for 20 samples), which roughly corresponds to 0.3 to 3 percent organic matter by volume. The types of organic matter include amorphous particulate material, spores, and wood, but amorphous organic matter greatly predominates in all samples. Spores are rare, and only a few wood fragments were found on bedding planes. Siltstones contain only small amounts of primary vitrinite and no recycled vitrinite (app. D), suggesting that terrigenous source areas had minimal plant cover and few carbonaceous rock exposures. Reflectance values range from 0.8 percent to 1.3 percent and are directly related to present-day burial depth (app. D).

Formation-Boundary Lithologies

Lower Contact

In the Permian Basin, contact between Silurian-Devonian carbonate rocks and the overlying Woodford Formation was preserved in two cores, the No. 1 A. E. State and the No. 1 Walker (app. B; C3, C5). In the No. 1 Walker core, the Woodford disconformably overlies Silurian-Devonian limestone that consists of mottled fine-grained grainstones and brachiopod grainstones (fig. 6a, b) that contain scattered chert lenses and nodules. The upper surface of the limestone is irregular, and locally it is bored. The basal Woodford layer is conglomeratic chert arenite that contains glauconite and phosphatic debris (fig. 6a, b) and is texturally and compositionally similar to the basal chert breccia in the Arbuckle Mountains described by Amsden (1975, 1980). Phosphatic debris includes conodonts, assorted fragments (bone, teeth, fish scales, *Lingula*), aggregates (fecal material), and ooids that exhibit both radial-fibrous and concentric fabric. Basal Woodford chert arenite is unsorted and has no current-induced primary sedimentary structures; thus it appears to be a residual lag produced by dissolution of the underlying cherty limestone. The fossils, glau-

conite, and phosphatic ooids indicate open-marine conditions and slow sedimentation.

In the No. 1 A. E. State core (from Lea County, New Mexico) brecciated, cavernous limestone is overlain disconformably by black shale. The uppermost 1 ft of limestone contains black shale clasts, and the basal Woodford contains scattered angular fragments of black shale and limestone (app. B; C3). The transition from limestone to black shale is abrupt; however, the contact is irregular and penetrative, and infiltration of mud tens of feet downward into the underlying limestone has occurred. Some of the solution cavities and fissures in the limestone are partly or completely filled by black shale that either has no structure or contains deformed, contorted laminae indicative of soft-sediment deformation (fig. 6c). The shale-filled cavities and fissures at Lea County, New Mexico, are similar to those in Andrews and Terry Counties, Texas, described by Peirce (1962).

Upper Contact

Contact between the Woodford and the overlying Mississippian limestone was preserved in two cores, the No. 1 Brennand and Price and the No. 1 Federal Elliott (app. B; C10, C13). In the No. 1 Brennand and Price, the uppermost Woodford contains articulate brachiopods, trilobite fragments, black shale clasts, dolomite grains, glauconite, and phosphatic debris (fig. 6d). The overlying Mississippian limestones are mostly laminated fine-grained grainstones along with some lime mudstones, sparsely fossiliferous grainstones, wackestones, and packstones. Locally these carbonate lithologies compose thin, graded beds. Chert beds, lenses, and nodules, locally spiculitic, are scattered throughout the Mississippian limestone section. Contact between the black shale and the overlying carbonate rocks is sharp and disconformable (fig. 6d), marking an abrupt change in lithology and fauna.

In the No. 1 Federal Elliott, Mississippian limestone rests conformably on the Woodford. Woodford black shale grades upward through 10 ft of interbedded dark-gray lime mudstone, black siltstone, and black glauconitic sandstone into medium to dark-gray fine-grained Mississippian grainstones and lime mudstones (app. B;

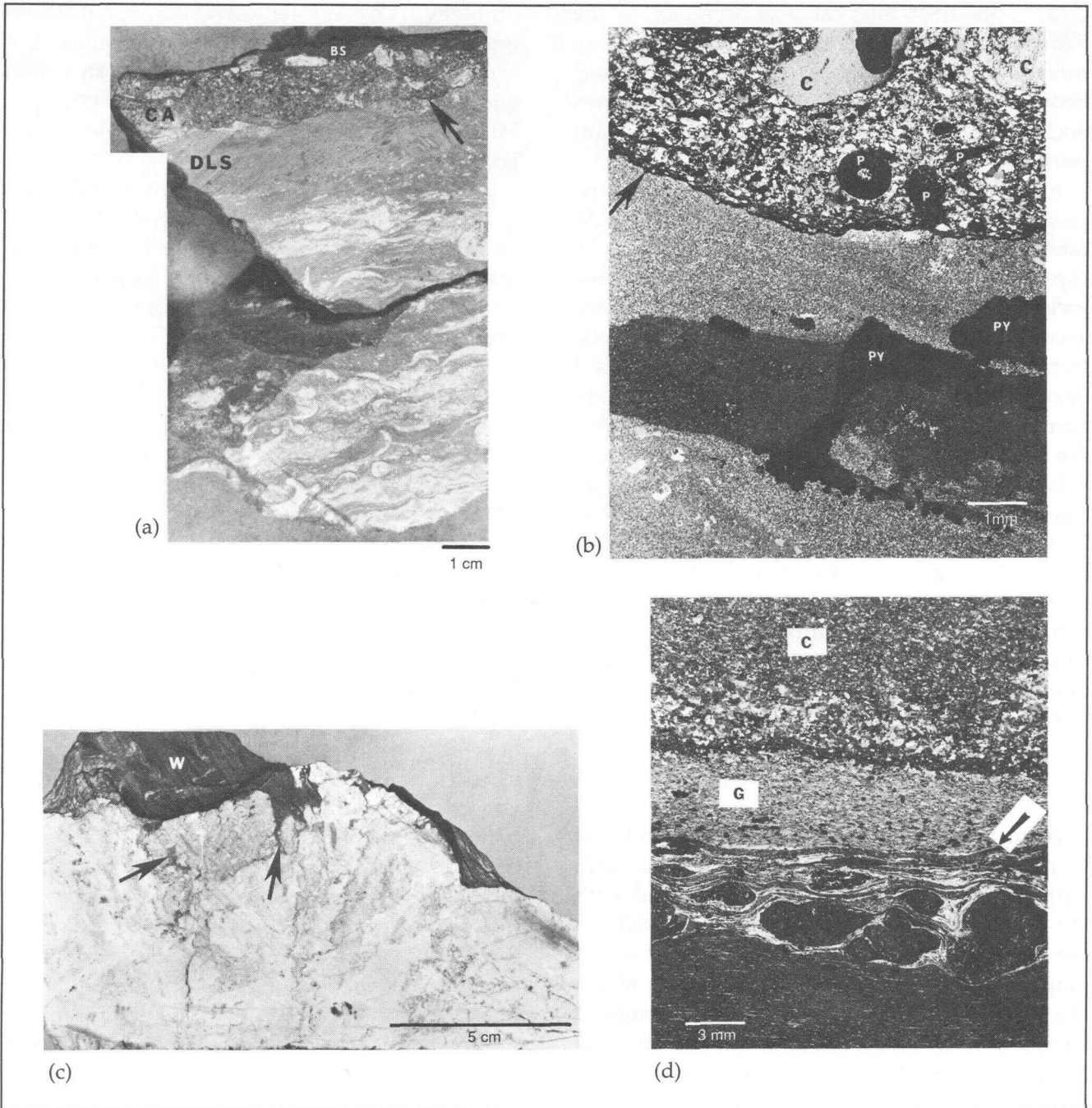


FIGURE 6. Photos of Woodford contacts, (a) Core slab showing lower contact, arrow, in No. 1 Walker at 11,689 ft (app. B; C5, sample C5-14). Silurian-Devonian limestone, DLS, overlain by basal Woodford chert arenite, CA, and black shale, BS, at top of core, (b) Thin-section photomicrograph of area at arrow in (a). Chert, C; pyrite, PY; phosphate, P. Three phosphatic grains from left to right are ooid containing a chert nucleus, aggregate of probable fecal origin, and skeletal fragment. Finer grains are chert (light) and phosphate (black). Below contact is fine-grained grainstone. Crossed nicols. (c) Core chip from 13,850 ft in No. 1 A. E. State (app. B; C3). Woodford black shale, W, in solution cavities in Silurian-Devonian limestone. Contorted laminae in shale and shale penetrating limestone crevices at arrows indicate soft-sediment infiltration of mud into the underlying limestone, (d) Thin-section photomicrograph of Woodford-Mississippian contact, arrow, at 8,459 ft in No. 1 Brennand and Price (app. B; C10, sample C10-1). Upper Woodford consists of brachiopod shells and trilobite carapaces (white ribbonlike material), black shale clasts, and silt-sized grains (white specks) that are mostly dolomite. Fine white streaks in black shale at base are brachiopod and trilobite fragments. Mississippian above contact is fine-grained grainstone, G, and chert bed containing scattered, unreplaced remnants of carbonate, C. Crossed nicols.

C13). This 10-ft interval was assigned to the Woodford Formation because it is markedly more radioactive than the overlying rocks and because it contains diagnostic Woodford features such as varvelike parallel laminae and abundant pyrite.

High concentrations of glauconite and phosphate in sedimentary rocks indicate low sedimentation rates (Odin and Letolle, 1980). The top stratum of the Woodford at these two localities is consequently inferred to have accumulated more slowly than the rest of the formation. Commonly, glauconitic grains and phosphatic ooids and pellets are unbroken, current-induced primary sedimentary structures are absent, and brachiopods possess articulated valves, indicating little or no active sediment transport at the close of Woodford deposition. The abundance of reduced iron, sulfur, and carbon and the absence of oxidized phases document absence of oxidation and imply absence of subaerial exposure. The upper boundary at these two localities thus suggests a submarine hiatus during which sedimentation slowed or ceased but the sea floor did not emerge.

Lithofacies Correlation

Basal siltstone in Woodford cores from the Northwestern Shelf and northern Midland Basin (app. B; C5, C9, C11) is herein correlated with the lower Woodford unit of Ellison (1950) on the basis of lithology, radioactivity, and stratigraphic position (fig. 7). Basal siltstone, which is a hybrid of silt-sized quartz and dolomite, is comparable to Ellison's lower unit in its high carbonate content and low radioactivity. Unfortunately, Ellison's cores were discarded, and direct comparison of lithologies was impossible. In the subsurface, both the lower unit and the basal siltstone immediately overlie the regional unconformity.

Stratigraphic position and lithology also suggest correlation of basal Woodford siltstone with the upper Middle to lower Upper Devonian Onate Formation in southeastern New Mexico. Both units rest on the regional unconformity surface and comprise a stratigraphic succession of interbedded siltstone, carbonate, and shale in which dolomitic siltstone is the dominant

lithology. The proposed correlation is consistent with that by Wright (1979), who suggested a correlation of the lower unit of Ellison (1950) with the Ives Breccia Member of the upper Middle Devonian to Lower Mississippian Houy Formation in Central Texas.

Basal siltstone also occupies the same stratigraphic position above the regional unconformity as the Canutillo Formation in West Texas and the Misener and Sylamore Sandstones in Oklahoma and Arkansas. These formally named units are mostly late Middle to early Late Devonian in age and are locally as young as Early Mississippian. Although the units are diachronous across the southern Midcontinent (Amsden and others, 1967; Freeman and Schumacher, 1969; Rosado, 1970; Amsden and Klapper, 1972; Amsden, 1975), they are at least partly correlative.

The black shale lithofacies is correlated with the middle and upper Woodford units of Ellison (1950) also on the basis of lithology, radioactivity, and stratigraphic position (fig. 7). Ellison's middle and upper units are not described as separate lithofacies in this report because striking lithologic differences between them are absent in cores (app. B; C1, C6). Although both units are pyritic black shale exhibiting parallel laminae, the middle unit is more radioactive (Ellison, 1950); hence, the middle and upper units can be mapped using gamma-ray logs (fig. 7; pls. 3 through 7). Wright (1979) correlated the middle unit with the Doublehorn Shale Member and the upper unit with the unnamed phosphatic member of the Houy Formation in Central Texas, thereby implying that the upper unit is partly Kinderhookian. Wright's correlation seems reasonable because the middle unit in both formations has higher radioactivity and more spores than does the upper unit (Ellison, 1950; Cloud and others, 1957).

Well log correlations (pls. 3 through 7) show that complete Woodford intervals containing all three units of Ellison (1950) are common only in the Midland, Delaware, and Val Verde Basins (pl. 3, A-A', wells 4, 9; pl. 4, B-B', well 5; pl. 5, C-C', wells 2 through 6, 9, 10; pl. 6, D-D', wells 9 through 12; pls. 7, E-E', wells 10, 11, 16, 17). Elsewhere Woodford sections are incomplete mostly because of the absence of the lower or

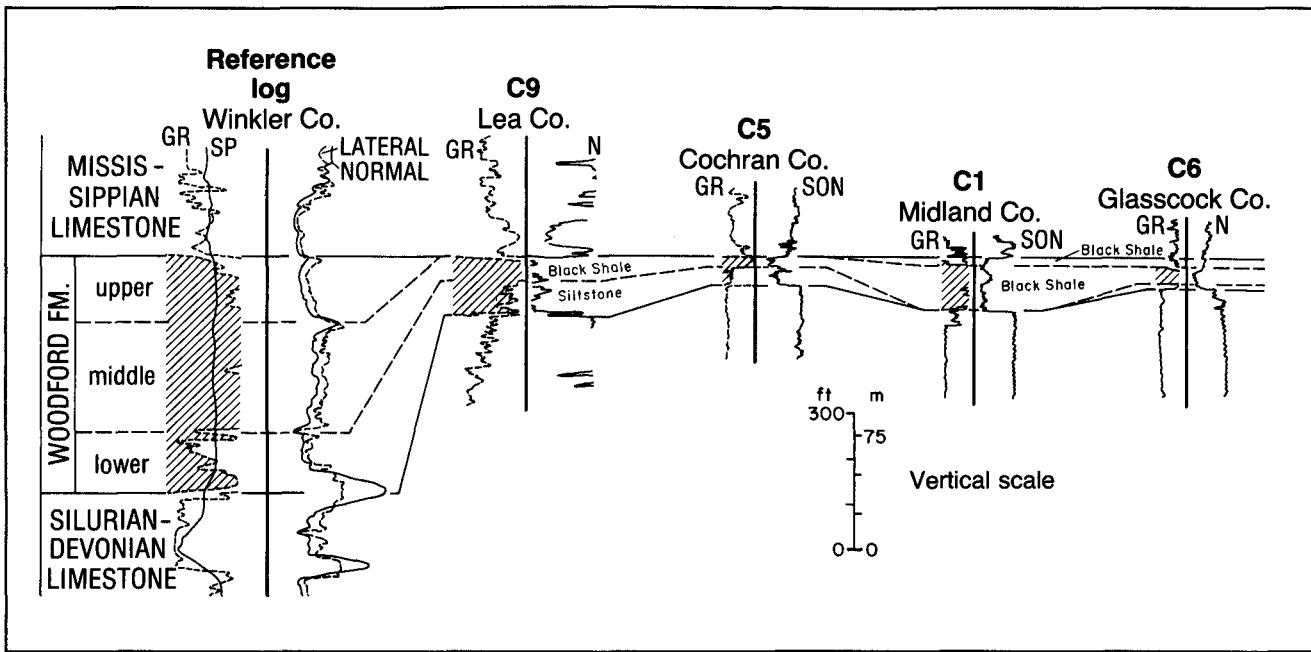


FIGURE 7. Log correlation of Woodford lithofacies. Reference log from Ellison (1950). Datum is top of Woodford. For detailed core descriptions see appendix B (C1, C5, C6, C9).

upper units. The lower unit gradually pinches out and is overstepped by the middle unit along the basin flanks (pls. 3 through 7), indicating depositional onlap. Lines of section showing onlap include (1) from the Midland Basin toward the Eastern Shelf (pl. 3, A-A', wells 9 through 13; pl. 4, B-B', wells 11 through 15; pl. 5, C-C', wells 9 through 12), (2) from the Midland Basin onto the Pecos Arch (pl. 7, E-E', wells 11 through 14), (3) westward from the Delaware Basin toward the Diablo Platform (pl. 4, B-B', wells 1 through 3; pl. 5, C-C', wells 1, 2), and (4) in the western Midland Basin (pl. 4, B-B', well 10). Many sections in which the upper unit is absent are overlain by Mississippian limestone, indicating nondeposition or erosional truncation that occurred after Woodford deposition but before Mississippian limestone deposition. Sections showing truncation include (1) along the eastern margin of the Central Basin Platform (pl. 3, A-A', well 8; pl. 4, B-B', well 9), (2) in the northern and central Midland Basin (pl. 7, E-E', wells 7, 8, 11), and (3) on the Northwestern Shelf (app. B; C5, C9). Most of the lines of section that show onlap also show evidence of increased truncation of the Woodford in the direction of onlap, suggesting that these were the last flooded and first exposed areas during the Late Devonian

transgression and latest Devonian regression. The patterns of onlap and truncation (pls. 3 through 7) indicate that all of the structural provinces shown in figure 1a had topographic expression in the Late Devonian. Onlap in the western Midland Basin supports the observation of Galley (1958) that a middle Paleozoic precursor of the Central Basin Platform lay slightly to the east of the present-day structure.

Lithofacies Distribution

Correlations shown in the cross sections (pls. 3 through 7) and the Woodford lithofacies distribution shown in a fence diagram (fig. 8) reveal that black shale is nearly ubiquitous and the most widely distributed lithofacies. Siltstone is more common in the northern part of the study area and in basinal depocenters. Silt-sized quartz is more abundant in northern and eastern areas, and silt-sized dolomite is more abundant in the far western outcrop belt and along the Central Basin Platform. Log correlations indicate that basal siltstone is areally restricted to deep parts of the Delaware, Midland, and Val Verde Basins, proximal areas on the Northwestern Shelf, and a few localities on the Central Basin Platform (pl. 3, A-A', wells 3 through 10; pl. 4, B-B', wells

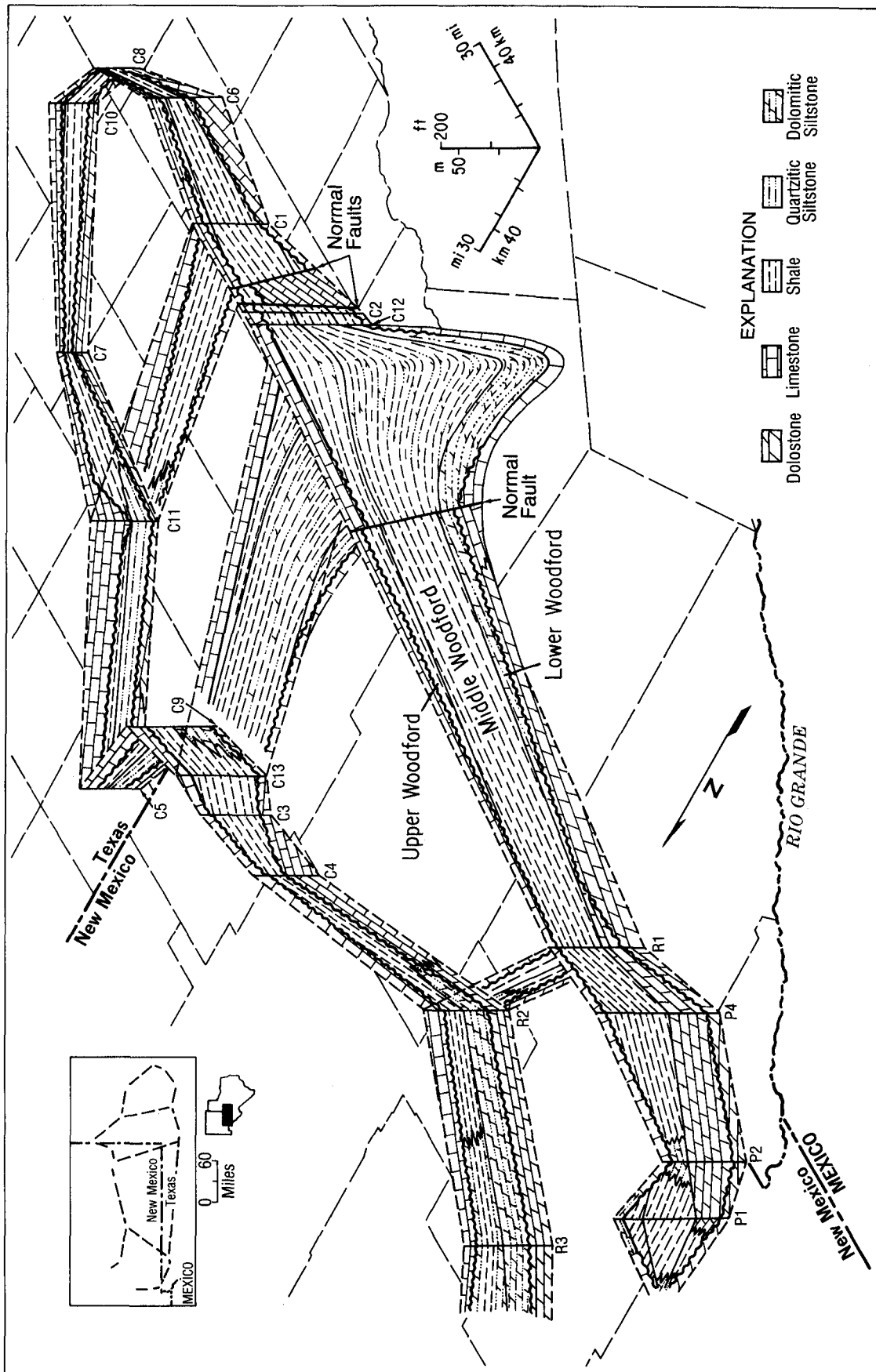


FIGURE 8. Fence diagram of Upper Devonian units. Correlation from outcrop to subsurface from Rosado (1970). Datum is top of Woodford. Locality numbers refer to map symbols in appendix A.

2 through 5, 7, 9, 11, 12; pl. 5, C–C', wells 2 through 6, 9, 10; pl. 6, D–D', wells 6 through 12; pl. 7, E–E', wells 7, 8, 10, 11, 16, 17).

Facies changes between black shale and siltstone appear in many parts of the study area (fig. 8; pls. 3 through 7). Siltstone beds common throughout the Sly Gap Formation in southeastern New Mexico correlate with black shale in the Percha and Woodford Formations to the south and east (Laudon and Bowsher, 1949; Ellison, 1950; Rosado, 1970). Dolomitic siltstones of the Onate Formation in New Mexico also correlate with dolostone and cherty dolostone beds of the Canutillo Formation in West Texas and with black shales in the Percha and Woodford Formations (King and others, 1945; Rosado, 1970). On the Northwestern Shelf, siltstone is the basal unit of the Woodford at some localities (app. B; C5, C9), but it is higher in the section at others (app. B; C3, C13). In the Delaware and Val Verde Basins, siltstone beds appear to be common throughout the formation, as indicated by the generally reduced radioactivity and the highly erratic nature of the gamma-ray log patterns shown in plates 5 through 7 (pl. 5, C–C', logs 4, 6; pl. 6, D–D', logs 9 through 13; pl. 7, E–E', logs 16, 17).

Depositional Processes

Siltstone

Many of the siltstone strata and siltstone-shale couplets in the Woodford Formation (fig. 5a through f) closely resemble the silt and mud turbidites described by Piper (1978) and Stow and Piper (1984) and the distal storm deposits described by Aigner (1982, 1984). In the Woodford, these strata range from laminae less than 2 mm thick to beds rarely more than 10 to 15 cm thick. They commonly contain graded layers (fig. 5a, d through f), climbing ripple cross-stratification (fig. 5d), horizontal stratification, fading (incipient) ripple forms (fig. 5e), flow-sheared laminae (fig. 5c), and laminae contorted by soft-sediment failure (fig. 5b). Many of these strata are partial or complete Bouma sequences that have scoured bases, normally graded sequences, and a vertical succession of primary sedimentary structures that indicate rapid deposition from a waning current during a single event.

Both fine-grained turbidites and distal storm deposits described in the literature have similar thicknesses and sedimentary structures (Piper, 1978; Aigner, 1982, 1984; Stanley, 1983; Stow and Piper, 1984; Schieber, 1987; Davis and others, 1989). Mud turbidites in the deep ocean consist of the division E mud of Bouma (1962), which Piper (1978) subdivided into laminated, graded, and ungraded units. The vertical pattern and the contained sedimentary structures, such as grading and low-amplitude climbing ripples, are diagnostic of turbidite origin (Stow and Piper, 1984). Silt turbidites are silt-dominated sequences that exhibit the same suite of sedimentary structures and the same divisions (Bouma A through F) as classical sandy turbidites (Stow and Piper, 1984). The siltstone and shale layers in the Woodford Formation (fig. 5a through f) differ from silt and mud turbidites described in the literature (for example, Piper, 1978; Stanley, 1983; Stow and Piper, 1984) only in the scarcity of bioturbation in the shale that is common at the top of the turbidite sequence (Bouma division E mud and division F pelagite). This difference indicates that anoxic bottom conditions toxic to benthic organisms prevailed throughout the basin during deposition of the shale laminae.

Sedimentary processes related to storms, such as wind-forced currents (Morton, 1981), ebb currents produced by storm surge setup (Nelson, 1982), and seaward-flowing currents caused by coastal downwelling (Swift and others, 1983), deposit sediment that has textures and structures virtually identical to those of turbidites. Distal storm deposits characteristically are fine grained, thinly stratified, and normally graded, having scoured bases and Bouma sequences (Aigner, 1982). They differ from proximal equivalents in grain size and layer thickness and in their having no hummocky stratification or oscillatory ripples, both of which, when present, indicate deposition under combined flow conditions above wave base (Aigner, 1982). Whether storms produce turbidity currents is debatable, but it is clear that storms generate bottom currents that transport large quantities of sediment (Hayes, 1967; Morton, 1981, 1988; Nelson, 1982; Walker, 1984, 1985). Storm-generated bottom flows and turbidity currents may represent end members of a single process if, as suggested by

Walker (1984, 1985), distal storm currents passing below wave base become turbidity currents. Such a subtle change in the transport mechanism may explain the present difficulty in distinguishing fine-grained turbidites from storm deposits in the stratigraphic record. Whether the siltstones and siltstone-shale couplets in the Woodford Formation are turbidites or storm deposits is likewise problematic, but the presence of grading and partial or complete Bouma sequences indicates deposition from bottom flows.

Black Shale

Most layers in the black shale lithofacies (fig. 4a through h) do not have grading or Bouma divisions as do beds in the siltstone. Black shale that displays undisturbed parallel laminae typically contains higher concentrations of marine organic matter, less clastic material, and more planktonic microfossils (for example, radiolarians, spores, conodonts) than do the Bouma E and F shales of the siltstone-shale couplets (fig. 5a through f). Shale displaying parallel laminae constitutes the bulk of the Woodford black shale lithofacies and is mostly pelagic in origin.

Origin of the thin varvelike siltstone and shale laminae in pelagic black shale (fig. 4a, b, e) is less certain. These laminae may represent mud turbidites or storm layers too small or far from the source to produce grading and recognizable Bouma divisions, or they may represent episodic fallout from the pycnocline. Pierce (1976), Maldonado and Stanley (1978), and Stanley (1983) described detachment of low-concentration turbidity plumes and entrainment of the muddy water along the isopycnals in strongly density stratified water columns. Episodic fallout of material (for example, terrigenous silt and planktonic tests) occurs as particle concentration builds up and exceeds the density of the pycnocline, producing a relatively clean, well-sorted, structureless lamina of widespread areal extent. Similar laminae are common in muddy marine sediments, such as those found in the eastern Mediterranean Sea near the Nile delta (Maldonado and Stanley, 1978; Stanley, 1983). Sediment deposition by this process seems likely

during Woodford accumulation because of the exclusively fine grained texture of the rocks and because of the strong density stratification that existed within the basin. Water-density stratification is an inherent property of the sea and, judging from the scarcity of bioturbation and its implicit link with bottom stagnation and anoxia (Byers, 1977; Arthur and Natland, 1979; Demaison and Moore, 1980; Leggett, 1980; Ettenshon and Barron, 1981; Stanley, 1983; Pratt, 1984; Ettensohn and Elam, 1985; Stein, 1986; Davis and others, 1989) strong density stratification probably occurred during Woodford black shale deposition. (See also *Paleoceanography*, p. 33.) In this context, the relative abundances of benthic fossils, trace fossils, and undisturbed parallel laminae in the Woodford (figs. 4a through h, 5a through h) indicate that the black shale and siltstone lithofacies represent anaerobic and dysaerobic biofacies, respectively (Rhoads and Morse, 1971; Byers, 1977).

Lithologic Patterns and Origin of Sediments

The Woodford Formation consists of varying proportions of terrigenous, pelagic, and authigenic constituents (app. C), and textural and compositional evidence indicates much re-sedimentation within the basin. Terrigenous material includes fine-grained quartz, muscovite, microcline feldspar, illite, wood and leaf fragments, vitrinite, and the trace heavy minerals (zircon and tourmaline). The silt-sized silicate minerals are most common in the northern basin. Locally, in rocks from the Northwestern Shelf, coarse-grained mica flakes glitter on fresh bedding surfaces (app. B; C4, C5), and the silt-sized fraction is subarkosic (app. C). The distribution and texture of these minerals indicate that the principal source was the land north of the basin, the Pedernal Massif and northern Concho Arch (fig. 1b).

Siltstone depocenters lie in the northern, central, southern, and westernmost parts of the basin (fig. 9a) in areas coincident with the modern-day Northwestern Shelf, the deepest parts of the Delaware, Val Verde, and Midland Basins, and the Sacramento Mountains. The patchy distribution of these depocenters suggests that sediment

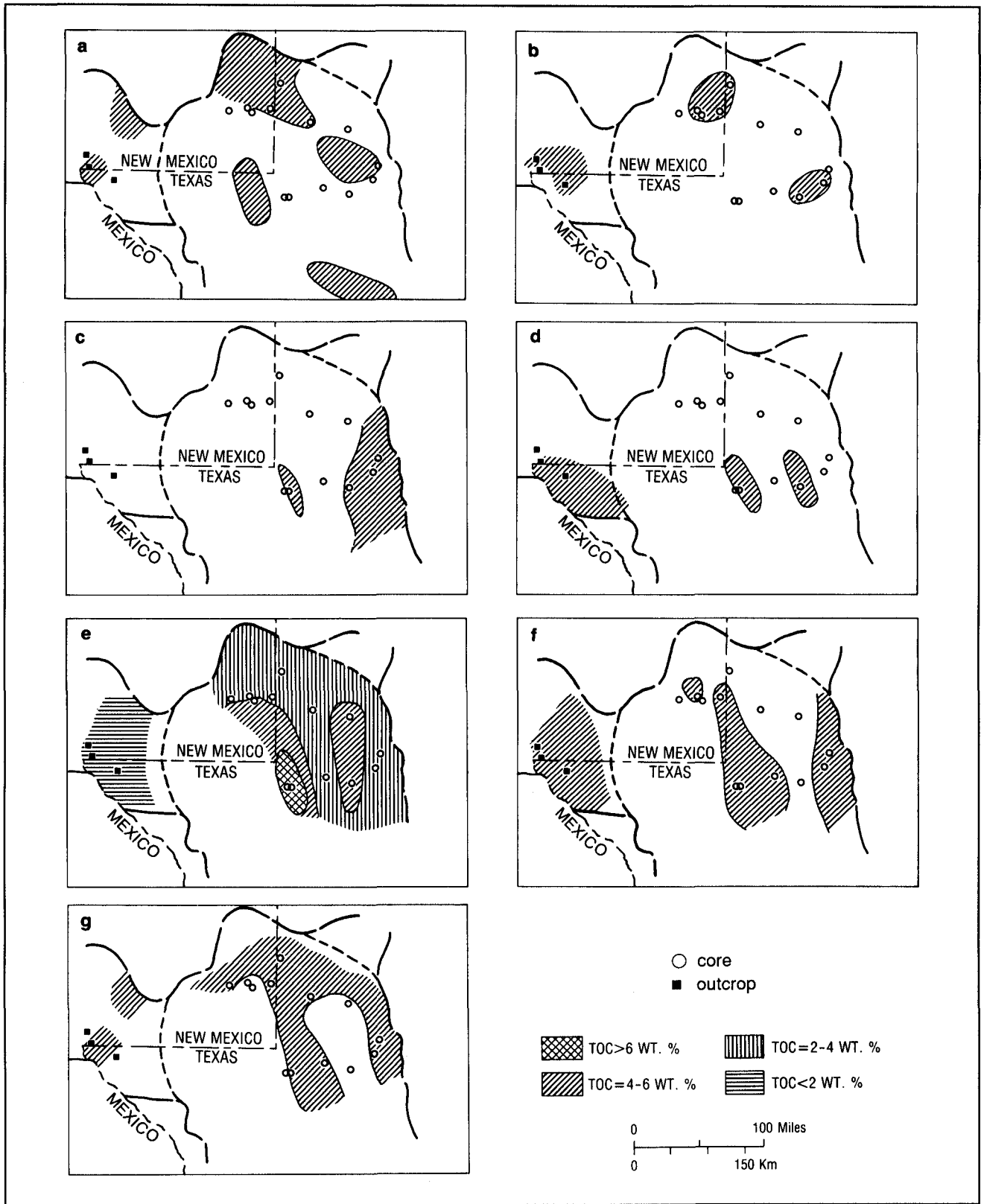


FIGURE 9. Regional lithologic variations in Upper Devonian rocks in West Texas and southeastern New Mexico. Maps show Late Devonian shoreline and limit of Tobosa Basin depocenter (fig. 1b). (a) Siltstone depocenters, (b) Illite depocenters, (c) Recycled vitrinite depocenters, (d) Radiolarian chert depocenters, (e) TOC concentration in black shale, (f) Depocenters of silt-sized dolomite where dolomite/quartz ratio is greater than 1. (g) Depocenters of dysaerobic, shallow-water sedimentary structures.

bypassing was common as silt and mud moved from siliciclastic source areas downslope into the basin. This inference is consistent with the interpretation that most silt was deposited from bottom flows, a mechanism sensitive to bottom irregularities and channelization.

The most abundant terrigenous component in the Woodford is illite (app. C). Detrital illite has an apparent Rb-Sr source age of 540 m.y., an age uncommon in North American basement rocks but common in regionally metamorphosed rocks found in large areas of Africa and South America (Morton, 1985). The source age and the good fit to the isochron for data from widely different localities in West and Central Texas are cited as evidence that illite came from a southern (Gondwana) source or was thoroughly mixed during transport from multiple sources (Morton, 1985). In the present study, the highest concentrations of illite (>60%) were found in northern, southeastern, and westernmost regions (fig. 9b) in the present-day Northwestern and Eastern Shelves, Midland Basin, and western outcrop belt. The wide distribution of illite depocenters and their proximity to northern siltstone depocenters and siliciclastic source areas suggest that illite came from multiple sources on the Pedernal Massif and Concho Arch (fig. 9b). The broad extent of the exposed land implies that it derived from diverse stratigraphic levels. Although contribution from a Gondwana source cannot be ruled out because of the absence of control in the southern part of the basin, a mixed provenance for illite seems most likely.

Trace amounts of vitrinite are ubiquitous, documenting a small contribution of land plant debris to all parts of the basin. Recycled vitrinite was found only in the eastern and central parts of the basin (fig. 9c) in black shale from the Central Basin Platform, southern Midland Basin, and Eastern Shelf (app. D), indicating that these areas were close to emergent land that displayed eroding bedrock. A few wood and leaf impressions were found mostly in northern and eastern parts of the basin in rocks from the Northwestern and Eastern Shelves (app. B; C4, C7, C13). Their distribution implies that land areas on the Pedernal Massif and Concho Arch

supported most of the terrestrial plant life in the study area during the Late Devonian. Abundances of vitrinite and land plant remains are low, however, even in the siltstones, indicating that terrestrial source areas were only sparsely vegetated.

Pelagic constituents include radiolarians, amorphous particulate organic matter, algal spores, conodonts, fish fragments, and associated fecal material. Radiolarian chert is most common in the central and eastern parts of the basin (fig. 9d) at localities on the present-day Central Basin Platform and in the southeastern Midland Basin (app. B; C2, C6). Chert is also abundant in the Canutillo Formation in West Texas (King and others, 1945; Rosado, 1970). Anomalously high biogenic silica is perhaps the best indication of nutrient-rich water upwelling in ancient seas (Parrish and Barron, 1986; Hein and Parrish, 1987) and suggests that upwelling occurred in the basin and was most pronounced in central and western areas. Intrabasinal upwelling is a likely consequence of the major oceanic upwelling that occurred adjacent to the study area along the margin of the North American craton during the Late Devonian. This upwelling episode is recorded as extensive Upper Devonian novaculite beds of biogenic origin in the Ouachita allochthon (Park and Croneis, 1969; Lowe, 1975; Parrish, 1982).

Volumetrically, amorphous organic matter (AOM), which accounts for nearly all of the TOC, is the most abundant pelagic constituent in the Woodford (app. C). The highest TOC concentrations (>6 wt %) are found in the center of the basin on the modern-day Central Basin Platform (fig. 9e). Somewhat lower TOC values (4 to 6 wt %) are found to the east and north in areas coincident with parts of the western and eastern Midland Basin, southern Northwestern Shelf, and western margin of the Eastern Shelf (fig. 9e). Localities that have the highest TOC concentrations also have the most radiolarian chert, suggesting that high TOC values record increased biologic productivity at sites of intrabasinal upwelling. The area that has the highest TOC's (fig. 9e) is surrounded by siltstone depocenters (fig. 9a), supporting the inference that it was bypassed by siliciclastic sediment.

Authigenic material includes dolomite, pyrite, secondary silica, glauconite, anhydrite, calcite, and phosphatic ooids. Some cored intervals on the Central Basin Platform and Northwestern Shelf (app. B; C2, C3) contain abundant pristine, euhedral dolomite rhombs floating in organic-rich black shale. The texture and association are similar to those observed in Deep Sea Drilling Project (DSDP) cores and in very young sediments in the Gulf of California (Baker and Kastner, 1981), suggesting that the rhombs are authigenic and formed in situ. Most of the dolomite in the Woodford, however, appears to be re-sedimented because it contains abraded anhedral and subhedral silt-sized grains and commonly appears randomly mixed with quartz in graded layers and Bouma sequences (fig. 5e, f, h). Derivation from ancient dolomitic rocks is not indicated. The poor durability of dolomite precludes long-distance subaerial transportation. Moreover, dolomite in the Woodford is typically monocrystalline and monotonously uniform in texture, whereas in older Paleozoic rocks, dolomite texture is quite variable. One would expect to see dolomitic rock fragments and a greater variety of textures if Woodford dolomite were terrigenous detritus.

If most of the dolomite in the Woodford is re-sedimented but not terrigenous in origin, then it must be penecontemporaneous. Early formation of dolomite in marine sediment is promoted by hypersaline brine (Zenger, 1972) and by low concentrations of dissolved sulfate that develop in organic-rich sediments as the result of microbial sulfate reduction (Baker and Kastner, 1981). Given the abundance of organic matter and the presence of anhydrite in the Woodford, both are plausible mechanisms for contemporaneous dolomitization in the Permian Basin during the Late Devonian.

Areas that have a high ratio of dolomite to quartz (fig. 9f) are found in the central, northern, eastern, and westernmost parts of the basin, suggesting that these were the areas of highest carbonate production. The highest dolomite/quartz ratio is in the center of the basin (app. C; C2) where very little detrital quartz is found, and the quartz typically is much finer grained than dolomite. This observation is further evidence that the basin center, which coincides with the modern-day Central Basin Platform, was bypassed by siliciclastic detritus.

Secondary silica is a common cement in primary sedimentary structures, such as burrows and syneresis cracks, where it is associated locally with calcite and anhydrite. Burrows and syneresis cracks are abundant in the northern, central, and eastern basin (fig. 9g) in areas that were overlapped by Woodford sediments (for example, the Northwestern and Eastern Shelves, Central Basin Platform, and western Midland Basin). They are less abundant or absent in cores farther east in the Midland Basin. The distribution and association with anhydrite suggest that these structures are shallow-water indicators formed under dysaerobic conditions above the anoxic zone.

Benthic components are scarce and include trilobite fragments, brachiopods, and biogenic pellets. Some of the pellets in siltstone and others associated with scattered trilobite fragments in shale may be fecal material from a sparse benthos. However, many are found in black shale that has parallel laminae and has no burrows or benthic fossils, suggesting that they originated in the upper water column amid a thriving, normal marine biota. Most benthic fossils are found in the shelf regions, but biogenic pellets are also common in rocks from the Central Basin Platform (app. C; C2, C12).

Depositional Setting

Paleogeography

Late Devonian paleogeography of the study area (fig. 10) was inferred from the patterns of onlap (pls. 3 through 7) and lithology (fig. 9) described earlier. The widespread, blanketlike distribution and nearly uniform lithology of the Woodford indicate that the entire region was one of low relief during the Late Devonian. Major topographic features in the model include (1) the land in the north and northwest representing the Pedernal Massif and Concho Arch, (2) the ancestral Delaware and Val Verde Basins, (3) the shallow Midland Basin, (4) an intrabasinal archipelago representing the ancestral Central Basin Platform and Pecos Arch, (5) shallow shelf regions to the north and east representing the ancestral Northwestern and Eastern Shelves, (6) a western shelf that had irregular channels and shoals representing parts of the Northwestern Shelf and Diablo Platform, and (7) a

land mass to the southwest representing the southern part of the Diablo Platform (fig. 10).

The Pedernal Massif and northern Concho Arch represent the southern end of the Transcontinental Arch, which was the dominant topographic high in the western North American craton during the Late Devonian (Poole and others, 1967; Poole, 1974; Heckel and Witzke, 1979). Grain size and composition of Woodford siltstones indicate that this arch supplied most of the terrigenous sediment to the basin and consequently must have had the highest elevations in the study area. The absence of deltas and coarse clastic wedges, however, indicates that elevations were not high enough to create an orographic barrier to winds or to introduce major rainfall, runoff, and clastic influx into the basin.

The Northwestern and Eastern Shelves and the Diablo Platform are onlapped by Woodford

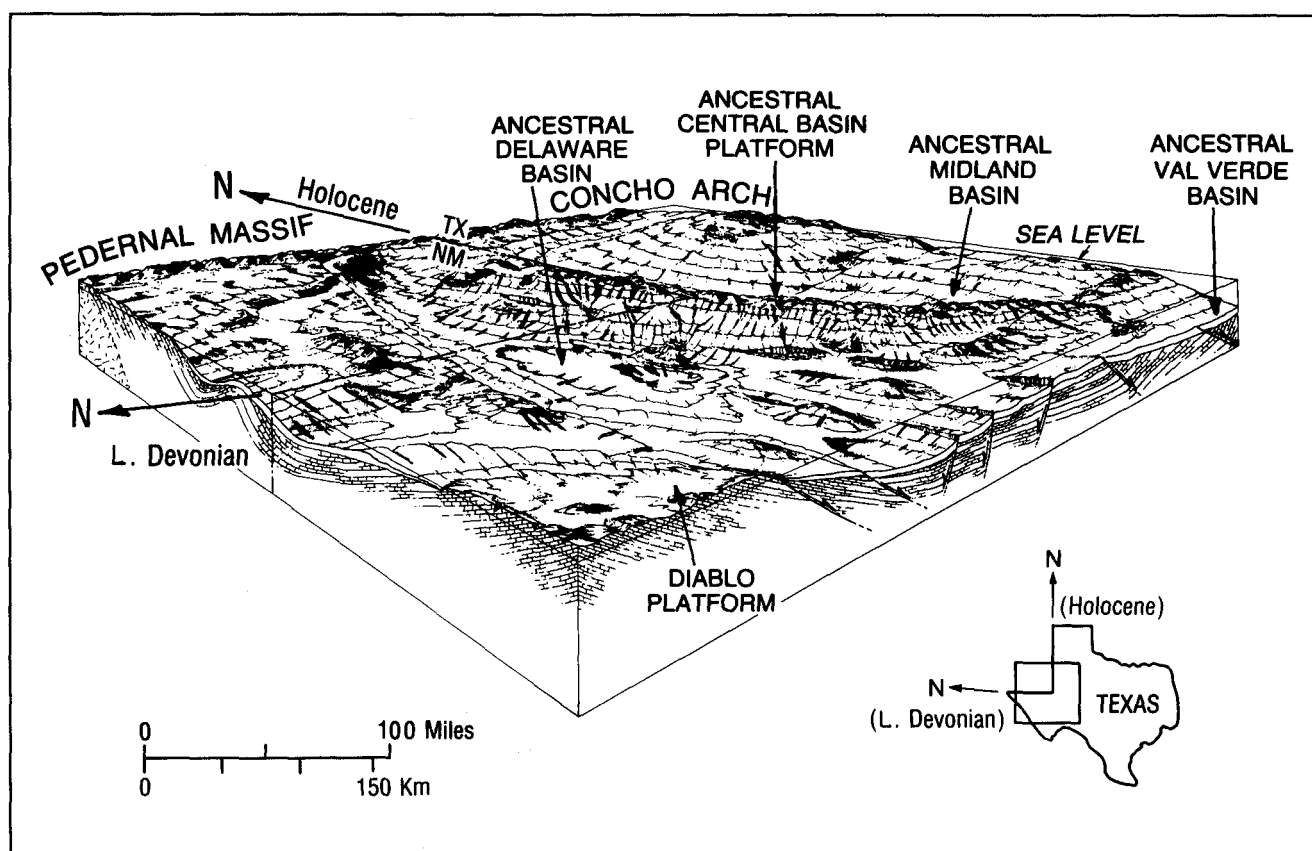


FIGURE 10. Late Devonian paleogeography of West Texas and southeastern New Mexico.

sediment (pls. 3 through 7), indicating that they were low-relief expanses of intermediate elevation, and that during the Late Devonian transgression they became shallow-water shelf environments that had local channels, scattered islands, and protected shoals. The westernmost outcrop belt is characterized by complex facies changes (Stevenson, 1945; Laudon and Bowsher, 1949; Rosado, 1970), indicating that it comprised an extensive, low-relief cratonic shelf that had prominent shoals and channels (Rosado, 1970). The southern Diablo Platform may have remained emergent, but it was not a major source of terrigenous sediment (Wright, 1979).

The deepest parts of the Late Devonian epeiric sea coincided with the deepest parts of the present-day Delaware and Val Verde Basins (fig. 10), where the thickest and most complete Woodford sections are found (pls. 3 through 7). Gradual changes in well log signatures at formation boundaries in these depocenters suggest that the Woodford may be conformable with the bounding formations (pl. 5, C–C', wells 4, 6; pl. 6, D–D', wells 10, 11, 13; pl. 7, E–E', wells 16, 17). That the Midland Basin was a topographic depression (fig. 10) is supported by the following evidence: (1) the Woodford thickens and contains all three units toward the basin axis and (2) the Woodford generally has no bottom features (such as anhydrite-bearing burrows and syneresis cracks), that would indicate elevations above the anoxic and sulfate-reducing zones.

The ancestral Central Basin Platform and Pecos Arch are shown as a continuous intra-basinal archipelago (fig. 10). Whether the two actually connected is unknown, but the onlap of both structures by the Woodford indicates that both were topographically high during the Late Devonian. Lithologic patterns (fig. 9) indicate that the Central Basin Platform was bypassed by terrigenous sediment, and stratigraphic onlap indicates that bypassing occurred because the platform was elevated above the surrounding provinces. The abundance of dysaerobic primary sedimentary structures on the platform (fig. 9g) suggests a shallow-water setting and supports this conclusion. Folk (1959) inferred the presence of an island chain along the platform during

the Early Ordovician on the basis of the abundance of feldspar in the Ellenburger Formation. Similarly, the presence of recycled vitrinite in the black shale lithofacies (fig. 9c) indicates that eroding bedrock existed nearby and that scattered islands lay along the platform during Late Devonian eustatic highstand.

Paleotectonics

Ellison (1950) recognized anomalously thin but complete Woodford intervals on structural highs along the Central Basin Platform and interpreted them as evidence of contemporaneous uplift during Woodford deposition. Pre-Mississippian truncation of the Woodford along the ancestral Central Basin Platform (for example, pl. 4, well 9) and on the Northwestern Shelf (app. B; C5, C9), where the lower unit is well developed and the upper unit is absent, is further evidence of contemporaneous uplift in these areas. Vertical tectonic adjustments in the Late Devonian most likely reflect reactivation of basement structures because truncated sections are found along zones of weakness in the basement and near the major Paleozoic fault systems (pls. 1, 2) that formed along reactivated basement faults (Walper, 1977; Muehlberger, 1980; Hills, 1984). In figure 10, contemporaneous vertical movements are illustrated by the schematic representations of normal faults in the Delaware and Val Verde Basins. These faults represent the dominant Paleozoic faults shown in plates 1 and 2.

Epeirogeny in the southern Midcontinent probably was linked to renewed tectonism along the continental margins. The Acadian orogeny produced highlands (fig. 11) that shed coarse terrigenous elastics toward the craton to form the Catskill delta (Ettensohn and Barron, 1981; Faill, 1985; Ettensohn, 1987). The Antler orogeny also produced a rising highland (fig. 11) that shed coarse elastics into a subsiding foreland basin (Poole and others, 1967; Poole, 1974). Forces transmitted from the Antler orogenic belt have been correlated with minor faulting, uplift, and subsidence in New Mexico (Poole and others, 1967) and are inferred to account for Late Devonian epeirogeny in the study area.

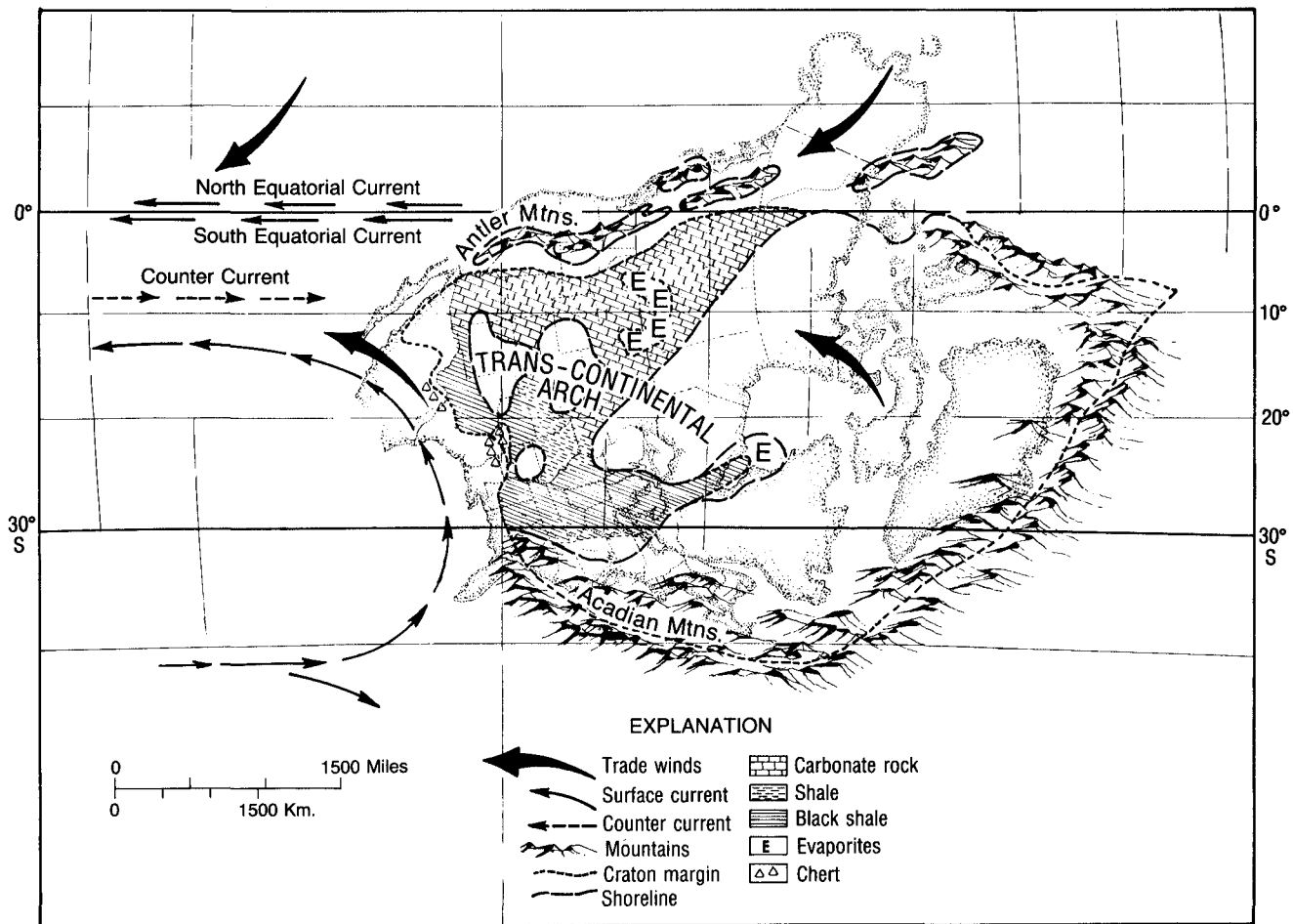


FIGURE 11. Late Devonian paleogeography of North America. After Heckel and Witzke (1979).

Paleoclimate

The paucity of terrestrial organic matter in the Woodford Formation, including the siltstone lithofacies, suggests that land in the region was mostly barren, and the absence of coarse-grained sediments and thick deltaic or fan deposits indicates that the land was low lying and not drained by large rivers. Furthermore, the presence of anhydrite in primary sedimentary structures documents hypersalinity within the basin. Together these observations indicate that the Permian Basin was arid during the Late Devonian. An arid paleoclimate and hypersalinity suggest that some of the dolomite in the Woodford formed in shallow-water evaporitic settings. Episodic resedimentation by bottom flows would account for the hybrid mixture of

dolomite and quartz grains composing graded layers and Bouma divisions.

Arid-climate indicators support a Paleogeographic reconstruction in which the study area lies along the western margin of North America at approximately 15 degrees south latitude in the warm, arid southern trade-wind belt between the wet equatorial doldrums and the wet southern temperate zone (Heckel and Witzke, 1979; fig. 11). In this reconstruction the Late Devonian paleoequator lies along the Antler orogenic belt and the Canadian Rockies from California to Alberta. Other plate tectonic reconstructions of the Late Devonian also place the study area at low southern latitudes in the warm tropics or on the paleoequator (Lowe, 1975; Ettensohn and Barron, 1981; Parrish, 1982).

Paleoceanography

Features characteristic of black shale in the Woodford, including high organic content, abundant pyrite, and parallel laminae, indicate that bottom waters were stagnant and anoxic during deposition. The abundance of pelagic marine fossils and marine types of organic matter indicates that surface waters supported a luxuriant, normal marine biota. Coexistence of a putrid bottom and fertile surface waters requires a strongly stratified water column and implies the presence of a pycnocline (Byers, 1977; Arthur and Natland, 1979; Demaison and Moore, 1980; Ettensohn and Barron, 1981; Stanley, 1983; Ettensohn and Elam, 1985; Stein, 1986). The arid climate and hypersaline indicators imply that a pycnocline formed as a result of the strong density contrast between warm, normal-salinity surface water and cold, somewhat hypersaline bottom water. Anaerobic conditions developed below the pycnocline because no vertical mixing was occurring and because oxygen had been depleted owing to the high demand created by decay of the large volume of organic matter.

The abundance of marine organic matter and pelagic fossils indicates that efficient circulation of surface water and continuous resupply of nutrients characterized the upper part of the water column. Upwelling off the west and southwest coasts of North America during the Late Devonian (Lowe, 1975; Heckel and Witzke, 1979; Parrish, 1982) was the most likely source of the nutrients. No record exists of large rivers discharging into the basin (that is, deltas or fans) that would indicate a significant, continuous terrestrial source. Published circulation models suggest that oceanic surface currents flowing along the continental margin were diverted northward and northeastward, carrying upwelled water onto the North American craton (Lowe, 1975; Heckel and Witzke, 1979; Ettensohn and Barron, 1981). The model shown in figure 12 suggests that upwelled water moved eastward into the basin primarily as counter currents. In the southeast trade-wind belt, net flow of surface water would have been directed westward out of the basin by the Coriolis force and the Ekman spiral. The arid climate that produced hyper-

salinity caused net evaporation of surface water, particularly over shallow-water shelves, platforms, and shoals. The loss of surface water via wind-driven currents and evaporation would have amplified the negative water balance required by eustatic rise, causing inflowing counter currents to be stronger than outflowing surface currents.

The model in figure 12 differs from other published models (Lowe, 1975; Heckel, 1977; Demaison and Moore, 1980; Witzke, 1987) in that the floor of the basin in this model remained stagnant and anoxic, receiving sulfide-rich mud that had parallel laminae, even though net evaporation, local brine production, and negative water balance was occurring. This happened because the circulation pattern developed during a major marine transgression; therefore, much of the increased volume of water flowing onto the craton can be accounted for by the addition of hypersaline brine to stagnant bottom waters. Consequently, dense water gradually filled depressions in the epeiric sea without deep circulation being necessary to maintain water balance.

The existence of only dysaerobic (siltstone) and anaerobic (black shale) biofacies in the Woodford Formation indicates that bottom water became depleted in oxygen soon after the Late Devonian transgression began. Early oxygen depletion most likely was related to the early development of hypersalinity and strong density stratification. Dense water accumulated at the bottom of the water column in topographic lows and probably caused many local pycnoclines to develop during the initial stages of transgression. Later, at transgressive highstand, a single pycnocline (fig. 12) apparently developed, allowing anaerobic mud, represented by the black shales of the middle Woodford unit, to accumulate uniformly across the entire region. Dysaerobic bottom indicators found locally in the black shale on topographic highs (burrows, syneresis cracks, and anhydrite) may record some of the small-scale eustatic regressions documented by Johnson and others (1985) and reflect short-term fall of the pycnocline caused by falling sea level.

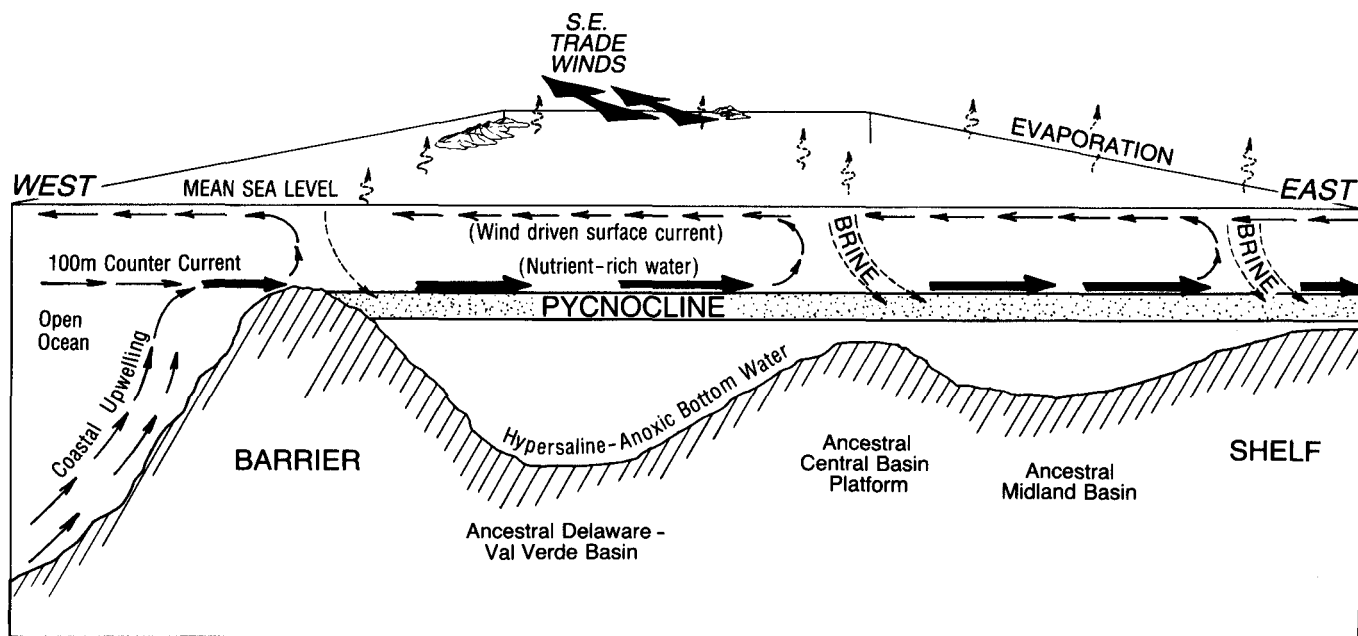


FIGURE 12. Model of Late Devonian circulation during eustatic highstand.

Depositional Mechanisms

Because the study area was once located in the tropics (fig. 11), and particularly because the Late Devonian was an epoch of worldwide transgression and global warming (Johnson and others, 1985), storms were most likely frequent and geologically significant events (Marsaglia and Klein, 1983; Morton, 1988; Barron, 1989). Frequent storms are therefore the most plausible mechanism for explaining the generation of bottom flows. Triggering mechanisms for bottom flows include (1) turbid, dense discharge from deltas, submarine fans, and rivers in flood, (2) spontaneous slumping of rapidly deposited, unconsolidated sediment, (3) slope failure resulting from earthquakes, and (4) sediment liquefaction and autosuspension during storms (Walker, 1984).

The absence of deltas and submarine fans in the Woodford precludes the first two mechanisms. What little turbid flood discharge entered the basin would not have been dense enough to sink beneath marine or hypersaline basin water (Drake, 1976; Pierce, 1976). Most likely, flood discharge was hypopycnal, or it produced detached turbidity layers by processes similar to those that had occurred in modern submarine canyons off southern California

(Pierce, 1976) and in the Nile cone and Hellenic trench regions of the Mediterranean Sea (Maldonado and Stanley, 1978; Stanley and Maldonado, 1981). Deposition from turbid, muddy plumes would not produce graded layers or Bouma sequences but could yield the varvelike laminae (Pierce, 1976; Stanley, 1983) characteristic of the black shale lithofacies in the Woodford.

Earthquakes associated with epeirogenic movements probably triggered some bottom flows, but the subtlety of structural displacement during the Late Devonian indicates that these movements probably were weak and infrequent. Furthermore, bottom flows starting in shallow water would be diverted along the pycnocline in strongly stratified seas (Pierce, 1976; Stanley, 1983), unless they entrained brine from restricted hypersaline basins, shelves, or shoals (Arthur and Natland, 1979).

Storms, rather than earthquakes, probably were the most frequent and powerful agents of sediment transport in the warm Late Devonian tropics. They can account for both the indiscriminate mixing of siliciclastic and dolomite grains and the generation of bottom flows that persisted into basinal depocenters. In modern seas, storms can disrupt density stratification

(Mooers, 1976a, b), a condition that could minimize flow detachment and promote sustained bottom flows. It is probable that such a process happened in Late Devonian times as well. Storm winds and surge would flush shallow-water, hypersaline environments and give rise to very dense bottom flows consisting of sediment-laden brine. Briny bottom flows would maintain their integrity below the pycnocline even in strongly stratified basins.

Evidence indicates that bottom flows periodically disturbed anoxia that existed beneath the pycnocline. In black shales, burrows are commonly confined to graded layers and Bouma divisions, indicating that the bottom was briefly inhabited by organisms after sediment deposition. Bottom flows originating in shallow, aerobic or dysaerobic environments apparently entrained enough oxygen to sustain a temporary benthic population. However, oxygen was quickly depleted by the meager fauna, decay of organic matter, and absence of oxygen resupply. And because bottom oxygenation was short-lived, anaerobic conditions quickly returned, killing the few allochthonous organisms. Burrowed layers in the Cretaceous Mowry Shale (Davis and others, 1989) and the Devonian Chattanooga Shale (Potter and others, 1982) have been similarly explained, and entrainment of oxygen and benthic organisms in turbidity currents apparently occurred in modern sediments in the Santa Barbara Basin (Sholkovitz and Soutar, 1975).

Basal siltstones in proximal shelf and basin environments (app. B; C5, C9, C11) consist of vertically stacked siltstone-shale couplets, documenting episodic deposition from bottom flows. The greater numbers and thicknesses of siltstones in the deepest parts of the Delaware, Midland, and Val Verde Basins indicate that these depocenters were locations where bottom flows, initiated in various parts of the basin, finally converged. The high frequency of bottom flows in basinal depocenters implies that basin axes were dysaerobic more often than were distal shelves, slopes, and platforms. Thus, the lower concentrations of organic matter in the basins (fig. 9e) can be attributed to the combined effects of dilution by clastic sediment and destruction

by oxidation, aerobic microbes, and the temporary benthos.

Synopsis of Depositional History

Woodford deposition began when the sea drowned marine embayments in what are now the deepest parts of the Delaware and Val Verde Basins and advanced over a subaerially eroded and dissected terrane composed mostly of carbonate rocks of Ordovician to Middle Devonian age. A broad epeiric sea formed that had irregular bottom topography and scattered, low-relief land masses. The basin lay in the arid midtropics surrounded by lands that supported little vegetation and few rivers. Oceanic water from an area of coastal upwelling flowed into the expanding epeiric sea and maintained a thriving, normal marine biota in the upper levels of the water column. Net evaporation locally produced hypersaline brines, and strong density stratification developed that restricted vertical circulation. The basin quickly became dysaerobic and then anaerobic as sea level continued to rise. Once oxygen was eliminated from the bottom, sulfide-rich mud began to accumulate. Rising sea level and persistent oceanographic and climatic patterns allowed anaerobic mud deposition to continue slowly during the rest of the Late Devonian Epoch. Frequent storms and occasional earthquakes triggered bottom flows that supplied silty mud to proximal shelves and deep basin troughs and caused much re-sedimentation throughout the basin. Tectonic stress arising from the Antler orogeny initiated epeirogenic movements throughout the region and caused contemporaneous movements along reactivated basement faults.

Woodford deposition probably ended because sea level stabilized or dropped and oceanographic patterns changed, thus halting the strong net flow of ocean water onto the craton and forcing deep circulation through most of the basin. Glauconite and calcified benthic epifauna accumulated on the floor of the epeiric sea, marking a change in bottom conditions from anaerobic to dysaerobic and locally aerobic and recording the improved vertical circulation through most of the basin.

Petroleum Potential

The Woodford Formation is currently generating oil in the Midland Basin, Central Basin Platform, and Eastern and Northwestern Shelves and is currently generating gas in the Delaware and Val Verde Basins. Thermal maturity of the Woodford Formation was deduced from the depth and R_0 data in appendix D and the depth versus R_0 log-normal relationship derived for the Woodford in the Anadarko Basin (Cardott, 1989). Oil generation in the Woodford occurs between R_0 values of 0.5 and 1.3 percent (Cardott, 1989) at depths between 6,000 and 13,000 ft in the Permian Basin. These depths correspond to depths below sea level of approximately 4,000 to 10,000 ft in the region east of the Central Basin Platform and 2,000 to 9,000 ft in the Delaware Basin and regions to the west (fig. 1a; pl. 1). Condensate and wet-gas generation occurs between R_0 values of 1.3 and 2.0 percent (Cardott, 1989) at depths between 13,000 and 18,000 ft common only in the Delaware and Val Verde Basins. These depths correspond to depths below sea level of approximately 9,000 to 14,000 ft in the region west of the Central Basin Platform and south of the Pecos Arch (fig. 1a; pl. 1). Dry gas is generated between R_0 values of 2.0 and 5.0 percent at depths between 18,000 and 26,000 ft (Cardott, 1989), or at depths below sea level of 14,000 to 22,000 ft in the Delaware and Val Verde Basins (fig. 1a; pl. 1).

Summary

The Woodford Formation is an organic-rich petroleum source rock that has long been recognized as an important marker unit because of its black shales, anomalously high radioactivity, widespread distribution, and stratigraphic position between carbonates. The Woodford is mostly Late Devonian in age and is stratigraphically equivalent to the Devonian black shales (for example, Chattanooga, Ohio, Antrim, New Albany, Bakken, Exshaw, and Percha) that are present in many North American basins. At most localities, the

Commercial production of hydrocarbons from the Woodford is possible in areas where the formation is highly fractured. The fractured Upper Devonian shales (Ohio, Chattanooga, Antrim, Bakken, and Woodford) that produce gas in the Appalachian and Michigan Basins and oil in the Williston and Ardmore Basins illustrate the commercial potential and provide appropriate geological models for exploration in the Permian Basin. In West Texas and southeastern New Mexico, optimum drilling targets are the siltstones and radiolarian cherts because they are competent lithologies that are the most likely to maintain open fracture systems. Areas that have the greatest density of major faults are the most prospective: these include the Central Basin Platform, southernmost Midland Basin, and parts of the Northwestern Shelf (fig. 1a; pls. 1, 2). Production may be possible from the well-developed basal siltstone in the northern part of the Midland Basin and adjacent Northwestern Shelf (for example, app. B; C5, C11 in Cochran and Gaines Counties, Texas). Although faults are uncommon there, commercial production could be established in zones where porosity has been enhanced or permeability can be artificially stimulated. Gas undoubtedly is present in siltstones and fractured shales in the Delaware and Val Verde Basins; however, drilling depths would make costs prohibitive in most places.

Woodford overlies a major regional unconformity and is diachronous.

In the Permian Basin, the Woodford is thickest (661 ft) in the Delaware Basin depocenter and locally is absent from structural highs on the Central Basin Platform and Pecos Arch. Structural relief in the subsurface is 20,000 ft; it developed primarily during the late Paleozoic as a response to orogenic activity in the Ouachita Fold Belt.

Two lithofacies, black shale and siltstone, compose the Woodford. The black shale exhibits

varvelike parallel laminae, abundant pyrite, very high radioactivity, and high concentrations of marine organic matter (mean = 4.5 ± 2.6 wt % TOC). It is the most widely distributed and distinctive rock type in the formation. Siltstone is a hybrid of silt-sized quartz and dolomite grains and exhibits discontinuous or disrupted stratification, graded layers, fine-grained Bouma sequences, and moderately high radioactivity. It is restricted to deep basin and proximal shelf settings and is commonly the basal unit. On the basis of lithology and stratigraphic position, basal siltstone is correlated with the Onate and Canutillo Formations in New Mexico and West Texas, the Misener and Sylamore Sandstones in Oklahoma and Arkansas, and the Ives Breccia Member of the Houy Formation in Central Texas. The black shale lithofacies is correlated with the Sly Gap and Percha Formations in the west and the Doublehorn Shale and phosphatic members of the Houy Formation in Central Texas. Black shale is mostly pelagic and represents an anaerobic biofacies, whereas siltstone was deposited by bottom flows and comprises a dysaerobic biofacies. Upward transition from basal siltstone to black shale locally records the worldwide marine transgression that occurred during the Late Devonian.

The Woodford onlaps Paleozoic structures flanking the Midland, Delaware, and Val Verde Basins, indicating that all of the major structural provinces in the modern-day Permian Basin had topographic expression in the Late Devonian. The blanketlike geometry and nearly uniform lithology, however, indicate that the region was one of low relief. The increased size and abundance of siliciclastic grains (quartz, muscovite, feldspar) and wood fragments in the northern part of the basin show that the Pedernal Massif and northern Concho Arch were the principal source areas of terrigenous sediment. In contrast, most dolomite formed contemporaneously on distal platforms and shelves in highly reduced, low-sulfate mud or restricted marine environments. Resedimentation of dolomite grains and mixing with siliciclastics were accomplished by bottom flows.

Woodford black shale records widespread bottom stagnation and anoxia during deposition and a strongly density-stratified water column.

High concentrations of marine organic matter and siliceous pelagic micro-organisms in the shale indicate high biological productivity in surface waters supported mainly by dynamic upwelling. Episodes of hypersalinity, documented by the presence of anhydrite in burrows and syneresis cracks, suggest an arid paleoclimate and indicate that density stratification was caused, at least partly, by accumulation of hypersaline bottom water.

The plate tectonic reconstruction most consistent with an arid paleoclimate and dynamic upwelling places the study area on the western margin of North America in the dry tropics near 15 degrees south latitude. In this setting, southeasterly trade winds and the Ekman spiral would push surface waters westward toward the open ocean and upwelled oceanic water eastward onto the craton as counter currents. The negative water balance required for marine transgression would be amplified by flow into the basin replacing water lost by evaporation.

This circulation model accounts for the large supply of nutrients needed to support high biological productivity in the upper part of the water column of the epeiric sea. Furthermore, the low-latitude paleogeography and Late Devonian global warming imply frequent tropical storms and suggest that the bottom flows that caused the deposition of hybrid quartz/dolomite siltstones were storm generated.

The end of Woodford deposition coincided with the end of the Late Devonian eustatic rise. Bottom oxygenation, recorded as accumulations of glauconite and calcitic benthic fossils, indicates that new oceanographic conditions included deep circulation in most of the basin. The stabilization or fall of sea level would have ended the strong net flow of ocean water containing upwelled nutrients onto the craton and forced deep circulation to maintain water balance.

The Woodford Formation is now in the oil window in the Midland Basin, Central Basin Platform, and Eastern and Northwestern Shelves, and it is in the gas window in the Delaware and Val Verde Basins. Commercial production of hydrocarbons is possible from intervals that are highly fractured, but optimum drilling targets are siltstone and radiolarian chert

beds in densely faulted regions, such as the Central Basin Platform, southernmost Midland Basin, and parts of the Northwestern Shelf.

Development of reserves in unusual geological settings such as the Woodford Formation in the Permian Basin undoubtedly will be required to meet future demands for petroleum. These

reserves can be discovered through comprehensive studies, similar to the present report, that integrate stratigraphic, petrologic, and geochemical data. Such studies can help predict the location and lithology of unconventional oil and gas reservoirs that are inherently difficult to find.

Acknowledgments

This study, funded by the Bureau of Economic Geology, at The University of Texas at Austin, was begun while the author was a Research Fellow at the Bureau on sabbatical from Tulsa University (TU). Peter K. Krynine, project Research Assistant, helped compile the well log data, describe core, and conduct the field work; his efforts are gratefully acknowledged. David V. LeMone (The University of Texas at El Paso [UTEP]) shared his thoughts on the stratigraphy and origin of the Percha, provided relevant UTEP theses, suggested appropriate outcrops for study, and accompanied the author to Bishop Cap, New Mexico. Paul C. Franks (TU) read parts of the manuscript and offered helpful suggestions. The manuscript benefited greatly from critical reviews by S. C. Ruppel, W. B. Ayers, Jr., E. H. Guevara, W. A. Ambrose, and A. R. Scott, all at the Bureau.

Cores were supplied by Shell Oil Company, Mobil Oil Corporation, and the Exxon Company.

Vitrinite reflectance and visual kerogen analyses were performed by Robert Littlejohn, Kerogen Prep, Inc., Tulsa, Oklahoma, and TOC was determined by Geochem Laboratories, Inc., Houston, Texas.

Maps and cross sections (pls. 1 through 7) were drafted at the Bureau of Economic Geology by Margaret D. Koenig and Kerza Prewitt, under the supervision of Richard L. Dillon. The text figures were drafted in Tulsa: the fence diagram by Sharon S. Scott and the lithology logs and Paleogeographic block diagram by Herbert S. Scott. Final modifications were made at the Indiana Geological Survey (IGS) and the Bureau. Drafts of the manuscript were typed by Margaret Andrews (TU) and Marilyn DeWees (IGS). Word processing and typesetting were done at the Bureau by Susan Lloyd under the supervision of Susann Doenges. Technical editing was by Tucker F. Hentz. Margaret L. Evans designed the report. Lana Dieterich was the editor.

References

- Aigner, Thomas, 1982, Calcareous tempestites: storm-dominated stratification in Upper Muschelkalk limestones (Middle Trias, SW-Germany), in Einsele, Gerhard, and Seilacher, Adolf, eds., *Cyclic and event stratification*: Berlin, Springer-Verlag, p. 180–198.
- 1984, Storm depositional systems, in Friedman, G. M., Neugebauer, H. J., and Seilacher, Adolf, eds., *Lecture notes in earth sciences*, v. 3: New York, Springer-Verlag, 174 p.
- Amsden, T. W., 1975, Hunton Group (Late Ordovician, Silurian, and Early Devonian) in the Anadarko Basin of Oklahoma: Oklahoma Geological Survey Bulletin 121, 214 p.
- 1980, Hunton Group (Late Ordovician, Silurian, and Early Devonian) in the Arkoma Basin of Oklahoma: Oklahoma Geological Survey Bulletin 129, 136 p.
- Amsden, T. W., Caplan, W. M., Hilpman, P. L., McGlasson, E. H., Rowland, T. L., and Wise, O. A., 1967, Devonian of the southern Midcontinent area, United States, in Oswald, D. H., ed., *International symposium on the Devonian System*: Calgary, Canada, Alberta Society of Petroleum Geologists, v.1, p. 913–932.
- Amsden, T. W., and Klapper, Gilbert, 1972, Misener sandstone (Middle-Upper Devonian), north-central Oklahoma: American Association of Petroleum Geologists Bulletin, v. 56, no. 12, p. 2323–2334.
- Arthur, M. A., and Natland, J. H., 1979, Carbonaceous sediments in the North and South Atlantic: the role of salinity in stable stratification of Early Cretaceous basins, in Talwani, Manik, Hay, William, and Ryan, W. B. P., eds., *Deep drilling results in the Atlantic Ocean: continental margins and paleo-environment*: American Geophysical Union, Maurice Ewing Series 3, p. 375–401.
- Baker, P. A., and Kastner, Miriam, 1981, Constraints on the formation of sedimentary dolomite: *Science*, v. 213, no. 4504, p. 214–216.
- Barron, E. J., 1989, Severe storms during Earth history: Geological Society of America Bulletin, v. 101, no. 5, p. 601–612.
- Bolton, Keith, Lane, H. R., and LeMone, D. V., 1982, Symposium on the paleoenvironmental setting and distribution of the Waulsortian facies: El Paso Geological Society and The University of Texas at El Paso, 202 p.
- Bouma, A. H., 1962, *Sedimentology of some flysch deposits*: Amsterdam, Elsevier, 168 p.
- Broadhead, R. R., Kepferle, R. C., and Potter, P. E., 1982, Stratigraphic and sedimentologic controls of gas in shale—example from Upper Devonian of northern Ohio: American Association of Petroleum Geologists Bulletin, v. 66, no. 1, p. 10–27.
- Burrowes, O. G., and Krause, F. F., 1987, Overview of the Devonian System: subsurface of Western Canada Basin, in Krause, F. F., and Burrowes, O. G., eds., *Devonian lithofacies and reservoir styles in Alberta*, 13th CSPG Core Conference and Display and Second International Symposium on the Devonian System: Calgary, Canada, Canadian Society of Petroleum Geologists, p. 1–20.
- Byers, C. W., 1977, Biofacies patterns in euxinic basins: a general model, in Cook, H. E., and Enos, Paul, eds., *Deep-water carbonate environments*: Society of Economic Paleontologists and Mineralogists Special Publication No. 25, p. 5–17.
- Cardott, B. J., 1989, Thermal maturation of the Woodford Shale in the Anadarko Basin, in Johnson, K. S., ed., *Anadarko Basin Symposium, 1988*: Oklahoma Geological Survey Circular 90, p. 32–46.
- Cloud, P. E., Barnes, V. E., and Hass, W. H., 1957, Devonian-Mississippian transition in central Texas: Geological Society of America Bulletin, v. 68, no. 7, p. 807–816.
- Cluff, R. M., 1980, Paleoenvironment of the New Albany Shale Group (Devonian-Mississippian) of Illinois: *Journal of Sedimentary Petrology*, v. 50, no. 3, p. 767–780.
- Cluff, R. M., Reinbold, M. L., and Lineback, J. A., 1981, The New Albany Shale Group of Illinois: Illinois State Geological Survey Circular 518, 83 p.
- Comer, J. B., and Hinch, H. H., 1987, Recognizing and quantifying expulsion of oil from the Woodford Formation and age-equivalent rocks in Oklahoma and Arkansas: American Association of Petroleum Geologists Bulletin, v. 71, no. 7, p. 844–858.
- Davis, H. R., Byers, C. W., and Pratt, L. M., 1989, Depositional mechanisms and organic matter in Mowry Shale (Cretaceous), Wyoming: American Association of Petroleum Geologists Bulletin, v. 73, no. 9, p. 1103–1116.
- Demaison, G. J., and Moore, G. T., 1980, Anoxic environments and oil source bed genesis: American Association of Petroleum Geologists Bulletin, v. 64, no. 8, p. 1179–1209.
- Dow, W. G., 1977, Kerogen studies and geological interpretations: *Journal of Geochemical Exploration*, v. 7, no. 2, p. 77–79.
- Drake, D. E., 1976, Suspended sediment transport and mud deposition on continental shelves, in Stanley, D. J., and Swift, D. J. P., eds., *Marine sediment transport and environmental management*: New York, John Wiley, American Geological Institute, p. 127–158.
- Duncan, D. C., and Swanson, V. E., 1965, Organic-rich shale of the United States and world land areas: U.S. Geological Survey Circular 523, 30 p.
- Dutton, S. P., Goldstein, A. G., and Ruppel, S. C., 1982, Petroleum potential of the Palo Duro Basin, Texas Panhandle: The University of Texas at Austin, Bureau of Economic Geology Report of Investigations No. 123, 87 p.
- Ellison, S. P., Jr., 1950, Subsurface Woodford black shale, West Texas and southeast New Mexico: University of Texas, Austin, Bureau of Economic Geology Report of Investigations No. 7, 20 p.
- Ettensohn, F. R., 1987, Rates of relative plate motion during the Acadian orogeny based on the spatial distribution of black shales: *Journal of Geology*, v. 95, no. 4, p. 572–582.
- Ettensohn, F. R., and Barron, L. S., 1981, Depositional model for the Devonian-Mississippian black shales of North America: a paleoclimatic-paleogeographic approach, in Roberts, T. G., ed., *Geological Society of America Cincinnati '81 Field Trip Guidebooks*, v. II: Economic Geology, Structure, p. 344–361.
- Ettensohn, F. R., and Ham, T. D., 1985, Defining the nature and location of a Late Devonian-Early Mississippian pycnocline in eastern Kentucky: Geological Society of America Bulletin, v. 96, no. 10, p. 1313–1321.

- Ettensohn, F. R., Fulton, L. P., and Kepferle, R. C., 1979, Use of scintillometer and gamma-ray logs for correlation and stratigraphy in homogeneous black shales: *Geological Society of America Bulletin*, v. 90, part I, p. 421–423; part n, p. 828–849.
- Ewing, T. E., 1991, Tectonic map of Texas: The University of Texas at Austin, Bureau of Economic Geology, scale 1:750,000.
- Faill, R. T., 1985, The Acadian orogeny and the Catskill delta, *in* Woodrow, D. L., and Sevon, W. D., eds., *The Catskill delta: Geological Society of America Special Paper 201*, p. 15–37.
- Folk, R. L., 1959, Thin-section examination of pre-Simpson Paleozoic rocks, *in* Barnes, V. E., ed., *Stratigraphy of the pre-Simpson Paleozoic subsurface rocks of Texas and southeast New Mexico*, v. 1: Austin, University of Texas Publication No. 5924, p. 95–130.
- Folk, R. L., and Pittman, J. S., 1971, Length-slow chalcedony: a new testament for vanished evaporites: *Journal of Sedimentary Petrology*, v. 41, no. 4, p. 1045–1058.
- Francis, B. M., 1988, Petrology and sedimentology of the Devonian Misener Formation, north-central Oklahoma: University of Tulsa, Master's thesis, 176 p.
- Freeman, Tom, and Schumacher, Dietmar, 1969, Qualitative pre-Sylamore (Devonian-Mississippian) physiography delineated by onlapping conodont zones, northern Arkansas: *Geological Society of America Bulletin*, v. 80, no. 11, p. 2327–2334.
- Frezon, S. E., and Jordan, Louise, 1979, Oklahoma, *in* Craig, L. G., and Connor, C. W., coordinators, *Paleotectonic investigations of the Mississippian System in the United States*, part I, Introduction and regional analyses of the Mississippian system: U.S. Geological Survey Professional Paper 1010-1, p. 146–159.
- Galley, J. E., 1958, Oil and geology in the Permian Basin of Texas and New Mexico, *in* Weeks, L. G., ed., *Habitat of oil: Tulsa, Oklahoma*, American Association of Petroleum Geologists, p. 395–446.
- Click, E. E., 1979, Arkansas, *in* Craig, L. C., and Connor, C. W., coordinators, *Paleotectonic investigations of the Mississippian System in the United States*, part I, Introduction and regional analyses of the Mississippian System: U.S. Geological Survey Professional Paper 1010-H, p. 125–145.
- Graves, R. W., 1952, Devonian conodonts from the Caballos Novaculite: *Journal of Paleontology*, v. 26, no. 4, p. 610–612.
- Ham, W. E., 1969, Regional geology of the Arbuckle Mountains, Oklahoma, *in* Ham, W. E., ed., *Geology of the Arbuckle Mountains: Oklahoma Geological Survey Guidebook 17*, p. 5–21.
- Ham, W. E., and Wilson, J. L., 1967, Paleozoic epeirogeny and orogeny in the central United States: *American Journal of Science*, v. 265, p. 332–407.
- Harlton, B. H., 1956, The Harrisburg Trough, Stephens and Carter Counties, Oklahoma, *in* Hicks, I. C., Westheimer, J. M., Thomlinson, C. W., Putman, D. M., and Selk, E. L., eds., *Petroleum geology of southern Oklahoma*, a symposium, v. 1; sponsored by the Ardmore Geological Society: Tulsa, American Association of Petroleum Geologists, p. 135–143.
- Hass, W. H., 1951, Age of Arkansas Novaculite: *American Association of Petroleum Geologists Bulletin*, v. 35, no. 12, p. 2526–2541.
- Hass, W. H., and Huddle, J. W., 1965, Late Devonian and Early Mississippian age of the Woodford Shale in Oklahoma, as determined from conodonts: U.S. Geological Survey Professional Paper 525-D, p. D125–D132.
- Hayes, M. O., 1967, Hurricanes as geological agents, south Texas coast: *American Association of Petroleum Geologists Bulletin*, v. 51, no. 6, p. 937–942.
- Heckel, P. H., 1977, Origin of phosphatic black shale facies in Pennsylvanian cyclothems of Mid-Continent North America: *American Association of Petroleum Geologists Bulletin*, v. 61, no. 7, p. 1045–1068.
- Heckel, P. H., and Witzke, B. J., 1979, Devonian world palaeogeography determined from distribution of carbonates and related lithic palaeoclimatic indicators, *in* House, M. R., Scrutton, C. T., and Bassett, M. G., eds., *The Devonian System: Special Papers in Palaeontology No. 23*, p. 99–123.
- Hein, J. R., and Parrish, J. T., 1987, Distribution of siliceous deposits in space and time, *in* Hein, J. R., ed., *Siliceous sedimentary rock-hosted ores and petroleum: New York, Van Nostrand Reinhold*, p. 10–57.
- Hills, J. M., 1984, Sedimentation, tectonism, and hydrocarbon generation in Delaware Basin, West Texas and southeastern New Mexico: *American Association of Petroleum Geologists Bulletin*, v. 68, no. 3, p. 250–267.
- Hoenig, M. A., 1976, Stratigraphy of the “Upper Silurian” and “Lower Devonian,” Permian Basin, West Texas: The University of Texas at El Paso, Master's thesis, 81 p.
- Horak, R. L., 1985, Tectonic and hydrocarbon maturation history in the Permian Basin: *Oil and Gas Journal*, v. 83, no. 21, p. 124–129.
- Huffman, G. G., 1958, Geology of the flanks of the Ozark uplift: *Oklahoma Geological Survey Bulletin No. 77*, 281 p.
- Huffman, G. G., and Starke, J. M., 1960, Noel shale in northeastern Oklahoma: *Oklahoma Geology Notes*, v. 20, p. 159–163.
- Hunt, J. M., 1979, *Petroleum geochemistry and geology*: San Francisco, Freeman, 617 p.
- Johnson, J. G., Klapper, Gilbert, and Sandberg, C. A., 1985, Devonian eustatic fluctuations in Euramerica: *Geological Society of America Bulletin*, v. 96, no. 5, p. 567–587.
- Jones, T. S., and Smith, H. M., 1965, Relationships of oil composition and stratigraphy in the Permian Basin of West Texas and New Mexico, *in* Young, Addison, and Galley, J. E., eds., *Fluids in subsurface environments: Tulsa, American Association of Petroleum Geologists*, p. 101–224.
- Keroher, G. C., and others, 1966, *Lexicon of geologic names of the United States for 1936–1960*: U.S. Geological Survey Bulletin 1200, part 3, P-Z, p. 4292–4293.
- King, P. B., King, R. E., and Knight, J. B., 1945, Geology of the Hueco Mountains, El Paso and Hudspeth Counties, Texas: U.S. Geological Survey, Oil and Gas Investigations Preliminary Map 36.
- Kottlowski, F. E., 1963, Paleozoic and Mesozoic strata of southwestern and south-central New Mexico: *New Mexico Bureau of Mines and Mineral Resources Bulletin 79*, p. 24–32.
- Landis, E. R., 1962, Uranium and other trace elements in Devonian and Mississippian black shales in the central Midcontinent area: *U.S. Geological Survey Bulletin 1107-E*, p. 289–336.
- Laudon, L. R., and Bowsher, A. L., 1949, Mississippian formations of southwestern New Mexico: *Geological Society of America Bulletin*, v. 60, no. 1, p. 1–88.

- Leggett, J. K., 1980, British lower Paleozoic black shales and their paleo-oceanographic significance: *Geological Society of London Journal*, v. 137, pt. 2, p. 139–156.
- LeMone, D. V., 1971, General stratigraphy of the Franklin Mountains, *in* Robledo Mountains, New Mexico, Franklin Mountains, Texas, 1971 Field Conference: Society of Economic Paleontologists and Mineralogists Permian Basin Section Publication 71-13, p. ix.
- Leventhal, J. S., 1981, Pyrolysis gas chromatography-mass spectrometry to characterize organic matter and its relationship to uranium content of Appalachian Devonian black shales: *Geochimica et Cosmochimica Acta*, v. 45, no. 6, p. 883–889.
- Lindberg, F. A., ed., 1983, Correlation of Stratigraphic Units of North America (COSUNA) Project, Southwest/Southwest Mid-Continent Region: Tulsa, American Association of Petroleum Geologists.
- Lloyd, E. R., 1949, Pre-San Andres stratigraphy and oil-producing zones in southeastern New Mexico: *New Mexico Bureau of Mines and Mineral Resources Bulletin* 29, 87 p.
- Lowe, D. R., 1975, Regional controls on silica sedimentation in the Ouachita system: *Geological Society of America Bulletin*, v. 86, no. 8, p. 1123–1127.
- Lucia, F. J., 1971, Lower Paleozoic history of the western Diablo Platform, West Texas and south central New Mexico, *in* Robledo Mountains, New Mexico, Franklin Mountains, Texas, 1971 Field Conference: Society of Economic Paleontologists and Mineralogists Permian Basin Section Guidebook Publication 71-13, p. 174–214.
- Maldonado, Andres, and Stanley, D. J., 1978, Nile cone depositional processes and patterns in the Late Quaternary, *in* Stanley, D. J., and Kelling, Gilbert, eds., *Sedimentation in submarine canyons, fans, and trenches: Stroudsburg, Pennsylvania, Dowden, Hutchinson and Ross*, p. 239–257.
- Marsaglia, K. M., and Klein, G. deV., 1983, The paleogeography of Paleozoic and Mesozoic storm depositional systems: *Journal of Geology*, v. 91, no. 4, p. 117–142.
- Mapel, W. J., Johnson, R. B., Bachman, G. O., and Varnes, K. L., 1979, Southern Midcontinent and southern Rocky Mountain region, *in* Paleotectonic investigations of the Mississippian System in the United States, part I, Introduction and regional analyses of the Mississippian System: U.S. Geological Survey Professional Paper 1010-J, p. 160–187.
- McGlasson, E. H., 1967, The Siluro-Devonian of West Texas and southeast New Mexico, *in* Oswald, D. H., ed., International symposium on the Devonian System: Calgary, Canada, Alberta Society of Petroleum Geologists, v. 2, p. 935–948.
- Meissner, F. F., 1978, Petroleum geology of the Bakken Formation, Williston Basin, North Dakota and Montana: Montana Geological Society 24th Annual Conference, 1978 Williston Basin Symposium, p. 207–227.
- Mooers, C. N. K., 1976a, Introduction to the physical oceanography and fluid dynamics of continental margins, *in* Stanley, D. J., and Swift, D. J. P., eds., *Marine sediment transport and environmental management*: New York, John Wiley, p. 7–21.
- 1976b, Wind-driven currents on the continental margin, *in* Stanley, D. J., and Swift, D. J. P., eds., *Marine sediment transport and environmental management*: New York, John Wiley, p. 29–52.
- Morton, J. P., 1985, Rb-Sr dating of diagenesis and source age of clays in Upper Devonian black shales of Texas: *Geological Society of America Bulletin*, v. 96, no. 8, p. 1043–1049.
- Morton, R. A., 1981, Formation of storm deposits by wind-forced currents in the Gulf of Mexico and the North Sea, *in* Nio, S. D., Shattenhelm, R. T. E., and Van Weering, T. C. E., eds., *Holocene marine sedimentation in the North Sea Basin: International Association of Sedimentologists Special Publication* 5, p. 385–396.
- 1988, Nearshore responses to great storms, *in* Clifton, H. E., ed., *Sedimentologic consequences of convulsive geologic events: Geological Society of America Special Paper* 229, p. 7–22.
- Muehlberger, W. R., 1980, Texas lineament revisited: New Mexico Geological Society Guidebook, 31st Field Conference, Trans-Pecos Region, p. 113–121.
- Munn, J. K., 1971, Breedlove field, Martin County, Texas: *American Association of Petroleum Geologists Bulletin*, v. 55, no. 3, p. 403–411.
- Nelson, C. H., 1982, Modern shallow-water graded sand layers from storm surges, Bering Shelf: a mimic of Bouma sequences and turbidite systems: *Journal of Sedimentary Petrology*, v. 52, no. 2, p. 537–545.
- Odin, G. S., and Letolle, Rene, 1980, Glauconitization and phosphatization environments: a tentative comparison, *in* Bentor, Y. K., ed., *Marine phosphorites—geochemistry, occurrence, genesis: Society of Economic Paleontologists and Mineralogists Special Publication No. 29*, p. 227–237.
- Park, D. E., and Croneis, Carey, 1969, Origin of Caballos and Arkansas Novaculite formations: *American Association of Petroleum Geologists Bulletin*, v. 53, no. 1, p. 94–111.
- Parrish, J. T., 1982, Upwelling and petroleum source beds, with reference to Paleozoic: *American Association of Petroleum Geologists Bulletin*, v. 66, no. 6, p. 750–774.
- Parrish, J. T., and Barron, E. J., 1986, Paleoclimates and economic geology: *Society of Economic Paleontologists and Mineralogists Short Course Notes No. 18*, 162 p.
- Pashin, J. C., and Ettensohn, F. R., 1987, An epeiric shelf-to-basin transition: Bedford-Berea sequence, northeastern Kentucky and south-central Ohio: *American Journal of Science*, v. 287, p. 893–926.
- Pedersen, T. F., and Calvert, S. E., 1990, Anoxia vs. productivity: what controls the formation of organic-carbon-rich sediments and sedimentary rocks: *American Association of Petroleum Geologists Bulletin*, v. 74, no. 4, p. 454–466.
- Peirce, F. L., 1962, Devonian cavity fillings in subsurface Silurian carbonates of West Texas: *American Association of Petroleum Geologists Bulletin*, v. 46, no. 1, p. 122–124.
- Pierce, J. W., 1976, Suspended sediment transport at the shelf break and over the outer margin, *in* Stanley, D. J., and Swift, D. J. P., eds., *Marine sediment transport and environmental management*: New York, John Wiley, p. 437–458.
- Piper, D. J. W., 1978, Turbidite muds and silts on deep sea fans and abyssal plains, *in* Stanley, D. J., and Kelling, Gilbert, eds., *Sedimentation in submarine canyons, fans, and trenches: Stroudsburg, Pennsylvania, Dowden, Hutchinson and Ross*, p. 163–176.
- Pittenger, H. A., 1981, Provenance, depositional environment and diagenesis of the Sylamore sandstone in northeastern Oklahoma and northern Arkansas: University of Tulsa, Master's thesis, 109 p.

- Poole, F. G., 1974, Flysch deposits of Antler foreland basin, western United States, *in* Dickinson, W. R., ed., *Tectonics and sedimentation: Society of Economic Paleontologists and Mineralogists Special Publication No. 22*, p. 58–82.
- Poole, R. G., Baars, D. L., Drewes, Harald, Hayes, P. T., Ketner, K. B., McKee, E. D., Teichert, Curt, and Williams, J. S., 1967, Devonian of the southwestern United States, *in* Oswald, D. H., ed., *International symposium on the Devonian System, v. 1: Calgary, Canada, Alberta Society of Petroleum Geologists*, p. 879–912.
- Potter, P. E., Maynard, J. B., and Pryor, W. A., 1982, Appalachian gas bearing Devonian shales: statements and discussions: *Oil and Gas Journal*, v. 80, no. 4, p. 290–318.
- Pratt, L. M., 1984, Influence of paleoenvironmental factors on preservation of organic matter in middle Cretaceous Greenhorn Formation, Pueblo, Colorado: *American Association of Petroleum Geologists Bulletin*, v. 68, no. 9, p. 1146–1159.
- Pray, L. C., 1961, Geology of the Sacramento Mountains escarpment, Otero County, New Mexico: *New Mexico Bureau of Mines and Mineral Resources Bulletin 35*, 144 p.
- Rhoads, D. C., and Morse, J. W., 1971, Evolutionary and ecologic significance of oxygen-deficient marine basins: *Lethaia*, v. 4, no. 4, p. 413–428.
- Roen, J. B., 1984, Geology of the Devonian black shales of the Appalachian basin: *Organic Geochemistry*, v. 5, no. 4, p. 241–254.
- Rosado, R. V., 1970, Devonian stratigraphy of south-central New Mexico and far West Texas: *The University of Texas at El Paso, Master's thesis*, 108 p.
- Ruppel, S. C., 1985, Stratigraphy and petroleum potential of pre-Pennsylvanian rocks, Palo Duro Basin, Texas Panhandle: *The University of Texas at Austin, Bureau of Economic Geology Report of Investigations No. 147*, 81 p.
- Schieber, Jiirgen, 1987, Storm-dominated epicontinental clastic sedimentation in the mid-Proterozoic Newland Formation, Montana, U.S.A.: *Neues Jahrbuch fur Geologic und Palaontologie Monatshefte*, v. 7, p. 417–439.
- Sholkovitz, Edward, and Soutar, Andrew, 1975, Changes in the composition of the bottom water of the Santa Barbara Basin: effect of turbidity currents: *Deep-Sea Research*, v. 22, no. 1, p. 13–21.
- Schopf, T. J. M., 1983, Paleozoic black shales in relation to continental margin upwelling, *in* Thiede, John, and Suess, Erwin, eds., *Sedimentary records of ancient coastal upwelling: coastal upwelling, its sediment record, part B: New York, Plenum Press*, p. 579–596.
- Stanley, D. J., 1983, Parallel laminated deep-sea muds and coupled gravity flow-hemipelagic settling in the Mediterranean: *Smithsonian Contributions to the Marine Sciences No. 19*, 19 p.
- Stanley, D. J., and Maldonado, Andres, 1981, Depositional models for fine-grained sediment in the western Hellenic trench, eastern Mediterranean: *Sedimentology*, v. 28, no. 2, p. 273–290.
- Stein, Ruediger, 1986, Organic carbon and sedimentation rate—further evidence for anoxic deep-water conditions in the Cenomanian/Turonian Atlantic Ocean: *Marine Geology*, v. 72, no. 3/4, p. 199–209.
- Stevenson, F. V., 1945, Devonian of New Mexico: *Journal of Geology*, v. 53, p. 217–245.
- Stow, D. A. V., and Piper, D. J. W., 1984, Deep-water fine-grained sediments: facies models, *in* Stow, D. A. V., and Piper, D. J. W., eds., *Fine-grained sediments: deep-water processes and facies: Geological Society of London, Special Publication No. 15*, p. 611–646.
- Sutherland, P. K., and Manger, W. L., 1979, Comparison of Ozark shelf and Ouachita basin facies for Upper Mississippian and Lower Pennsylvanian series in eastern Oklahoma and western Arkansas, *in* Sutherland, P. K., and Manger, W. L., eds., *Ozark and Ouachita shelf-to-basin transition, Oklahoma-Arkansas: Norman, Oklahoma, Oklahoma Geological Survey Guidebook 19*, p. 1–13.
- Swanson, V. E., 1960, Oil yield and uranium content of black shales: *U.S. Geological Survey Professional Paper 356-A*, 44 p.
- 1961, Geology and geochemistry of uranium in marine black shales—a review: *U.S. Geological Survey Professional Paper 356-C*, 112 p.
- Swift, D. J. P., Figueiredo, A. G., Freeland, G. L., and Oertel, G. P., 1983, Hummocky cross-stratification and megaripples: a geological double standard: *Journal of Sedimentary Petrology*, v. 53, no. 4, p. 1295–1317.
- Taff, J. A., 1902, *Geological atlas of the United States: U.S. Geological Survey Atoka Folio No. 79*.
- Tissot, B. P., Demaison, G. J., Masson, Peter, Delteil, J. R., and Combaz, Andre, 1980, Paleoenvironment and petroleum potential of Middle Cretaceous black shale in Atlantic basins: *American Association of Petroleum Geologists Bulletin*, v. 64, no. 12, p. 2051–2163.
- Tissot, B. P., and Welte, D. H., 1984, *Petroleum formation and occurrence*, 2d ed.: New York, Springer-Verlag, 699 p.
- Walker, R. G., 1984, Turbidites and associated coarse clastic deposits, *in* Walker, R. G., ed., *Facies models*, 2d ed.: *Geoscience Canada, Reprint Series 1*, p. 171–188.
- 1985, Geological evidence for storm transportation and deposition on ancient shelves, *in* Tillman, R. W., Swift, D. J. P., and Walker, R. G., eds., *Shelf sands and sandstone reservoirs: Society of Economic Paleontologists and Mineralogists Short Course Notes 13*, p. 243–302.
- Walper, J. L., 1977, Paleozoic tectonics of the southern margin of North America: *Gulf Coast Association of Geological Societies Transactions*, v. 27, p. 230–241.
- Witzke, B. J., 1987, Models for circulation patterns in epicontinental seas applied to Paleozoic facies of North America craton: *Paleoceanography*, v. 2, no. 2, p. 229–248.
- Wright, W. F., 1979, *Petroleum geology of the Permian Basin: Midland, Texas, West Texas Geological Society*, 98 p.
- Zenger, D. H., 1972, Dolomitization and uniformitarianism: *Journal of Geological Education*, v. 20, no. 3, p. 107–124.

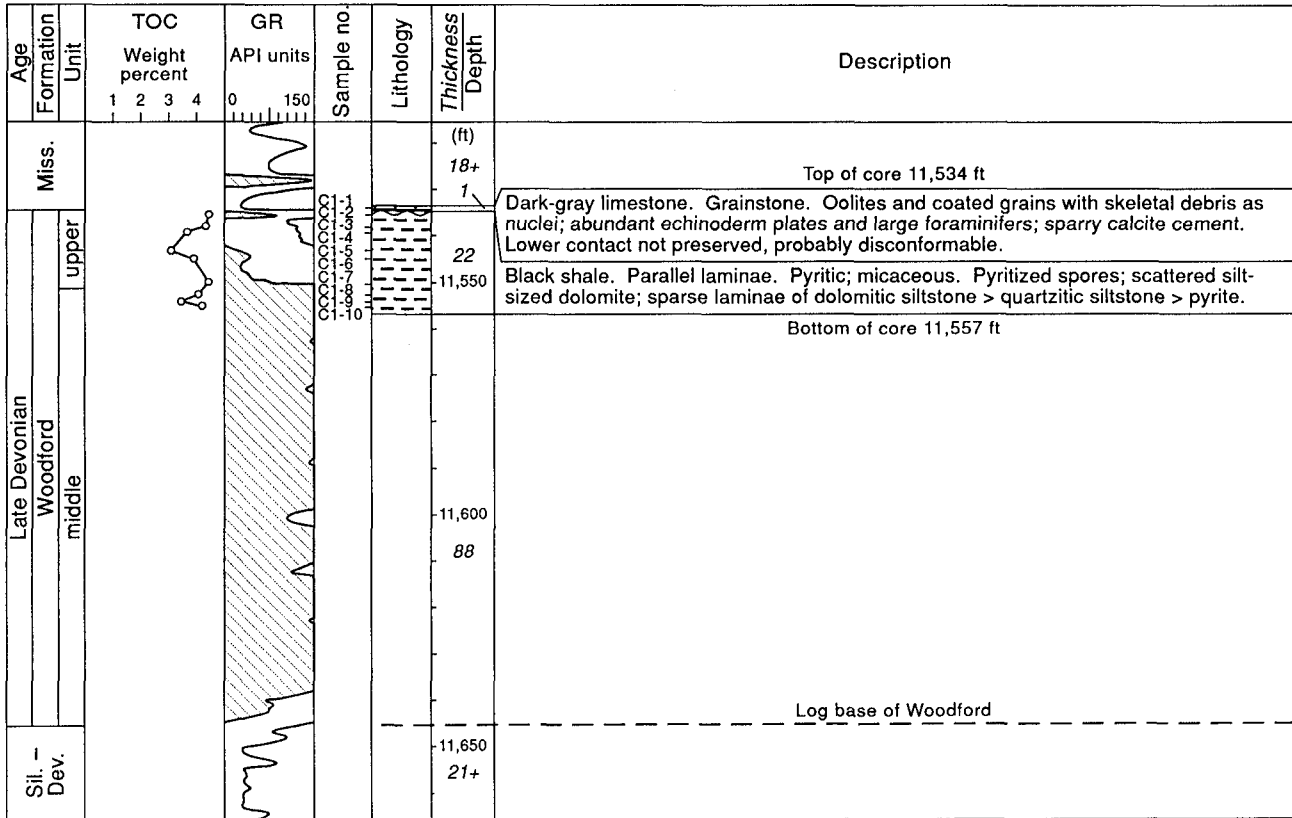
APPENDICES

Appendix A. Location of cores and measured sections.

Map symbol	Operator	Well	County	State	Location
Cores					
C1	Mobil	#1918 Parks Unit 2	Midland	Texas	Sec. 14, Block 40, C.F. O'Neal Survey
C2	Humble	#43 Yarborough & Allen	Ward	Texas	Sec. 66, E.J. Brady Survey
C3	Humble	#1 A. E. State	Lea	New Mexico	Sec. 16, T.15S., R.33E.
C4	Shell	#1 Champeau Federal	Chaves	New Mexico	Sec. 31, T.15S., R.30E.
C5	Pan American	#1 Walker	Cochran	Texas	Sec. 8, Block Z, PSL Survey
C6	Shell	#1 Chrieseman	Glasscock	Texas	Sec. 12, Block 36, T.5S., T&P Survey
C7	Standard of Texas	#1-28 Canon	Dawson	Texas	Sec. 28, Block 33, T.5N., T&P Survey
C8	Roden & Cosden	#1 Reed	Sterling	Texas	Sec. 9, Block 30, W&NW Survey
C9	Shell	#5 Pacific Royalty	Lea	New Mexico	Sec. 10, T.15S., R.37E.
C10	McGrath & Smith	#1 Brennand & Price	Mitchell	Texas	Sec. 7, Block 17, SPRR Survey
C11	Shell	A#1 Williamson	Gaines	Texas	Sec. 110, Block H, D&WRR Survey
C12	Shell	#1 Sealy Smith	Ward	Texas	Sec. 38, Block A, G&MMB&A Survey
C13	Humble	#1 Federal Elliott	Lea	New Mexico	Sec. 1, T.16S., R.34E.
Measured Sections					
P1	Bishop Gap		Doña Ana	New Mexico	Sec. 25, T.24S., R.3E.
P2	Anthony Gap, Northern Franklin Mountains		Doña Ana	New Mexico	Sec. 34, T.26S., R.4E.
P4	Martin Canyon, Hueco Mountains		El Paso	Texas	106°00'30" W. Longitude, 31°48'30" N. Latitude
Sections from Rosado (1970)					
R1	Magnolia	#1 University 39881	Hudspeth	Texas	Sec. 19, Block C, University Lands Survey
R2	Gulf	#1 Munson Federal	Chaves	New Mexico	Sec. 28, T.19S., R.18E.
R3	Alamo Canyon, Sacramento Mountains		Otero	New Mexico	Sec. 2, T.17S., R.10E.

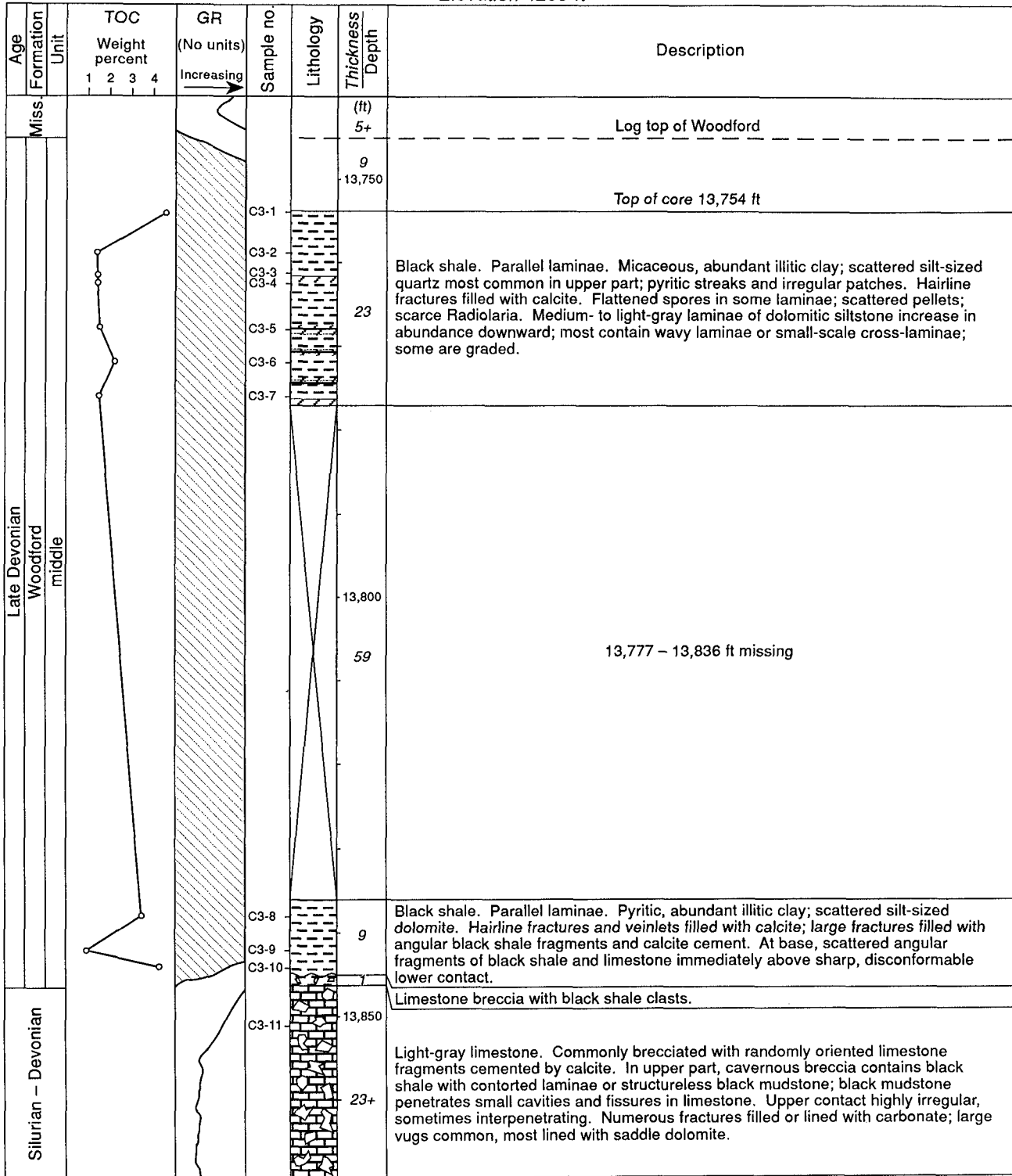
Appendix B. Description of cores and measured sections. For map locations, see figure 2 and plates 1 and 2.

C1
 Mobil No. 1918, Parks Unit 2
 Midland County, Texas
 Section 14, Block 40, C. F. O'Neal Survey
 Elevation 2825 ft



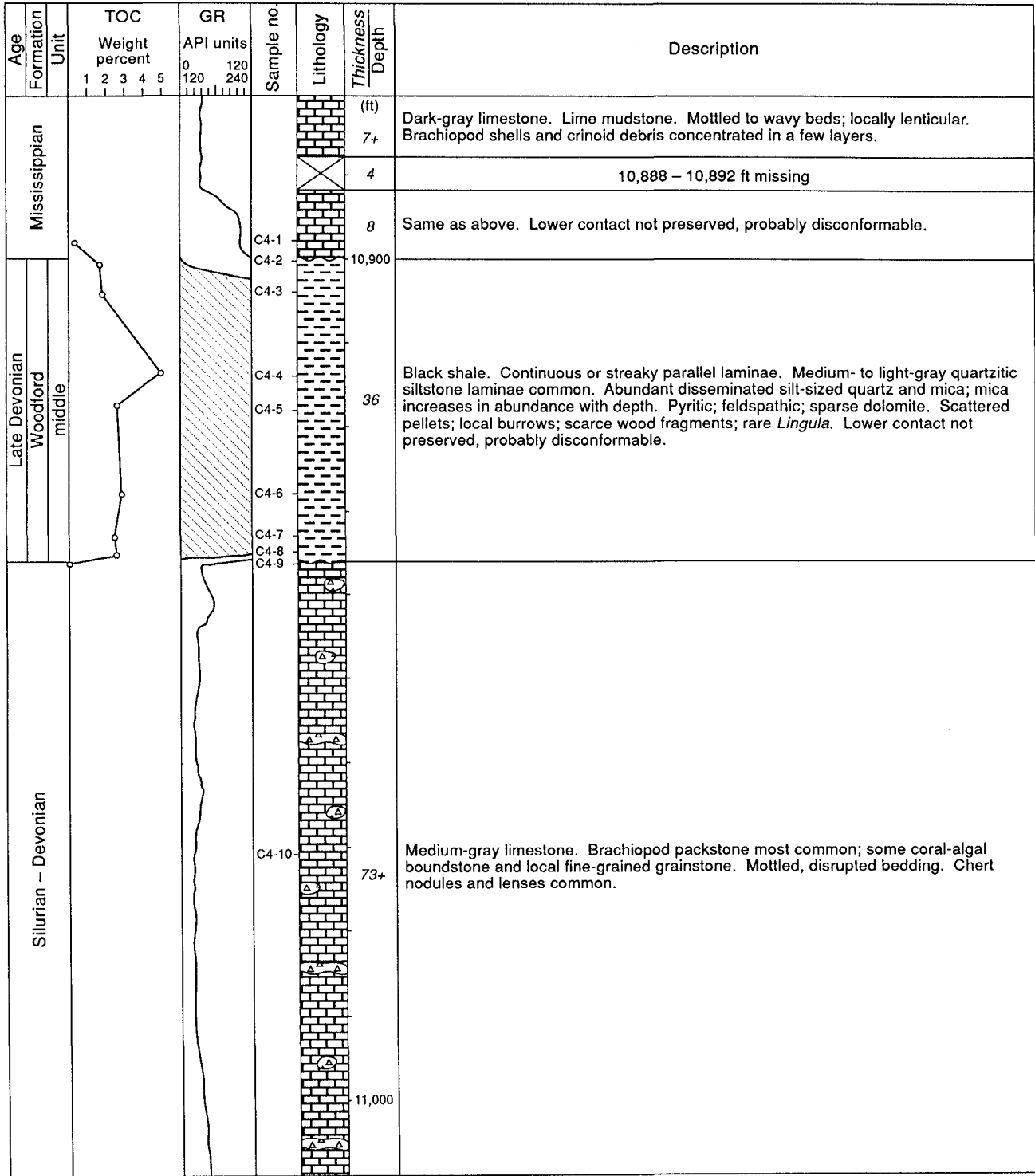
QA 14570c

C3
Humble No. 1 A. E. State
Lea County, New Mexico
Section 16, T 15 S – R 33 E
Elevation 4203 ft



QA 14572c

C4
 Shell No. 1 Champeau Federal
 Chaves County, New Mexico
 Section 31, T 15 S – R 30 E
 Elevation 3923 ft



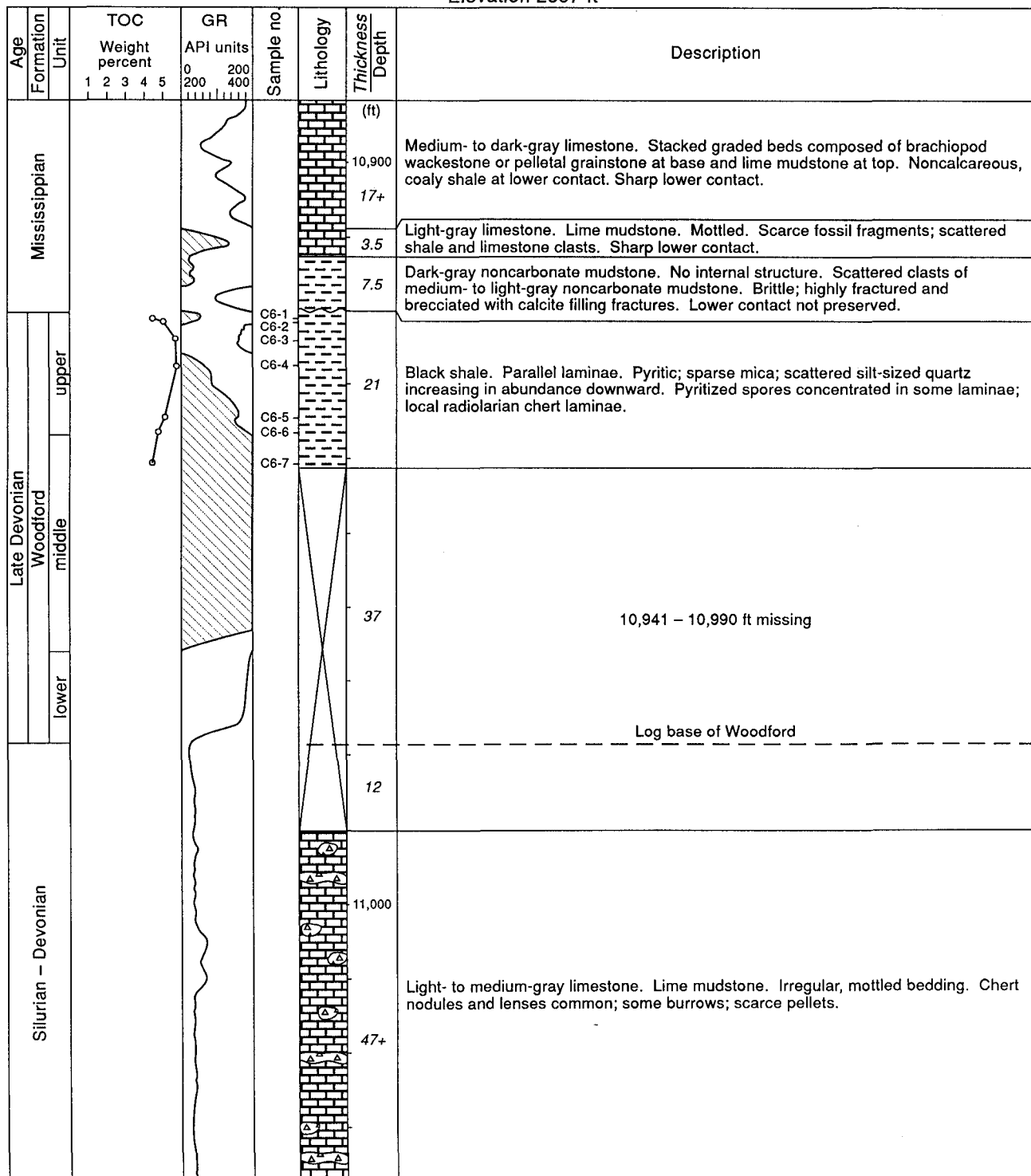
QA 14573c

C5
 Pan American No. 1 Walker
 Cochran County, Texas
 Section 8, Block Z, PSL Survey
 Elevation 3883 ft

Age Formation Unit	TOC Weight percent			GR API units		Sample no.	Lithology	Thickness Depth	Description
	1	2	3	0	100				
Mississippian						C5-1		31+	Medium- to dark-gray limestone. Mottled to wavy beds; graded beds composed of brachiopod wackestone overlain by mottled lime mudstone; rare cross-stratified fine grainstone overlain by burrowed lime mudstone. Lower contact not preserved.
	Late Devonian Woodford lower						C5-2		19
					C5-3		8.5	Medium- to dark-gray quartzitic siltstone. Mottled to wavy beds; dark-gray shale layers common. Dolomitic; micaceous; feldspathic. Local burrows. Sharp lower contact.	
					C5-4		3.5	Light-gray quartzitic siltstone. Well-sorted coarse silt. Low-angle simple cross-laminae between horizontal laminae; 1 – 3-cm strata. Dolomitic, feldspathic, micaceous. Sharp lower contact.	
					C5-5		19.5	Light-gray quartzitic siltstone. Well-sorted coarse silt. Low-angle simple cross-laminae between horizontal laminae; 1 – 3-cm strata. Dolomitic, feldspathic, micaceous. Sharp lower contact.	
					C5-6		0.5	Light-gray quartzitic siltstone. Well-sorted coarse silt. Low-angle simple cross-laminae between horizontal laminae; 1 – 3-cm strata. Dolomitic, feldspathic, micaceous. Sharp lower contact.	
					C5-7		11,700	Medium- to dark-gray quartzitic siltstone. Mottled, discontinuous, and wavy beds. Dark-gray shale layers common. Dolomitic, micaceous, feldspathic. Local burrows. Lower contact sharp and irregular but conformable.	
					C5-8		31	Light-gray to black speckled conglomeratic sandstone. Phosphatic chert arenite. No internal structure. Abundant chert grains, mostly sand-sized, some granule- to pebble-sized. Abundant phosphatic fossil fragments; some phosphatic ooids and large coprolites; scattered sand-sized quartz; scarce mica. Lower contact sharp, irregular, and disconformable.	
					C5-9		65	Light-gray limestone. Fine-grained grainstone and brachiopod packstone; local boundstone. Irregular, discontinuous beds. Chert nodules and lenses common.	
								11,720 - 11,785 ft missing	
Silurian – Devonian							C5-10		17.5+
						C5-11		11,800	

QA 14574c

C6
 Shell No. 1 Chriesman
 Glasscock County, Texas
 Section 12, Block 36, T 5 S, T and P Survey
 Elevation 2697 ft



QA 14575c

C7
 Standard of Texas No. 1-28 Canon
 Dawson County, Texas
 Section 28, Block 33, T 5 N, T and P Survey
 Elevation 2711 ft

Age Formation Unit	TOC Weight percent					GR API units			Sample no.	Lithology	Thickness Depth	Description
	1	2	3	4	5	0	125	250				
Mississippian											(ft)	
											14+	
Log top of Woodford												
Late Devonian Woodford middle											10	
Top of core 10,174 ft												
Silurian Fusselman						C7-1 C7-2 C7-3					3	Black shale. Continuous, discontinuous, and wavy parallel laminae. Pyritic; clay-rich. Scattered grains of silt-sized quartz, dolomite, and mica. Scattered pellets; sparse wood fragments; scarce conodonts. Lower contact not preserved.
											26	Pale brown to pink and light-gray finely crystalline dolostone. No obvious bedding. Chert nodules and lenses common. Lower contact not preserved, possibly gradational.
											10,200	
Ordovician Montoya Sylvan											1	
											5	Green shale. Platy parting. Clay-rich. Grades from pale green and dolomitic above into medium green and nondolomitic below.
Bottom of core 10,204 ft												
											6+	
Log base of Sylvan												

QA 14576c

C8
 Roden and Cosden No. 1 Reed
 Sterling County, Texas
 Section 9, Block 30, W and NW Survey
 Elevation 2569 ft

Age	Formation Unit	TOC			GR		Sample no.	Lithology	Thickness Depth	Description
		Weight percent	1	2	3	API units				
Late Devonian	Miss. Woodford upper								(ft)	
									5+	
	9000									
Late Devonian	Woodford middle								38	
									Top of core 9033 ft	
Ordovician	Sylv.						C8-1 C8-2		5	Black shale. Wavy laminae. Pyritic; micaceous; scattered grains of silt-sized quartz; sparse dolomite. Lower contact not preserved.
									3	Green shale. Platy parting. Clay-rich. Lower contact not preserved, possibly conformable.
	Montoya									
33+										

QA 14577c

C9
 Shell No. 5 Pacific Royalty
 Lea County, New Mexico
 Section 10, T 15 S – R 37 E
 Elevation 3814 ft

Age Formation Unit	TOC Weight percent					GR µgm Ra- eq/ton				Sample no.	Lithology	Thickness Depth	Description	
	1	2	3	4	5	1	2	3	4					
Mississippian Late Devonian Woodford middle lower Silurian – Devonian												(ft)	Medium- to dark-gray limestone. Lime mudstone with a few thin beds of brachiopod wackestone and skeletal and pellet grainstone. Some intervals highly fractured; all fractures are filled, some with calcite, some with silica. Lower contact not preserved, probably conformable.	
												35+		
												12,200		
													5	Green limestone. Clay rich. Lower contact not preserved, probably disconformable.
														C9-1
														C9-2
														C9-3
														C9-4
														C9-5
														C9-6
														C9-7
														C9-8
													73	Medium-gray dolomitic siltstone. Abundant silt-sized anhedral and subhedral dolomite; silt-sized quartz common. Interbedded and interlaminated dark-gray shale and medium-gray fine-grained calcite grainstone, packstone, and lime mudstone. Wavy to discontinuous beds near top; becomes more discontinuous, contorted, and mottled downward; shales have parallel to wavy laminae. Pyritic; micaceous. Sparse burrows; rare <i>Lingula</i> and wood fragments. Grades downward into lighter gray dolomitic siltstone with fewer shale interbeds. Lower contact not preserved, probably disconformable.
												12,300		
													C9-9	
													C9-10	
													C9-11	
													C9-12	
												8	Pale brownish-pink crystalline dolostone. Vuggy.	
													C9-13	
												4	Medium-gray shale. Dolomitic; silty.	
												69+	Pale brownish-pink crystalline dolostone. Vuggy.	
												12,400		

QA 14578c

C10
 McGrath and Smith No. 1 Brennan and Price
 Mitchell County, Texas
 Section 7, Block 17, SPRR Survey
 Elevation 2332 ft

Age	Formation	TOC					Res -ohms m ² /m	Sample no	Lithology	Thickness Depth	Description
		1	2	3	4	5					
Mississippian										(ft)	
										8440	Medium- to dark-gray limestone. Fine-grained grainstone with sparse interbeds of fossiliferous grainstone and wackestone. Parallel laminae or thin beds; some beds lenticular, others mottled, some graded. Scattered thin dolomitic beds and lenses. Fossils include disarticulated shells and fragments of brachiopods, bryozoans, crinoids, and ostracodes; scarce pellets; sparse burrows. Chert nodules and lenses common, some spiculitic. Fractures common. Lower contact sharp and disconformable.
Late Devonian	Woodford							C10-1		23+	Uppermost Woodford. No internal structures. Crushed, thin-walled brachiopods, many still articulated; trilobite carapaces; black shale clasts; scattered glauconite pellets and organic matter; phosphatic debris. Lower contact locally sharp or abruptly gradational.
										1	Black shale. Parallel to wavy laminae. Pyritic; slightly calcareous. Scattered spores, most filled with pyrite or silica, some replaced by pyrite; scattered brachiopod and trilobite fragments near top.
										8470	
										35	8459 – 8494 ft missing
Silurian - Devonian								C10-2		8	Black shale. Indistinct laminae; essentially parallel but discontinuous. Pyritic; abundant silt-sized quartz and dolomite; micaceous; scattered spores and Radiolaria. Scarce dolomitic siltstone laminae containing scattered silt-sized chert grains and nodules, glauconite, well-rounded sand-sized quartz, and phosphatic debris; sparsely burrowed.
								C10-3		8500	8502 – 8510 ft missing
								C10-4		8	Dark-gray shale. Discontinuous to lenticular laminae. Clay-rich. Scattered lenses of coarse-grained, glauconitic, sparsely burrowed siltstone containing nearly equal proportions of silt-sized quartz and dolomite. Lower contact not preserved, probably disconformable.
								C10-5		3	Medium-gray dolostone. Fine- to medium-grained, glauconitic grainstone. Bedding indistinct; locally mottled and burrowed.
										6	Light-gray to white dolostone. Grainstone. Mottled to lenticular beds. Mixed lithic clasts; glauconite; chert nodules and lenses common.
								6	Light-gray to pale brownish-pink dolostone. Fine-grained grainstone. Bedding indistinct; locally mottled and burrowed.		
								4+			

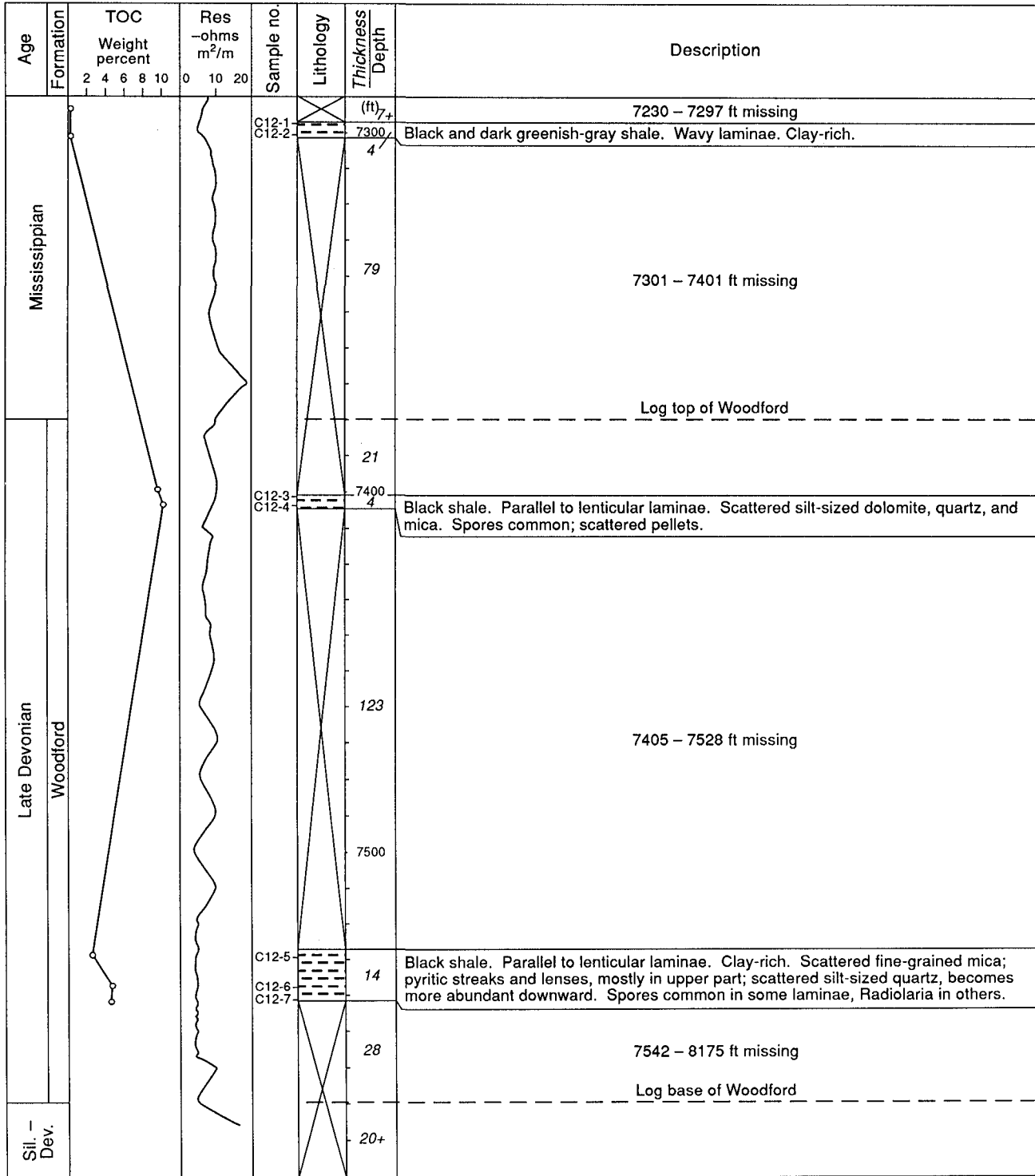
QA 14579c

C11
 Shell A No. 1 Williamson
 Gaines County, Texas
 Section 110, Block H, D and W RR Survey
 Elevation 3229 ft

Age Formation Unit	TOC Weight percent		GR μgm Ra-eq/ton	Sample no.	Lithology	Thickness Depth	Description
	1	2					
Mississippian						(ft)	
						12,950	
						81+	Medium- to dark-gray limestone. Fine-grained grainstone. Bedding thin, discontinuous to wavy; locally mottled and burrowed. Chert nodules and lenses common, many spiculitic. Scattered pyrite; sparse glauconitic beds. Fractures common, some filled with calcite, some with silica. Lower contact not preserved, probably disconformable.
						13,000	
				C11-1			
				C11-2			
				C11-3			
				C11-4			
				C11-5			
				C11-6			
				C11-7			
Late Devonian Woodford lower						42	Medium- to greenish-gray quartzitic siltstone. Abundant silt-sized quartz and subequal amounts of silt-sized dolomite. Interbedded and interlaminated dark-gray shale and rare fine-grained calcite grainstone and lime mudstone. Siltstone layers mottled to discontinuous, also contorted and wavy; local burrows; shales have parallel to wavy laminae. Pyritic; some layers micaceous; scattered glauconite. Lower contact not preserved, probably disconformable.
						13,050	
				C11-8			
				C11-9			
Sil. - Dev.						11+	Pale brownish-pink dolostone. Vuggy with dolomite crystals lining vugs.
				C11-10			
			C11-11				

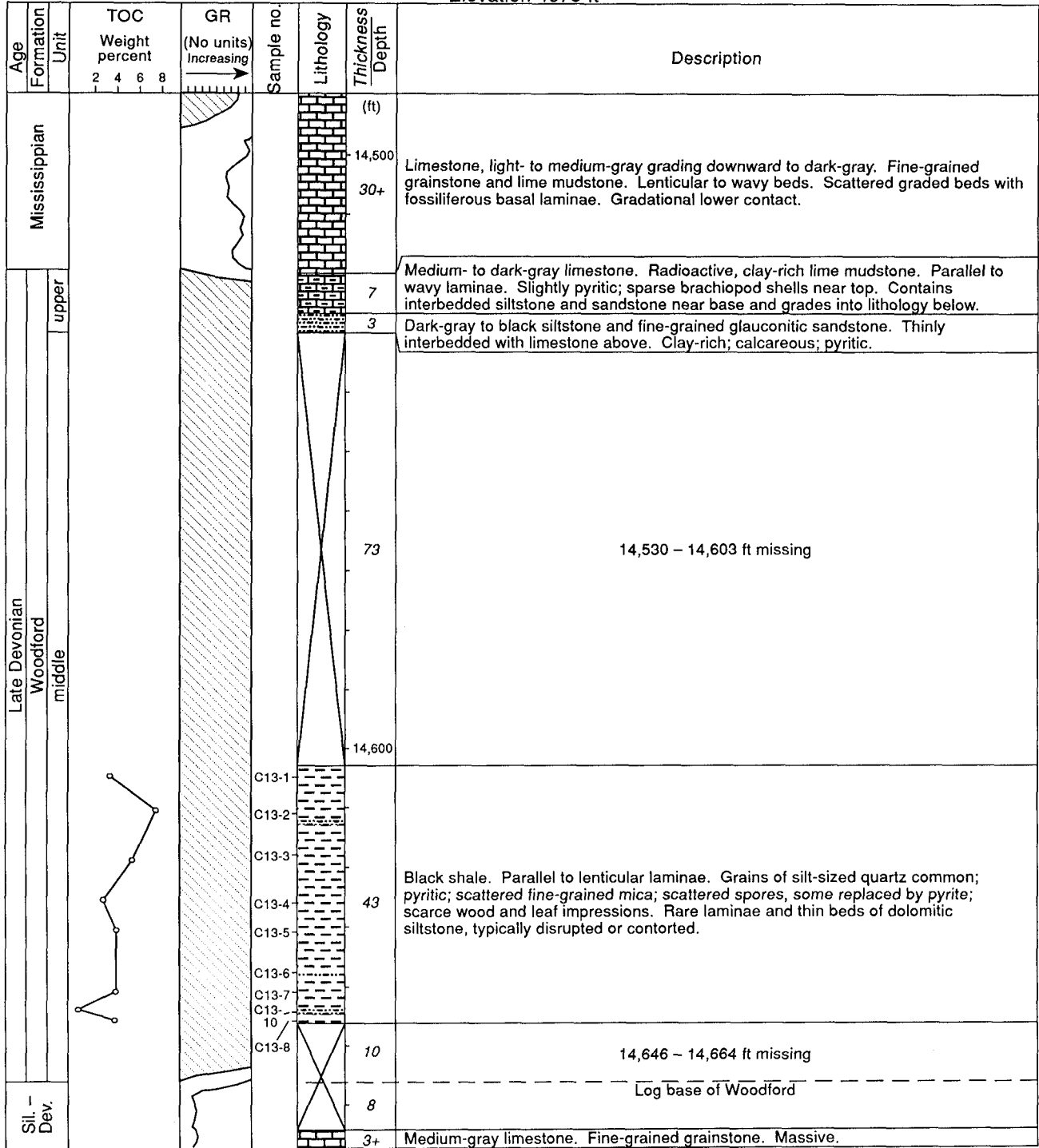
QA 14580c

C12
 Shell No. 1 Sealy Smith
 Ward County, Texas
 Section 38, Block A, G and MMB and A Survey
 Elevation 2736 ft



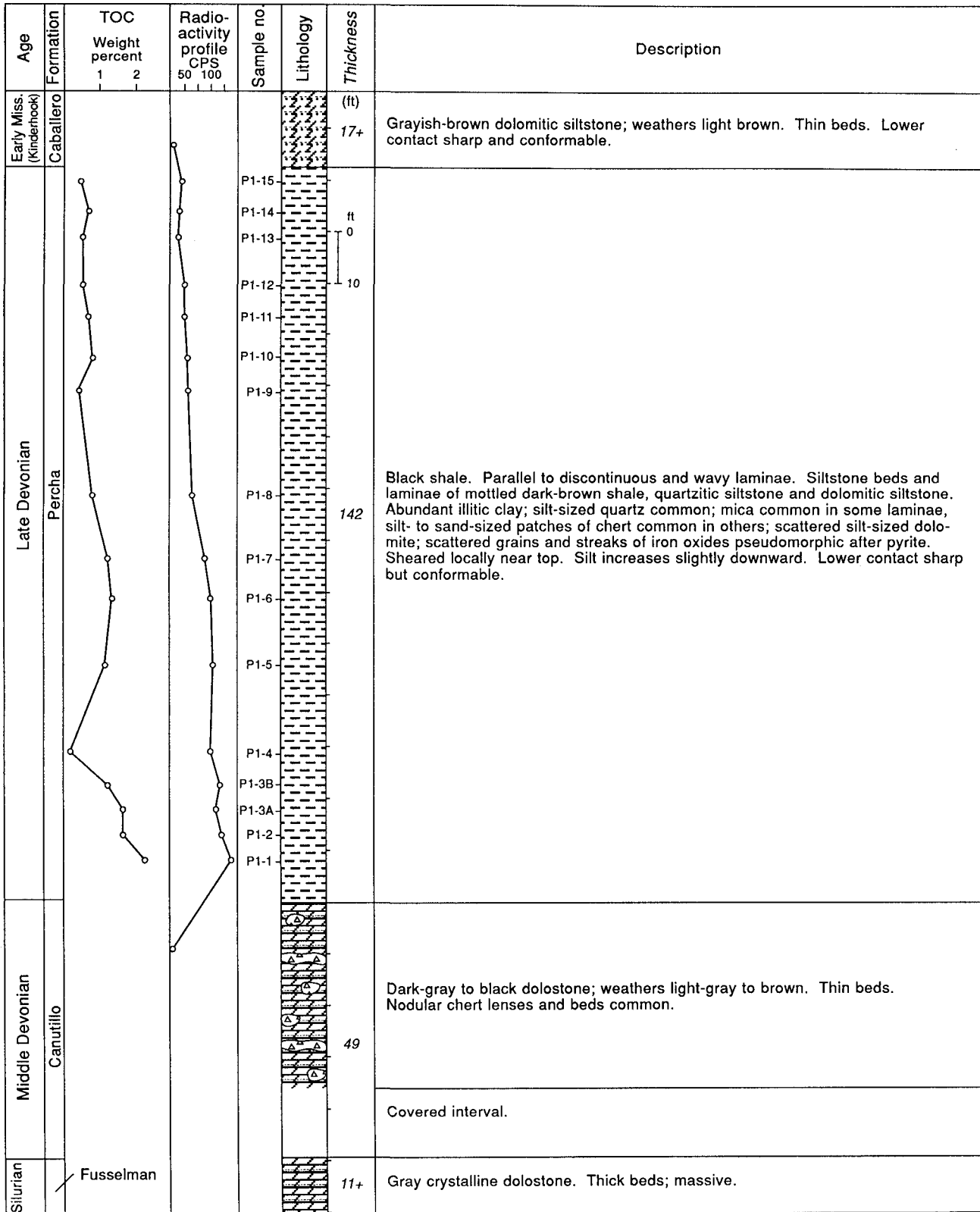
QA 14581c

C13
 Humble No. 1 Federal Elliott
 Lea County, New Mexico
 Section 1, T 16 S - R 34 E
 Elevation 4078 ft



QA 14582c

P1
 Bishop Cap
 Doña Ana County, New Mexico
 NE/4 Section 25, T 24 S – R 3 E



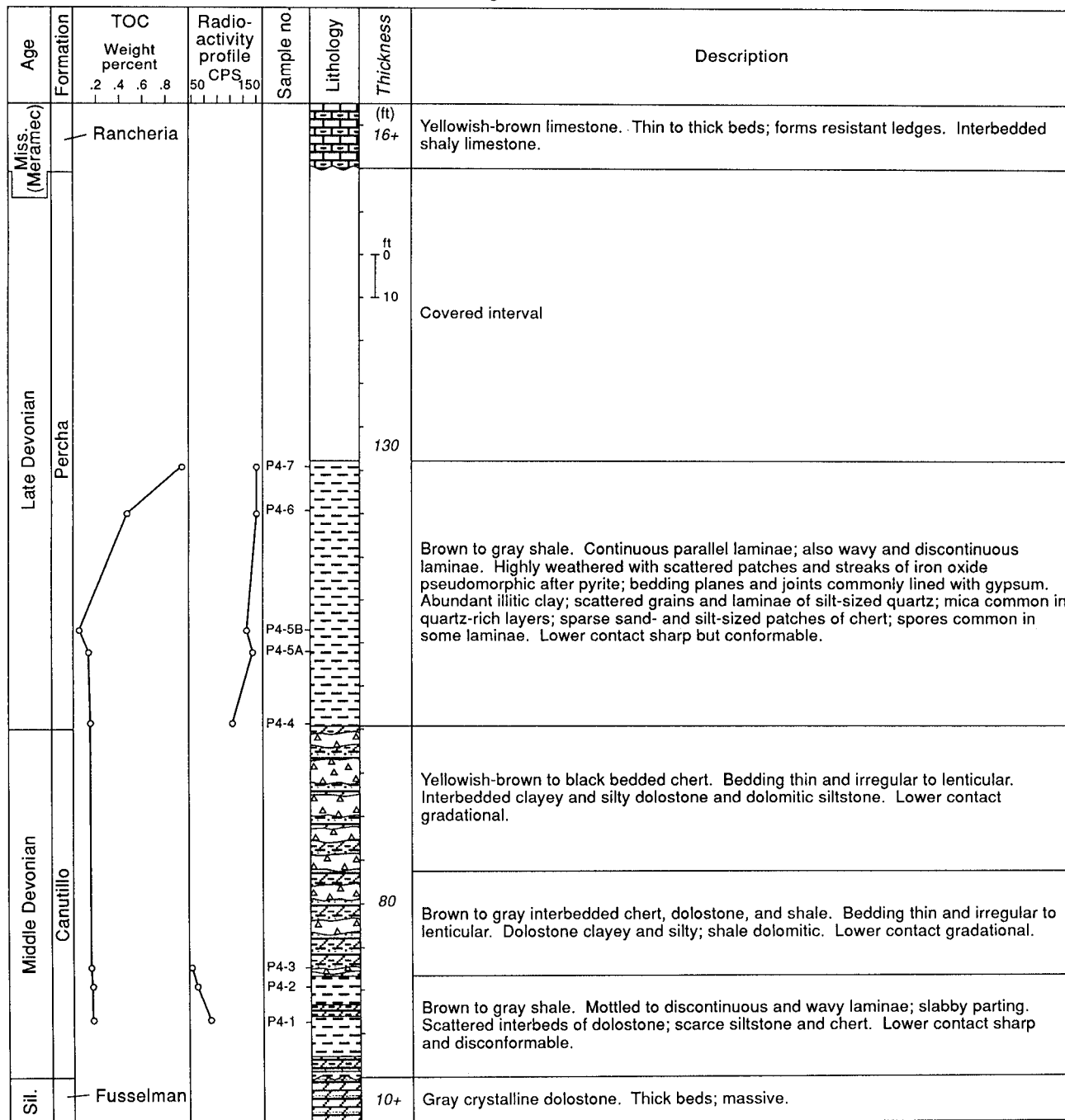
QA 14583c

P2
 Anthony Gap
 North Franklin Mountains
 Doña Ana County, New Mexico
 SE/4 Section 34, T 26 S - R 4 E

Age	Formation	TOC		Radio-activity profile	Sample no.	Lithology	Thickness	Description
		Weight percent	CPS					
		.2 .4 .6 .8	20 30 40					
Miss.	Las Cruces						5+	Gray limestone. Thin beds. Shaly. Lower contact sharp and disconformable.
Late Devonian	Percha				P2-4			Gray dolomitic siltstone; weathers brown. Discontinuous and wavy laminae to thin beds; slabby parting. Slightly calcareous; abundant silt-sized quartz; phosphatic debris common; sparse mica. Rare burrows. Lower contact sharp and conformable.
					P2-3		28	
					P2-2			
					P2-1			
Middle Devonian	Canutillo						ft 0 10 92	Gray dolostone; weathers brown. Thin beds. Nodular chert lenses and beds common.
								Covered interval.
Silurian	Fusselman						18+	Gray crystalline dolostone. Thick beds; massive.

QA 14584c

P4
 Martin Canyon
 Hueco Mountains
 El Paso County, Texas
 106° 00' 30" W. Longitude – 31° 48' 30" N. Latitude



QA 14585c

Appendix C. Point-count data for the Woodford Formation.

Core and sample no.	Depth (ft)	Terrigenous				Pelagic		Authigenic		Other (%)
		Quartz (%)	Mica (%)	Feldspar (%)	Illite (%)	AOM* (%)	Pellets (%)	Dolomite (%)	Pyrite (%)	
BLACK SHALE										
C1-4	11,540	6	3	— **	68	11	—	1	—	—
C1-9	11,555	14	2	1	45	10	—	22	6	—
C2-3	7,172	3	—	—	43	25	4	23	1	1
C2-8	7,181	—	—	1	34	35	5	19	2	4
C3-1	13,754	1	—	—	76	14	5	1	2	1
C3-10	13,884	2	—	—	53	13	—	20	—	12
C4-2	10,899	15	1	1	52	5	8	3	13	2
C4-7	10,933	17	2	2	56	8	—	6	8	1
C5-2	11,639	5	—	—	67	8	11	—	7	2
C5-5	11,648	6	—	—	64	9	2	15	2	2
C6-3	10,924	2	1	—	77	17	—	1	—	2
C7-2	10,176	16	—	—	53	15	3	7	5	1
C8-1	9,033	2	—	—	79	12	—	5	2	—
C9-2	12,228	9	—	—	69	10	—	2	3	7
C10-4	8,502	9	—	—	57	6	—	25	3	—
C12-4	7,404	3	2	—	50	31	7	4	2	1
C13-4	14,626	10	3	1	61	9	—	9	6	1
SILTSTONE										
C3-6	13,772	6	—	—	—	—	—	68	24	2
C5-8	11,662	36	4	2	28	—	—	30	—	—
C10-4	8,502	32	—	—	—	—	—	39	—	29 ***
C11-5	13,033	43	—	1	14	—	—	41	—	2

* Volume percent of amorphous organic matter (AOM) = wt % TOC × 3. The conversion factor, 3, represents the density difference between organic matter and minerals, ~2.5, and a generalized value of carbon in kerogen, 80 wt %, or 2.5/0.8 ≈ 3.

** Less than 1.

*** Fossils, calcite cement, and phosphate.

Appendix D. Organic content of the Woodford Formation.

Core no.	Depth (ft)	TOC* (wt %)	Kerogen morphology	Primary (%)	Recycled (%)
BLACK SHALE					
C1	11,536–11,555	3.9	Amorphous**	1.14	ND
C2	7,169–7,184	9.0	Amorphous	0.55	0.87
C3	13,745–13,776	2.3	Amorphous	1.44	ND
C3	13,838–13,844	2.9	Amorphous	1.66	ND
C4	10,898–10,936	2.7	Amorphous	1.05	ND
C5	11,639–11,657	3.2	Amorphous	0.79	ND
C6	10,921–10,941	5.1	Amorphous	1.52	2.21
C7	10,174–10,177	4.6	Amorphous	0.68	ND
C8	9,033–9,036	2.4	Amorphous	0.78	1.15
C9	12,219–12,263	3.3	Amorphous	0.92	ND
C10	8,459–8,513	2.2	Amorphous	0.61	0.99
C12	7,401–7,542	6.3	Amorphous	0.54	ND
C13	14,605–14,644	4.2	Amorphous	1.64	ND
P1	Outcrop	1.1	Amorphous	1.92	ND
P3	Outcrop	0.1	Amorphous	NA	NA
P4	Outcrop	0.4	Amorphous	NA	NA
SILTSTONE					
C5***	11,662–11,688	0.9	Amorphous	0.85	ND
C9****	12,266–12,333	0.7	Amorphous	0.99	ND
C11***	13,026–13,068	0.4	Amorphous	1.32	ND
P2****	Outcrop	0.4	Amorphous	NA	ND

* Data represent mean values of samples in designated depth interval.

** Amorphous kerogen is aquatic, nonterrestrial organic matter that yields oil during thermal maturation (Hunt, 1979; Tissot and Welte, 1984).

*** Quartz-dominated siltstone.

**** Dolomite-dominated siltstone.

ND not detected.

NA not analyzed.